eman ta zabal zazu

Universidad del País Vasco
Euskal Herriko Unibertsitatea

FACULTY OF ENGINEERING BILBAO
UNIVERSITY OF THE BASQUE COUNTRY

Departamento de Ingeniería de Comunicaciones

Komunikazioen Ingeniaritza Saila

Department of Communications Engineering

Ph.D. Thesis

Advanced Constellation and Demapper Schemes for Next Generation Digital Terrestrial Television Broadcasting Systems

Author Jon Barrueco Gutiérrez
Advisor Dr. Pablo Angueira Buceta
Co-Advisor Dr. Jon Montalbán Sánchez

February 2019

(cc)2019 JON BARRUECO GUTIERREZ (cc by-nc 4.0)

ABSTRACT

Nowadays, the users' demand of high quality multimedia contents and the available spectrum resources drive the Digital Terrestrial Television (DTT) market. Next generation DTT broadcast systems have to cope with very demanding TV services in terms of bitrate and robustness and a reduction of the frequencies assigned to broadcast systems. This challenge is faced with the design of advanced techniques that provide an efficient use of the radioelectric spectrum, increasing the capacities of the previous DTT systems.

There are three main strategies that can improve capacity and performance of DTT standards: network planning, video coding and physical layer efficiency optimization. The first two fields are well covered in the latest DTT systems. Regarding physical layer technologies, the recent advances in Forward Error Correction (FEC) techniques such as Low Density Parity Check (LDPC) codes and Non-Orthogonal Multiple Access (NOMA) solutions as Layered Division Multiplexing (LDM) have improved the efficiency and robustness of DTT systems. However, the advances in constellation design have not been included in DTT broadcast standards. State-of-the-art works related to constellation design via Geometrical Shaping (GS) demonstrate that the channel capacity of wireless communication systems can be highly improved with respect to standard Quadrature Amplitude Modulation (QAM) schemes commonly used in DTT. Non-Uniform Constellations (NUCs) are a sort of constellations designed via GS and their geometrical characteristics are given by the Signal-to-Noise Ratio (SNR) and channel model. NUCs arise as a candidate to be included in upcoming DTT systems as they provide higher channel capacity than QAM.

This dissertation analyzes and compares the system performance of NUCs with respect to QAM schemes in DTT broadcast systems. The joint system performance of NUCs with the Rotated Constellation (RC) technique is also evaluated in order to improve the robustness of DTT systems under fading scenarios. After the evaluation of several Modulation (from 16 to 256 constellation points) and Coding (from 3/15 to 12/15) (ModCod) configurations, it is demonstrated that NUCs outperform QAM for all ModCods with the highest gain of 1.1 dB. It is also proved that for the same throughput, the combination of low code rate and high order constellation outperforms the combination of high code rate and low order constellation with RC technique under fading scenarios.

Regarding the design of NUCs, there are several works which deal with the optimization of such constellation schemes. However, the proposed solutions are

both too complex and computationally expensive. Besides, the importance of initial conditions is not considered and some of the post-processing steps are not included. The computational complexity of the state-of-the-art methods may result into hours or even days to design even the simplest constellation, i.e., 16 constellation points. This thesis proposes an efficient optimization algorithm to design NUCs for both AWGN and Rayleigh channels. The optimization problem is analyzed showing the different possible methodologies to solve the problem and proposing the solution that best fits to the optimization challenge. Constellations from 16 to 4096 constellation points are designed in a very sort optimization time, i.e., in terms of minutes. The results of the system performance demonstrate that gains up to 1.8 dB are obtained with the designed NUCs with respect to QAM schemes.

The development of techniques at the transmitter side which improve the spectral efficiency and robustness commonly implies an increase of the computational complexity at the receiver. In the case of NUCs, the number of computations required at the demapper is highly incremented. Most of the state-of-the-art demappers are not efficient for NUCs as they do not consider their geometrical characteristics. Two different demappers are proposed reducing the computational complexity associated with NUCs. The first one consists of a lattice reduction demapper for massive order One-Dimensional NUCs (1D-NUC). A demapping complexity reduction up to 87.5% of the number of Euclidean Distances (EDs) computed for 1D-4096NUCs is achieved with negligible system performance losses and memory requirements if compared with the Maximum Likelihood (ML) decoder. The second demapper is designed for 2D-NUCs considering their geometrical characteritics for different SNR and channel models. The demapper is based on condensation and adaptive sub-region techniques achieving up to 95.4% of computational complexity reduction when compared to the ML demapper. When other 2D-NUC demapping proposals are considered, the proposed demapper still shows complexity reduction (from 6% to 27%) and better system performance (degradation always below 0.1 dB).

LABURPENA

Gaur egungo *Lurreko Telebista Digitala*-ren (LTD) merkatua, kalitate handiko multimedia edukien eskakizunen eta erabilgarri dagoen frekuentzia-espektroaren arabera arautzen da. Hurrengo belaunaldiko irrati-difusio sistemek, telebista zerbitzu berrien beharrei aurre egin beharko diete. Horretarako, transmisioaren fidagarritasuna ziurtatu eta erabilitako banda-zabalera txikiagotu beharko da. Erronka honi aurre egiteko, irrati-frekuentzien erabilera eraginkorra bermatzen duten teknikak garatu behar dira, LTD sistemen gaitasunak areagotuz.

Oro har, hiru estrategia ezberdin identifikatu daitezke LTD klasikoaren ahalmena eta errendimendua hobetzeko: sarearen planifikazioa optimizatzea, bideo-kodifikazioa eraginkorra izatea edota geruza fisikoaren ahalmenak garatzea. Geruza fisikoaren alorrean, erroreak kontrolatzeko tekniken inguruan egindako aurrerapenak, (*Low Density Parity Check* (LDPC)) kodeak, eta espektroa partekatzeko metodologia berriak, (*Layered Division Multiplexing* (LDM)), nabarmendu behar dira. Bestetik, geruza fisikoaren baitan konstelazioen diseinurako metodologia berriak ez dira LTD sistemen estandarren parte izan orain arte (ATSC 3.0-ean salbu). Proiektu honen lehenengo ekarpena *Geometrical Shaping* (GS) izeneko konstelazioen diseinuaren bidez haririk gabeko komunikazioak hobetu daitezkeela frogatzea izan da. Horrenbestez, alde batera utz daitezke aurreko LTD sistemetan erabili ohi izan diren konstelazioak, hots, *Quadrature Amplitude Modulation* (QAM) konstelazioak. *Non-Uniform Constellations* (NUCs) GS-aren bidez diseinatutako konstelazioak dira, eta haien ezaugarri geometrikoak *Signal-to-Noise Ratio* (SNR)-aren balioaren eta kanalaren ezaugarrien arabera definitzen dira. NUC-ek aukera paregabea dute etorkizuneko LTD sistemak hobetzeko, QAM-ek baino ahalmen handiagoa eskaintzen baitute.

Ikerkuntza lan honek, NUC eta QAM konstelazioen errendimendua aztertzen du LTD komunikazio sistemetan. Horrez gain, beste aukera bat ere aztertuko da: NUC konstelazioak eta *Rotated Constellation* (RC) teknika sistema berdinean uztartzea. Modulazio (16 konstelazio puntutik 256 puntura) eta LDPC (3/15-etik 12/15-era) desberdinen ebaluazioa egin ondoren, NUC sistemek QAM sistema klasikoak 1,1 dB-tan gainditzen dituztela frogatu daiteke. Halaber, datu transmisio berdinerako, modulazio altuen eta kodifikazio sendoen arteko konbinaketek errendimendu onenak eskaintzen dituzte.

NUC-en diseinuari dagokionez, metodologia ugari daude konstelazio eskema mota hauen optimizazioa garatzeko. Orokorrean, proposatutako soluzioak oso konplexuak eta garestiak izaten dira. Gainera, hasierako baldintzen garrantzia ez da

kontuan hartzen eta bukaerako urrats batzuk ez daude guztiz garatuta. Izan ere, konplexutasun konputazionala dela eta orduak edota egunak beharko lirateke lan horietan azaltzen diren metodoen bidez konstelaziorik sinpleena lortzeko. Tesi honetan nabarmenki eraginkorragoa den algoritmo bat proposatzen da, bai AWGN kanaletan baita Rayleigh kanaletan ere errendimendu ona eskaintzen duena. Lan honetan, optimizazio arazoa aztertzen da hainbat metodologia proposatuz eta optimizazio erronkari hobekien egokitzen zaion irtenbidea bilatuz. 16 eta 4096 puntuetako konstelazioak oso denbora laburrean diseinatzeko aukera eskaintzen da eta sistemaren errendimenduaren emaitzen arabera 1,8 dB-ko hobekuntza lor daiteke.

Orokorrean, transmisorean egindako aldaketek hargailuaren konplexutasuna handiagotzen dute. NUC-ei dagokienez, hargailuan eskatutako eragiketa kopurua exponentzialki handitzen da. Bibliografian aurkitu daitezkeen detektagailu gehienak ez dira eraginkorrak NUC sistementzat, haien ezaugarri geometrikoak ez baitira kontuan hartzen. Lan honetan bi detektagailu desberdin proposatzen dira konplexutasun konputazionala murrizteko. Lehendabizikoa *lattice reduction* izeneko detektagailuan oinarritzen da. Dimentsio bateko NUC-etara (1D-NUC) bideratua dago, eta konplexutasuna % 87,5 murriz dezake *Maximun Likelihood* (ML) detektagailuarekin alderatuta. Gainera, bai memoriaren tamaina, bai sistemaren galerak ML-en berdinak dira. Bigarren detektagailuak 2D-NUC-en ezaugarri geometrikoak aintzakotzat hartzen ditu SNR balio eta kanal eredu desberdinetan aplikatu ahal izateko. Detektagailua kondentsazioan eta *adaptive sub-region* tekniketan oinarritzen da. Kasu honetan, konplexutasun konputazionala % 95,4 murriz daiteke ML irtenbidearekin alderatuta. Beste 2D-NUC detektagailu proposamen batzuk kontuan hartzen direnean ere konplexutasun murrizketa handiak (% 6tik % 27ra) eta sistemaren funtzionamendu orokor hobea (degradazioa beti 0,1 dB azpitik) agertzen dira.

RESUMEN

Hoy en día, hay dos principales corrientes que dirigen el mercado de la Televisión Digital Terrestre (TDT). La primera es la demanda por parte de los usuarios de contenidos multimedia de alta calidad. La segunda son los recursos espectrales disponibles. Los sistemas de radiodifusión terrestre de siguiente generación tienen que adaptarse a los requerimientos de los servicios de televisión futuros, es decir, alta tasa de bit y fiabilidad del sistema. Además, también tienen que sufrir los recortes de las frecuencias asignadas a los sistemas de radiodifusión. Este reto se encara a partir del diseño de técnicas avanzadas que hacen un uso eficiente del espectro radioeléctrico, de forma que las capacidades de los sistemas TDT se incrementan.

Hay tres estrategias principales que permiten mejorar la capacidad y desempeño de los estándares de TDT: planificación de red, codificación de vídeo y optimización de la eficiencia de la capa física. Los primeros dos campos tienen un amplio desarrollo en los últimos estándares TDT. En cuanto a las tecnologías de capa física, los avances recientes tanto en técnicas de codificación, códigos LDPC, como en soluciones de acceso múltiple no ortogonal, LDM, han mejorados la eficiencia y robustez de los sistemas TDT. Sin embargo, los diferentes avances realizados en constelaciones no han sido aplicados a estándares de radiodifusión terrestre salvo en el recientemente implementado ATSC 3.0. El estado del arte de trabajos sobre constelaciones diseñadas a partir del moldeado geométrico demuestra que la capacidad de los sistemas de comunicaciones inalámbricos se puede mejorar considerablemente si se aplica este tipo de constelaciones en vez de las QAM, ampliamente utilizadas en los sistemas TDT. Un tipo de constelaciones moldeadas geométricamente son las llamadas constelaciones no uniformes (NUC). Las NUC se muestran como candidatas a ser incluidas en los próximos sistemas TDT ya que mejoran la capacidad del canal con respecto a las QAM.

Esta tesis analiza y compara el desempeño de las NUC con respecto a los esquemas QAM en sistemas de radiodifusión TDT. Además, este trabajo evalúa la unión de dos técnicas de modificación de constelaciones, NUC y constelaciones rotadas, con el objetivo de mejorar la robustez de los sistemas TDT bajo condiciones de desvanecimientos. Después de evaluar diferentes modulaciones (desde 16 a 256 puntos de constelación) y codificaciones (desde 3/15 a 12/15), a cuyas combinaciones se les llama ModCod, los resultados demuestran que las NUC mejoran a las QAM para todos los ModCod con un máximo de 1,1 dB. También se demuestra que para la misma capacidad de ModCod y para bajo condiciones de desvanecimientos, las combinaciones de tasas de codificación (code rate) bajas y

constelaciones de alto orden mejoran a las de tasas de codificación altas y constelaciones de bajo orden junto con la técnica de RC.

En cuanto al diseño de NUC, ya existen varios trabajos que tratan sobre la optimización de tales constelaciones. Sin embargo, estos trabajos proponen soluciones que son complejas y computacionalmente costosas. Además, no consideran la importancia de las condiciones iniciales y no incluyen varios de los pasos de procesado necesarios. La complejidad computacional de estas soluciones puede significar desde horas a días en diseñar incluso la constelación más simple, es decir, la de 16 puntos de constelación. Esta tesis propone un algoritmo eficiente de diseño de NUC para canales AWGN y Rayleigh. El problema de optimización es analizado mostrando las posibles metodologías para solucionar el problema y se propone la solución que mejor encaja en el reto de la optimización. Se diseñan constelaciones desde 16 a 4096 puntos en un tiempo de simulación muy bajo, esto es, minutos. Los resultados demuestran que se pueden alcanzar ganancias de hasta 1,8 dB con las NUC diseñadas a partir del método propuesto con respecto a los esquemas QAM.

El desarrollo de técnicas en la parte del transmisor que mejoran la eficiencia espectral y robustez normalmente implica un incremento de la complejidad computacional en la parte del receptor. En el caso de las NUC, el número de computaciones requeridas en la parte del demapeo se incrementa de forma acusada.

La mayoría de los demapeos que aparecen en el estado del arte no son eficientes para las NUC porque no consideran sus características geométricas. Esta tesis propone dos demapeos diferentes que reducen la complejidad computacional asociada a las NUC. El primero se basa en el demapeo llamado lattice reduction para constelaciones masivas de una dimensión. Este demapeo consigue hasta una reducción del 87,5% en la complejidad computacional en el caso de NUC de una dimensión y 4096 puntos con pérdidas y requerimientos de memoria insignificantes si se compara con el demapeo óptimo (maximum likelihood). El segundo demapeo se diseña para NUC de dos dimensiones considerando sus características geométricas para diferentes valores de SNR y modelos de canal. El demapeo se basa en las técnicas de condensación y subregión adaptativa consiguiendo hasta un 95,4% de reducción computacional si se compara con el demapeo óptimo. Cuando se compara con otros demapeos existentes, el demapeo propuesto sigue reduciendo la complejidad (desde el 6% al 27%) y, al mismo tiempo, mejora el rendimiento del sistema (degradación por debajo de 0,1 dB).

Index

Figure Index

Table Index

CHAPTER 1: **INTRODUCTION AND OBJECTIVES**

1. Terrestrial Broadcasting: Up to Date Roadmap and Future Expectations

1.1 From Analogue to Digital TV

The end of World War II got television (TV) underway, which is still considered one of the most popular communication systems. From 1950, TV has served as the main mean of information delivery for thousands of families around the World. At first, the content delivered was composed of sound and images in black and white. It was not until the mid-1960s that color broadcasting appeared. The created content (baseband signal) and the transmissions were both analogue, occupying frequency bands of the Ultra-High Frequency (UHF) and Very-High Frequency (VHF) spectrum. The transmission of signals composed of analogue content occupied a wide range of the bandwith available for TV and, thus, only few analogue programs could be delivered to the end users.

In order to make an efficient use of the available spectral resources, the TV media content delivered was switched from analogue to digital, also known as analogue swith off. The first generation of Digital Terrestrial Television (DTT) broadcasting systems appeared in the 90s to improve the spectral occupancy of the analogue services. These systems were enough to provide the digital media contents of that era.

Since the analogue switch off several DTT broadcasting systems have been designed. The Terrestrial Digital Video Broadcasting (DVB-T) [1] and Advanced Television System Committee (ATSC) [2] were the first DTT standards developed in Europe and United States (U.S.) in 1994 and 1996, respectively. Next, Japan developed its own DTT system called Terrestrial Integrated Services Digital Broadcasting (ISDB-T) [3] in 2001. Following the tendency, in 2006 China designed its own standard, the Digital Terrestrial Multimedia Broadcast (DTMB) [4].

ATSC is based on the 8 Level Vestigial Side Band (8-VSB), which suffers from multipath distortions. Besides, ATSC considers 2/3 code rate that together with the single-carrier modulation provides one single operational point with a maximum bitrate around 19.63 Mbps over a channel of one 6 MHz. In order to improve the system performance, the rest of first-generation DTT broadcasting standards included the Coded Orthogonal Frequency Division Multiplexing (OFDM) modulation [5]. In OFDM, the data information is protected with Forward Error Correction (FEC) codes and the subcarriers are allocated at a

determine frequency with a spacing inversely proportional to the useful symbol duration between adjacent subcarriers for a given bandwidth. The inclusion of several modulation orders, Code Rates (CR), Guard Intervals (GI) and Fast Fourier Transform (FFT) sizes enables the transmission of very robust signals or high bitrate services in the range of 19 to 25 Mbps.

In the early 2000s, with the appearance of portable devices the necessity of a DTT system supporting mobile scenarios came up. The Handheld (DVB-H) [6] system developed in Europe in 2004 was a first attempt to deal with mobile scenarios, but this system was not successful.

The advent of new media contents and the request of the consumers asking for high quality services, meant that already existing systems were insufficient to provide the desirable data rate without increasing the bandwidth. Therefore, in 2009 the Second Generation (DVB-T2) [7] system was published by the European Telecommunications Standards Institute (ETSI) improving the system performance and quality of service of the prior DTT standards. Figure 1.1 shows the worldwide map of the different DTT broadcasting systems in use [8].

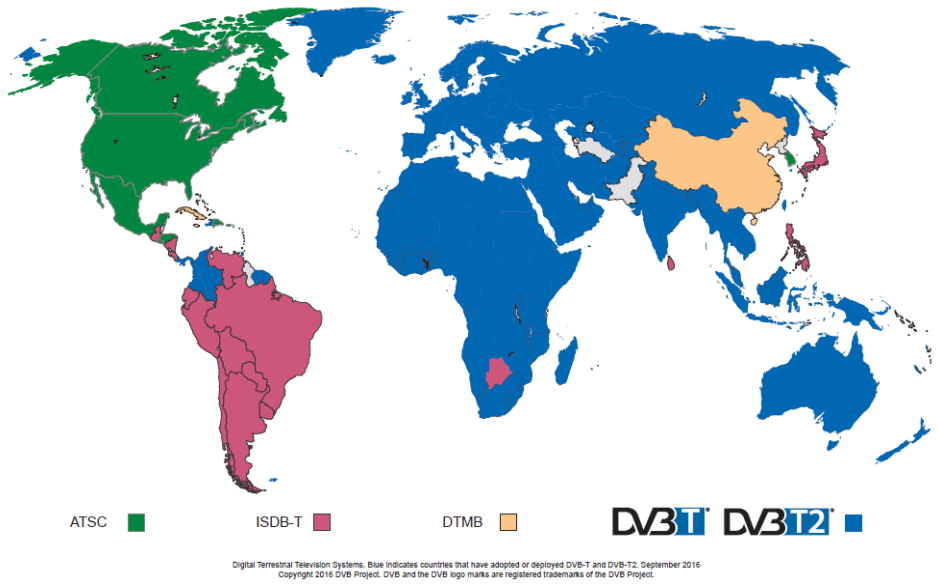

Figure 1.1. Map of countries with the different DTT systems adopted.

The third generation ATSC DTT system (ATSC 3.0) is developed in the U.S. The Physical Layer Standard is accessible in [9]. ATSC 3.0 includes new techniques

to provide Ultra High Definition (UHDTV) content and mobile services using the same spectral resources as prior DTT systems [10].

1.2 **Digital Dividends**

The switch-off of the analogue television and the introduction of the digital terrestrial television supposed the liberation of part of the radio spectrum over the VHF and UHF bands, also known as Digital Dividend [11], [12]. UHF bands are appealing for mobile communication systems as the propagation and penetration properties inside buildings of the signals are better than in higher frequency bands. In 2007, the International Telecommunications Union (ITU) decided to assign the upper part of the TV broadcasting band to International Mobile Telecommunications (IMT), i.e., Long Term Evolution (LTE) during the World Radiocommunication Conference (WRC). More in detail, the 700 MHz band (from 694 MHz to 790 MHz) was released by ITU Region 2 (America). ITU Regions 1 and 3 (Europe, Africa, Asia and Oceania) released the 800 MHz band (from 790 MHz to 862 MHz) [13].

Later on, the second Digital Dividend led to released frequency spectrum in the 700 MHz band in ITU Regions 1 and 3. In WRC 2015, the ITU decided to allocate IMT the 700 MHz band in ITU Regions 1 and 3 before 2020 to IMT services [14]. In the same year, the Federal Communications Commission (FCC) recommended U.S. broadcasters to voluntarily give up the 600 MHz band (used for broadcasting up to date) to Mobile Network Operators (MNOs) [15].

1.3 **The Evolution of Multimedia Content**

The multimedia content delivered by DTT broadcasting systems needs to adapt to the consumers demand in order to remain attractive and, as a consequence, maintain the incoming revenues from advertising media. The analysis of users demand presented in [16] predicts a steady and important increase of the multimedia content in Internet traffic. One of the main findings refers to the increment of the presence of high-resolution content, i.e., UHDTV, 3DTV and, in the near future virtual and augmented reality.

The demand in platforms such as the Internet must be taken into account in the upcoming next-generation DTT systems. These systems must respond to all the necessities for different types of scenarios, i.e., fixed, mobile, indoor reception.

To sum up, users are demanding very high quality multimedia content and the signal transmitted faces very challenging scenarios. As a consequence, three main characteristics of DTT broadcasting systems must be improved: i) Maximum achievable data rates ii) Signal robustness iii) Spectral efficiency of the transmited signal.

1.4 New Generation DTT Broadcasting Systems

The latest DTT broadcasting systems aim at responding to the high quality services for a wide range of reception scenarios with an efficient use of the available bandwidth. In Europe, the DVB-T2 system was released in 2009 improving significantly the robustness and spectral efficiency of its predecessor DVB-T. Currently, the most advanced DTT system has been developed in North America (ATSC 3.0) with even higher spectral efficiency, data rates and robustness.

1.4.1 DVB-T2

DVB-T2 is compatible with advanced coding techniques such as MPEG-4 or H.265 (HEVC) for audio and video data compression. DVB-T2 also provides flexibility in its configuration in order to efficiently adapt to defined sort of reception scenarios [17], i.e., portable, mobile or fixed-rooftop.

Although the modulation block (OFDM) is similar to DVB-T, in DVB-T2 additional configurations are included to provide an appropriate trade-off between system capacity and robustness. The number of guard interval values, FFT sizes and scattered pilot choices is increased. The maximum data rate is 50.3 Mbps for an 8 MHz bandwidth channel with a SNR maximum operational value of 22 dB under AWGN channel. The inclusion of a time interleaver makes this system more robust than DVB-T under fading and low Doppler scenarios [18]. DVB-T2 features Time Division Multiplexing (TDM) using Physical Layer Pipes (PLP) in order to provide simultaneously mobile and fixed services.

DVB-T2 makes use of the BICM system model using FEC structure based on Bose Chadhuri Hocquenghem (BCH) outer code and Low Density Parity Check (LDPC) as inner code. Quadrature Phase Shift Keying (QPSK), 16QAM, 64QAM and 256QAM constellations are included. The Signal Space Diversity (SSD) technique called Rotated Constellation (RC) is adopted in this standard showing very good performance in frequency selective fading channels and Rayleigh Memoryless with Erasures (RME) channels [19].

1.4.2 ATSC 3.0

ATSC 3.0 is the most recent DTT broadcasting system addressing the consumers' changing habits and demands [20]. The standardization process started in October 2013. The physical layer was published in September 2016 and in November 2017 the FCC authorized its deployment. South Korea has deployed ATSC 3.0 in 2017 in order to broadcast huge impact events, such as the 2018 Winter Olympic Games [21]. One of the main capabilities of ATSC 3.0 is the provision of hybrid content services to fixed and mobile receivers seamlessly with HD and Ultra HD resolutions and has demonstrated superior coverage and capacity performance than DVB-T2 [10].

ATSC 3.0 includes novel techniques, as a low-complexity Non-Orthogonal Multiplexing (NOM) also known as Layered Division Multiplexing (LDM) [22]–[23], and Channel Bonding (CB) [24]. It also takes advantage of some of the features included in DVB-T2, like an improved version of the time interleaver [25], LDPC coding with a wider range of code rates and an improved version of the OFDM chain [26]. Bit-Interleaved Coded Modulation (BICM) is chosen as the system model. The FEC is composed of an outer code and an inner code. There are 3 options for the outer coder: BCH code, Cyclic Redundancy Check (CRC) or none, whereas the inner code is LDPC with a new strcture of Parity Check Matrix (PCM) specially designed to enable operation below 0 dB SNR. The bit interleaver consists of a parity interleaver followed by a group-wise interleaver and a block interleaver. This structure enables parallel LDPC decoding and the performance of the FEC codes can be optimized to any constellation. A new constellation scheme called Non-Uniform Constellation (NUC) is adopted, providing up to 1.8 dB gain with respect to *M*-ary Quadrature Amplitude Modulation (QAM) [27], [28]. Although One-Dimensional NUCs (1D-NUC) were already proposed in DVB-NGH, Two-Dimensional NUCs (2D-NUC) are used for the first time in a DTT broadcast standard.

For Single-Input Single-Output (SISO) configuration, ATSC 3.0 provides a wider Signal-to-Noise Ratio (SNR) operational range. Under Additive White Gaussian Noise (AWGN) channel (from -6.2 dB to 32 dB) with a bit rate range from 1 Mbps to 57 Mbps for a 6 MHz channel bandwidth. Table 1.1 compares the main characteristics of the two latest DTT broadcast systems.

Table 1.1. Comparison of physical layer configuration parameters from DVB-T2 and ATSC 3.0

Parameter	DVB-T2	ATSC 3.0
Video Coding	H.264 & HEVC	H.264 & HEVC
Channel Coding **(Inner)** **(Outer)**	BCH LDPC	BCH. CRC, None LPDC
Code Rate	1/2, 3/5, 2/3, 3/4, 4/5, 5/6	{2 – 13}/15
Bit Interleaver	Block	Parity, Block-wise and Block
Constellation	QPSK, 16QAM, 64QAM, 256QAM	QPSK, 2D-16NUC, 2D-64NUC, 2D-256NUC, 1D-1024NUC, 1D-4096NUC
Time Interleaver	Block Interleaver	Convolutional Interleaver & Hybrid Block + Convolutional Interleaver
Frequency Interelaver	Random interleaving on every OFDM symbol (except P1)	Random interleaving on a per OFDM symbol basis
Multiplexing	TDM	LDM, FDM, TDM
Guard Interval	1/128, 1/32, 1/16, 19/256, 1/8, 19/128, 1/4	3/512, 3/256, 1/64, 3/128, 1/32, 3/64, 1/16, 19/256, 3/32, 57/512, 3/16, 1/8, 19/128, 1/4
FFT	1k, 2k, 4k, 8k, 16k, 32k	8k, 16k, 32k
Channel Bandwidth	1.7, 6, 7, 8, 10 MHz	6, 7, 8 MHz
Bit Rate (Mbps)	3.9 Mbps to 50.3 Mbps (8 MHz channel)	1 Mbps to 57 Mbps (6 MHz channel)
SNR operational region under AWGN channel	1 dB to 22 dB	-6.2 dB to 32 dB

2. MOTIVATION OF THIS THESIS

DTT systems have to respond to higher data rates and robustness and, at the same time, the electromagnetic spectrum resources associated to these systems are being cut back. To overcome these challenges, new communications tools must be developed to make an efficient use of the radio spectrum.

The upper bound at which digital data can be transmitted from a single source with no errors under an AWGN channel is given by Shannon's limit [29], [30] considering the Nyquist-Hartley theorem described in [31], [32] and [33]. During the last decades, researchers have focused on getting as close as possible to that limit by improving the error correction and modulation techniques. Error correction techniques, such as LDPC codes and turbo codes have shown to be very close to Shannon's capacity limit [34]. DTT broadcast systems have taken advantage of the evolution of those error coding techniques and each standard has included their latest version. Modulation techniques have been also improved along the last decades, but DTT broadcast systems have not paid attention to this evolution. Classical QAM schemes, which are far from Shannon`s limit, have been used since the first system (DVB-T) was developed.

Researchers who take part in the design of the most advanced DTT broadcast system up to date, i.e., ATSC 3.0 (included the author of this thesis) have focused on novel modulation schemes to improve spectral efficiency and system robustness. However, there are plenty of techniques to design capacity approaching constellations. These must be gathered and analyzed to propose the solution that best fits in the DTT broadcast environment.

The system performance of the selected modulation must be evaluated and compared with previous DTT systems under different system conditions to check out its feasibility and viability.

The viability of a constellation scheme is not only evaluated in terms of system performance, but also in terms of design and receiver complexity. Any optimization problem is known as a complex procedure, above all when the objective function is a very complex equation, as it is the case of the BICM capacity equation for DTT broadcast systems. The computation complexity is normally converted into time consumption, resulting into hours or even days to design even the simplest constellation, i.e., 16 constellation points. The time and computational resources used for the design of a constellation is a key parameter in the standardization process of a DTT broadcast system as there is a short period of time (since the system requirements are published) to propose a whole set of

constellations, e.g., from 4 to 4096 constellation points. Therefore, there is a challenging gap in order to reduce the designing time of constellations via BICM channel capacity maximization. If the optimization time is highly reduced, the success of such constellations and patents derived in the standardization process is guaranteed.

This thesis is focused on the efficient design of constellation schemes for BICM systems. The optimization problem must be studied in-depth to propose an efficient solution. The proposed solution must be validated and compared to standard modulation techniques using metrics for complexity and system performance evaluation.

The inclusion of new constellation schemes in a communication systems does not come for free. The optimal Maximum Likelihood (ML) decoder is an expensive solution in terms of computational requirements and low complexity detectors must be designed in order to reduce the receiver complexity. This thesis reduces receiver complexity with two different demapping approaches which highly reduce the computational requirements for the designed constellations.

3. OBJECTIVES

The principal objective is to design advanced modulation and demodulation schemes to increase the spectral efficiency and robustness of DTT broadcasting systems. In order to reach the main objective, several partial objectives are defined:

- **Analysis of the existing constellation and demapping design methods for digital communication systems**. To propose the most appropriate constellation type for DTT broadcast systems, the first step must be a detailed analysis of the state-of-the-art of existing constellation techniques. The main objective of increasing the spectral efficiency of the system comes with no minimal cost of complexity at the receiver. Therefore, a deep study of the demapper choice for digital communication systems must be carried out. This detailed analysis requires a set of sub-objectives:

    - Compilation of all the research related with constellation and detector design up to date.
    - Search of similarities between the work compiled and definition of families of constellations and detectors.
    - Characterisation of each family: advantages and disadvantages.
    - Description of the main contribution of the work divided by families.
    - Detection of the constellation scheme that fits best with the characteristics of a DTT broadcast system.

- **Analysis of the system performance of advanced constellation techniques for DTT broadcasting systems**. The system performance of new constellation schemes must be evaluated in conjunction with error correction codes in order to study their viability in DTT broadcast systems. This system performance study requires a set of sub-objectives:

    - Definition of the evaluation methodology: metrics, cases and tools.
    - Design of a BICM and OFDM simulation platform.
    - Analysis of the system performance of GS constellations for BICM systems under AWGN and Rayleigh independent and identically distributed (iid).
    - Analysis of the system performance of GS constellations with RC technique in fading scenarios.
    - Evaluation of the performance of same throughput Modulation and Coding (ModCod) combinations with and without RC under fading channels.

- **Propose an efficient design of capacity-approaching constellation schemes**. Up to now, proposed solutions to design efficient constellation schemes are very time consuming and there is not a detailed analysis of the optimization problem and the best way to proceed. As a consequence, the objective is to propose an efficient algorithm to design efficient constellation schemes following the next sub-objectives:

    - Analysis of the optimization problem and proposal of an efficient solution.
    - Creation of an optimization methodology to design advanced constellation schemes.
    - Study of the key factors and characteristics in the design of the constellations to provide heuristics for reducing the optimization time.
    - Design of a whole set of constellations from low order (16 constellation points) to high order (4096 constellation points) reducing the optimization time in one or two orders of magnitude.

- **Design low complexity demappers for NUCs**. The constellation schemes designed in the aforementioned objective require new demapping techniques that reduce the associated computational complexity. Depending on the geometrical characteristics of the designed constellations, different demapping methodologies must be designed. The associated objectives are:

    - Study of the characteristics of the designed constellations as a function of the code rate, constellation order, number of degrees of freedom and channel model.
    - Proposal of new demapping techniques associated to the different characteristics of the constellations.
    - Validatation of the proposed solutions via demapping complexity analysis and system performance.

The objectives defined in this section aim to provide solutions to increase the spectral efficiency of upcoming DTT broadcasting systems, such as ATSC 3.0. The range of applicability of the solutions provided can be extended to any wireless communication system (satellite, mobile…).

4. THESIS OUTLINE AND CONTRIBUTIONS

This thesis is divided in six chapters. The first chapter introduces the existing challenges in DTT broadcasting systems and establishes the objectives of the work. The publications derived from this thesis are found in Chapter 1, Section 5. Chapters 2, 3, 4 and 5 represent the core parts of this thesis gathering all the contributions. The methodology carried out alongside the work is explained in detail in each of the chapters. Chapter 6 concludes the work developed in this thesis showing the main contributions and presenting future lines of research in the field of efficient modulation and demodulation techniques for the upcoming digital communication systems.

The key contributions of each chapter and the publications derived are presented below:

Chapter 2: Technical Background and Related Work

This chapter presents a survey of the existing constellation types and low complexity demapping design techniques. First, the background of constellation and detection schemes families are studied in order to establish the basis of the state of the art contributions. In the field of constellation design, two main strategies are differenciated, i.e., geometrical and probabilistic shaping approaches. A deep analysis of the existing works is carried out highlighting the main contributions and objectives of each reference. In the field of low complexity demappers, two main cases are distinguished: single and multiple antenna systems. Up to date, the main works in the field of demapping solutions are presented and listed considering their contributions to the field of analysis. Finally, the different approaches of constellations and demapping designs are classified in different use cases, i.e., terrestrial, satellite, optical and broadband systems. This study represents the first comprehensive survey of existing constellation and low complexity demapping design solutions.

Chapter 3: System Performance Analysis of Advanced Modulation Techniques in DTT Broadcast Systems

This chapter evaluates the system performance of NUCs in DTT systems. The evaluation methodology is proposed considering the metrics, cases and tools for the evaluation. Two main contributions are gathered in this chapter. The first part presents the comparison of QAM schemes and NUCs in conjuction with the

LDPC codes proposed in ATSC 3.0. The results show that NUCs outperforms QAM in terms of system performance for AWGN and Rayleigh iid channels.

In the case of RC technique, the analysis is carried out considering Rayleigh and 0 dB Echo showing poor system performance. Even if the RC technique is applied to high code rates and low order constellations, the system performance is poor compared with low code rates and high order constellations with similar throughput and without RC. Publication [C4] and standardization activities [S1], listed in Section 5, are derived from this chapter.

Chapter 4: Design of Advanced Constellations Schemes to Improve BICM System Channel Capacity

This chapter investigates the low complexity design of spectral efficient constellation schemes for BICM systems. Constellation orders from 16 to 4096 points are considered and 1D and 2D geometrically shaping approach is followed. The novel contribution is an algorithm based on simulation optimization via the particle swarm optimization (PSO). If compared to state of the art proposals, the new algorithm provides significant lower design and computational complexity for both AWGN and Rayleigh iid channels. The proposed methodology jointly optimizes the constellation set and bit labeling. A significant contribution is the proposal of a systematic procedure to set up initial conditions of the optimization problem. An additional contribution is the new module that accounts for the specifics to each NUC and SNR value taking the optimization process to the best achievable limit. The last contribution is the design of two different condensation techniques providing very efficient design for massive order (from 1024 constellation points) constellations. Publications [J2] and [C2], [C3], [C5] listed in Section 5, are derived from this chapter.

Chapter 5: Low Complexity Demapping Solutions for NUCs

Chapter 5 contains two different contributions. First, a low complexity demapper for 1D-NUCs is designed. The basis of the demapper is to find the closest constellation points to the received observation via transformation of the non-uniform grid into uniform lattices. This is the first demapper in the literature for massive order 1D-NUCs.

Second, a novel low complexity demapper switching between two different demapping techniques based on condensation and on adaptive sub-region (SCASR) for 2D-NUCs is proposed. The first contribution of this work is the

design of an adaptive sub-region demapper closely suited to the shaping of 2D-NUCs. A metric to appropriately condense 2D-NUCs to provide low demapping complexity with negligible impact on performance represents the second contribution. The proposed demapper outperforms state of the art 2D-NUCs demappers with negligible system performance losses. Publications [J1] and [C1] listed in Section 5, are derived from this chapter.

Chapter 6: Contributions and Future Work

This chapter resumes the different contributions of this dissertation. The contributions derived from each chapter are explained and supported by the results shown in this chapter.

Finally, future research lines aligned with the topics of this thesis are presented considering a follow-up of the work derived from this dissertation. Some of the research lines are:

- The design of massive order 2D-NUCs (from 1024 to higher constellation points) to provide ultra high spectral efficiency to future communication systems.
- Development of advanced modulation techniques based on coding information bits in the injection level of the LDM systems.
- Creation of an advanced LDM profile consisting of non-uniform constellation schemes properly designed for such systems.

5. LIST OF PUBLICATIONS

5.1 Publications and Activities Related to this Thesis

International Journals

[J1] **J. Barrueco**, J. Montalban, P. Angueira, C. Abdel Nour, and C. Douillard, "Low Complexity Adaptive Demapper for Two-Dimensional Non-Uniform Constellations," *IEEE Trans. Broadcast., DOI: 10.1109/TBC.2018.2811619*

[J2] **J. Barrueco**, J. Montalban, C. Regueiro, M. Velez, J.L. Ordiales, H-M. Kim, S-I. Park, and S. Kwon, "Constellation Design for Bit-interleaved Coded Modulation (BICM) Systems in Advanced Broadcast Standards," *IEEE. Trans. Broadcast*., vol. 63, no. 4, pp. 603 – 614, Dec. 2017.

International Conferences

[C1] **J. Barrueco**, J. Montalban, P. Angueira, C. Abdel Nour, and C. Douillard, "Low Complexity Lattice Reduction Demapper for Massive Order One-Dimensional Non-Uniform Constellations," in *Proc. IEEE Int. Symp. Broadband Multimedia Syst. Broadcast. (BMSB)*, Valencia, Spain, Jun. 2018.

[C2] **J. Barrueco**, C. Regueiro, J. Montalban, M. Velez, P. Angueira, H-M. Kim, S-I. Park, and S. Kwon, "Condensation Methodologies for Two-Dimensional Non-Uniform Constellations," in *Proc. IEEE Int. Symp. Broadband Multimedia Syst. Broadcast. (BMSB)*, Cagliary, Italy, Jun. 2017.

[C3] **J. Barrueco**, C. Regueiro, J. Montalban, M. Velez, P. Angueira, H-M. Kim, S-I. Park, and S. Kwon, "Low Complexity and High Order Two-Dimensional Non-Uniform Constellation for High Capacity Broadcasting Systems," in *Proc. IEEE Int. Symp. Broadband Multimedia Syst. Broadcast. (BMSB)*, Nara, Japan, Jun. 2016.

[C4] **J. Barrueco**, C. Regueiro, J. Montalban, M. Velez, P. Angueira, H-M. Kim, S-I. Park, and J-Y. Lee, "Combining Advanced Constellations and SSD Techniques for Optimal BICM Capacity," in *Proc. IEEE Int. Symp. Broadband Multimedia Syst. Broadcast. (BMSB)*, Ghent, Belgium, Jun. 2015.

National Conferences

[C5] **J. Barrueco**, P. Angueira, and J.L. Ordiales, "Técnicas de Radiodifusión Avanzadas para Sistemas LDM," in *Jornadas Doctorales de la Universidad de Murcia*,

Murcia, Spain, Apr. 2015.

International Research Visits

[V1] Telecom Bretagne. Brest (France). September – November 2016 (3 months).

Standardization Activities

[S1] 9 contributions to the TG3/S32-2 Ad-hoc group on Modulation and Coding in the standardization process of ATSC 3.0:

- Rotation gain trend on NUC
- I/Q interleaving gain on NUC
- RC performance in BICM and OFDM chains and a preliminary ModCod reduction analysis
- RC gain on NUC over Rayleigh P1 and 0 dB echo channels
- Crosscheck of BICM system performance
- Test platform for V&V process
- ATSC 3.0 compliant BICM system
- ATSC 3.0 compliant OFDM system
- ATSC 3.0 Recommended Practice for the demapper

International Research Projects

[P1] Advanced Constellation Design for Future Broadcast and Wireless Broadband Communications

- Funding institution: Electronics and Telecommunications Research Institute Korea ETRI, South Korea.
- Start date: June 2016
- Duration: 7 months

[P2] Advanced Constellation Schemes for Layered Division Multiplexing System

- Funding institution: Electronics and Telecommunications Research Institute Korea ETRI, South Korea.

- Start date: June 2015
- Duration: 7 months

[P3] Advanced Constellation Schemes for Terrestrial Broadcast Systems

- Funding institution: Electronics and Telecommunications Research Institute Korea ETRI, South Korea.
- Start date: June 2014
- Duration: 7 months

National Research Projects

[P4] New Broadcast Technologies for a 5G Ecosystem (5G-newBROS) (TEC2015-66153)

- Funding institution: Ministry of Economy and Competitiveness. Applied R&D&I Program, Spanish Government.
- Start date: January 2016
- Duration: 36 months

[P5] High Efficiency Dynamic Technologies for Future Green Broadband-Broadcast Multimedia Systems (HEDYT GGB)

- Funding institution: Ministry of Economy and Competitiveness. Applied R&D&I Program, Spanish Government.
- Start date: January 2013
- Duration: 36 months

5.2 **Other Publications**

Apart from the publications directly related with this thesis, there are some publications that I have carried out during the realization of the dissemation.

International Journals

[J4] C. Regueiro, **J. Barrueco**, J. Montalban, P. Angueira, J.L. Ordiales, and M. Velez, "LLR Reliability Improvement for Multilayer Signals," *IEEE. Trans. Broadcast.*, vol. 63, no. 1, pp.

[J5] C. Regueiro, J. Montalban, **J. Barrueco**, M. Velez, P. Angueira, Y. Wu, L. Zhang, S-I. Park, J-Y. Lee, and H-M. Kim, "LDM Core Services: Indoor and Mobile Performance in ATSC 3.0," *IEEE. Trans. Broadcast.*, vol. 62, no. 1, pp.

International Conferences

[C5] J. Montalban, **J. Barrueco**, C. Regueiro, M. Velez, P. Angueira, and J.L. Ordiales, "New Transmitter Identification Mechanism for DVB-T2," in *Proc. IEEE Int. Symp. Broadband Multimedia Syst. Broadcast. (BMSB)*, Cagliary, Italy, Jun. 2017.

[C6] C. Regueiro, **J. Barrueco**, J. Montalban, I. Eizmendi, and M. Velez, "Improving LDPC Decoding Performance for ATSC 3.0 LDM Profiles," in *Proc. IEEE Int. Symp. Broadband Multimedia Syst. Broadcast. (BMSB)*, Cagliary, Italy, Jun. 2017.

[C7] C. Regueiro, **J. Barrueco**, J. Montalban, I. Sobron, I. Eizmendi, and M. Velez, "Performance Evaluation of Different Doppler Noise Estimation Methods," in *Proc. IEEE Int. Symp. Advances in Wireless and Optical Communications. (RTUWO)*, Riga, Latvia, Nov. 2016.

[C8] J. Montalban, **J. Barrueco**, P. Angueira, L. Zhang, Y. Wu, W. Li, H-M. Kim, S-I. Park, and J-Y. Lee , "Asynchronous N-Layered Division Multiplexing (N-LDM)," in *Proc. IEEE Int. Symp. Broadband Multimedia Syst. Broadcast. (BMSB)*, Nara, Japan, Jun. 2016.

[C9] C. Regueiro, **J. Barrueco**, J. Montalban, I. Eizmendi, and M. Velez, "ATSC 3.0 Interleavers Influence in Reception Performance," in *Proc. IEEE Int. Symp. Broadband Multimedia Syst. Broadcast. (BMSB)*, Nara, Japan, Jun. 2016.

[C10] J. Montalban, **J. Barrueco**, I. Angulo, L. Zhang, Y. Wu, W. Li, H-M. Kim, S-I. Park, and J-Y. Lee , "Peak-toAverage Power Ratio Analysis to LDM Signals," in *Proc. IEEE Int. Symp. Broadband Multimedia Syst. Broadcast. (BMSB)*, Ghent, Belgium, Jun. 2015.

[C11] C. Regueiro, **J. Barrueco**, J. Montalban, U. Gil, I. Angulo, I. Eizmendi, P.

Angueira, and M. Velez, "SVC and LDM Techniques for HD/UHD TV Indoor Reception," in *Proc. IEEE Int. Symp. Broadband Multimedia Syst. Broadcast. (BMSB)*, Ghent, Belgium, Jun. 2015.

CHAPTER 2: **TECHNICAL BACKGROUND AND RELATED WORK**

This chapter introduces the technical background and discusses the state-of-the-art related to the research carried out in this thesis. The chapter overviews the existing background technologies, which are fundamental for the development of advanced constellations and detection schemes for DTT systems. Meaningful research works in the fields of interest of this thesis are analyzed and compared in detail. First, the basis of the communication system models and the design of constellations schemes are detailed. Next, fundamentals on digital data detection are further described and their applications are presented. Finally, a short summary of the chapter is included.

1. SYSTEM MODELS

1.1 Overview

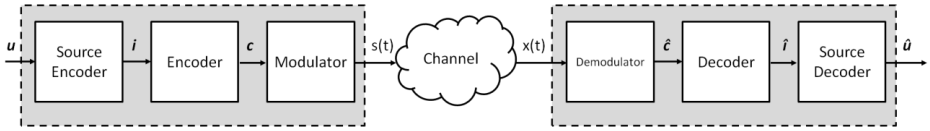

Figure 2.1. Basic transmitter/receiver system model.

One of the major challenges in communication systems engineering is to ensure reliable transmission of digital information through a noisy channel. We are considering the basic transmitter/receiver communication system shown in Figure 2.1. The first works related with this field are found in [31], [32] and [33] made by H. Nyquist and R. V. L. Hartley. However, it was not until the years 1948 and 1949 when C. E. Shannon introduced a unified mathematical theory of communication [29], [30]. In 1949 Shannon established the upper bound of a communication system for error free reception under AWGN channel. Since then, many experts have put their efforts in getting close to that limit to design the most efficient communication system. Indeed, in the power-limited regime (low SNR) where a binary signal, i.e., M=2 with a binary channel encoder is used, there are already two coding techniques that approach to the upper bound: the turbo codes defined in [35] by Berrou *et al.* in 1993 and the LDPC codes proposed by Gallager in 1962 [36] and reinforced by MacKay and Neal in 1997 [34]. Both alternatives have been included in commercial communication systems such as LTE (Turbo codes) and DVB-T2 (LDPC) and several studies have demonstrated their capacity to approach closely the Shannon's limit in the low SNR region [37]. The maximum channel capacity for the power-limited regime is bounded by one bit per symbol.

When the channel conditions are good enough, more than one bit per symbol can be transmitted in the bandwidth-limited regime (high SNR). The transmitted signal is comprised of more than two constellation symbols and the goal is to find the most efficient way to transmit the information bits. The most widely solution is the Coded-Modulation (CM) scheme in which the channel encoder is directly connected to the modulator, associating several bits to one constellation symbol. The main problem is the construction of a CM system that operates close to the Shannon's limit with a reasonable complexity.

For the bandwidth-limited regime, several proposals have been published during the last years in order to construct efficient CM systems. Trellis Coded Modulation (TCM) was the first popular CM scheme described by Ungerboeck in [38] and [39]. Next, Multi-Level Coding (MLC) was proposed in [40] by Imai and Hirakawa. Both systems aim at providing good system performance under AWGN noise scenarios maximizing the Euclidean distance (ED). However, these schemes cannot cope appropriately with fading channels. Indeed, this fact represents a major problem in current communication systems. The key aspect to improve the system performance in fading channels is to provide code diversity. As a solution, in 1992 Zehavi [41] introduced the so-called Bit-Interleaved Coded Modulation (BICM) system, which makes the encoder and the modulator independent blocks introducing a bit interleaver between them. Although the ED measure of BICM decreases with respect to TCM and MLC, the code diversity is increased providing better system performance under fading conditions. Next sub-sections contain the description of the main existing system models in digital communication systems.

1.2 **Trellis Coded Modulation (TCM)**

Ungerboeck proposed in 1982 TCM with set partitioning. This technique is based on successive partitioning of the expanded *M*-ary signal set into subsets with increasing minimum Euclidean distance.

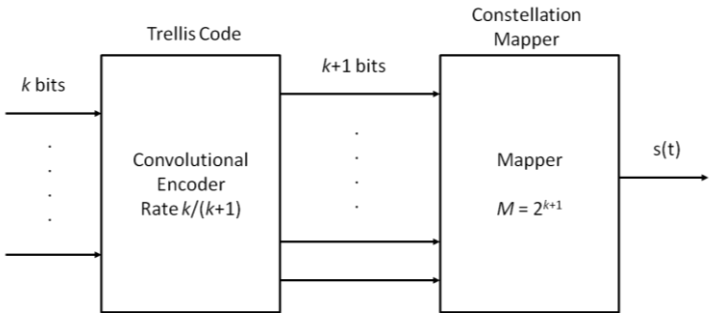

Figure 2.2. Trellis Coded Modulation scheme.

TCM is a combination of coding and modulation. The word Trellis stands for the use of Trellis/Convolutional codes. Due to the combined structure of the coding and modulation, a code with optimum performance independently may not be optimum in TCM. Figure 2.2 shows the functions of a general TCM system where a convolutional coder of rate $R=k/k+1$ is combined with an *M*-ary signal.

The Trellis coder outputs $M=2k$ points and the constellation mapper converts them into $M=2^{k+1}$ constellation points.

The use of convolutional coding allows TCM to be a bandwidth efficient modulation. The reduction of EDs provided by the increase of the constellation size is compensated by sequence coding gain, which constrains the allowed symbol transitions. The detection is accomplished via Viterbi algorithm [42].

1.3 **Multi-Level Coding (MLC)**

The main idea of Imea's MLC is to protect each bit of the signal point with an individual binary code using m parallel encoders connected to one of the m bit positions of the mapper. In contrast to Ungerböck's TCM, MLC provides flexible transmission rates and block codes. The system block of MLC is shown in Figure 2.3.

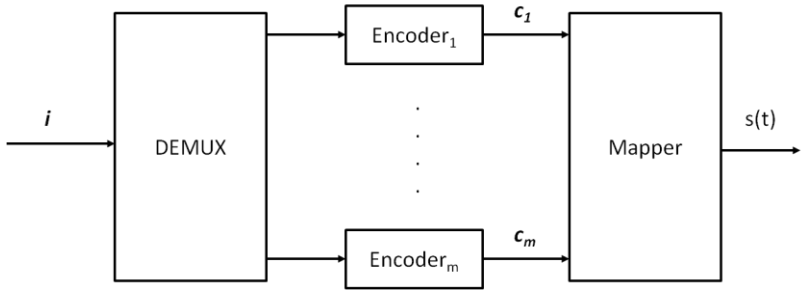

Figure 2.3. Multi-Level Coding scheme.

On the decoder side, there are two main decoding strategies for MLC: Multi-Stage Decoding (MSD) [43] and Parallel Decoding of the individual Levels (PDL). Regarding MLC schemes for fading channels, a solution was proposed in [44]. In [45], MLC with capacity-approaching turbo codes was considered.

1.4 **Bit-Interleaved Coded Modulation (BICM)**

BICM was firstly proposed by Zehavi in 1992 as a way to approach system capacity limits for fading channels. Zehavi proved that coded modulation performance can be improved over a Rayleigh fading channel by providing coding diversity using a bit interleaver between the encoder and modulator blocks. Later, in 1998 Caire *et al.* [46] provided the necessary mathematical tools in order to

evaluate the design of the BICM structure. The BICM scheme is shown in Figure 2.4.

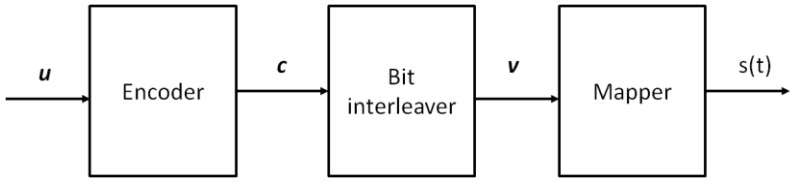

Figure 2.4. Bit-Interleaved Coded Modulation scheme.

The purpose of the bit interleaver is to disperse the burst errors and maximize the diversity order of the system and to decorrelate the bits associated with the given transmitted symbol. As Caire stated, the combination of binary encoding, bit-wise interleaving and *M*-ary modulation yields better performance in fading channels than symbol-wise interleaving and TCM. One of the key components of a BICM system is the bit labelling. In [47], the optimal alphabets and binary labelings for BICM at low SNR were proposed. The classical BICM decoder makes use of the Maximum A Posteriori (MAP) metric, which will be discussed in Section 4.4.

An update of the classical BICM is made in Iterative Decoding BICM (BICM-ID) where iterative decoding is performed. In [48], authors demonstrated that iterative decoding increases the minimum ED of BICM, providing good performance for AWGN and fading channels. The design of BICM-ID for fading channels is studied taking into account the diversity order and ED criteria.

In conclusion, as shown in [49] for AWGN channels and a given complexity TCM outperforms BICM. In the case of uncorrelated narrowband Rayleigh fading channels, BICM provides better performance. If iterative decoding is taken into account, BICM-ID shows superior performance than the others CM schemes studied for AWGN and uncorrelated narrowband Rayleigh channels. However, in real time systems where the latency is a key aspect, iterative decoding schemes are not appropriate.

2. BASIC CONSTELLATION SCHEMES

2.1 Overview

In the context of constellation and modulation schemes, there are five main classes of modulations used in digital data transmission: cubic, orthogonal, circular, rectangular and hexagonal [50]. These classes provide different geometric approaches in order to construct different constellation schemes depending on the basis functions $\varphi(t)$. The set of basis functions must fulfil two main requirements: each basis function must be orthogonal to all others and must be normalized. Cubic constellations are commonly used for simple data communications and in OFDM systems for channel estimation. They provide robustness against noise and channel impairments at the cost of low channel capacity. Orthogonal signal sets are not widely used as they provide low spectral efficiency. They are used for communication systems such as amateur radio, caller ID and emergency broadcasts. Cubic and circular constellations are commonly used in satellite communications as they provide low Peak-to-Average Power Ratio (PAPR) [51]. Rectangular signal constellations are widely used in broadcast, broadband systems and terrestrial wireless links. They offer a good trade-off between system capacity and robustness. Hexagonal constellations are used in Spatial Modulation (SM) [53]. They reduce the PAPR in OFDM systems and have comparable bandwidth efficiency and minimum Euclidean distance with respect to QAM constellations.

The number of basis functions used to transmit the constellation symbols is defined by N. Therefore, depending on the value of N an N-dimensional signal constellation can be constructed. Figure 2.5 shows a classification of the different constellation topologies and different types of constellation schemes for each topology.

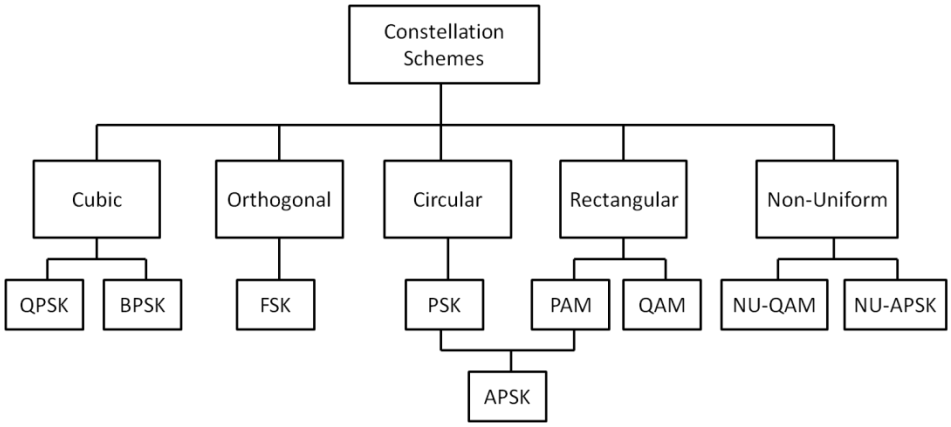

Figure 2.5. Diagram of basic constellations schemes.

Next, the basic constellation schemes commonly used in digital communication systems are explained.

2.2 Cubic Constellations

Cubic constellation refers to a direct mapping of a sequence of $N = b$ bits into the components of the basis vectors in a corresponding N-dimensional signal constellation, where b is the number of bits per constellation symbol. The next sub-sections show different types of well-known cubic constellations.

2.2.1 Binary Phase Shift Keying (BPSK)

BPSK constellation is composed by one basis function (sinusoid) which modulates the sequence of data symbols.

$$\varphi_1(t) = \begin{cases} \sqrt{\frac{2}{T}} \sin \frac{2\pi t}{T} & 0 \le t \le T \\ 0 & \text{elsewhere} \end{cases} \tag{2.1}$$

Where T is the symbol period. BPSK is composed by two constellation points, each one carrying one bit, with a separation of 180 degrees in the constellation diagram. It is the most robust modulation technique and its main applications are long distance wireless communications data channels, e.g., CDMA, WiMAX, WLAN, DVB-S2, DVB-T2, etc.

2.2.2 Quadrature Phase Shift Keying (QPSK)

In contrast to BPSK, QPSK constellations make use of two orthogonal basis functions in order to carry two bits per symbol with the same amplitude and with phase shifts of multiples of 90 degrees.

$$\varphi_1(t) = \begin{cases} \sqrt{\frac{2}{T}}\cos\frac{2\pi t}{T} & 0 \le t \le T \\ 0 & \text{elsewhere} \end{cases} \tag{2.2}$$

$$\varphi_2(t) = \begin{cases} \sqrt{\frac{2}{T}}\sin\frac{2\pi t}{T} & 0 \le t \le T \\ 0 & \text{elsewhere} \end{cases} \tag{2.3}$$

The linear combination of both basis functions with their respective carrier amplitudes composes the transmitted signal. QPSK is used in several space communication systems [52], satellite, broadband and broadcast wireless standards such as DVB-S2, LTE, DVB-T2 and ATSC 3.0. It is less robust than BPSK but doubles the system data rate.

2.3 Orthogonal Constellations

The main characteristic of orthogonal constellations is that the number of basis functions increases linearly with the number of constellation symbols. Therefore, the number of bits per dimension is lower than for cubic constellations. One of the most well known orthogonal constellations is the Frequency Shift Keying (FSK).

2.3.1 Frequency Shift Keying (FSK)

In Frequency Modulation (FM), the information bits are encoded into the frequency component of the transmitted signal. Therefore, the transmitted signal has a constant envelope which enables the use of non-linear amplifiers and the modulated signal sensitivity to channel or hardware amplitude distortion is lowered. However, the spectral bandwidth occupied is higher than amplitude and phase modulation. Only one basis function per symbol period is transmitted. FSK uses two basis functions:

$$\varphi_1(t) = \begin{cases} \sqrt{\frac{2}{T}} \sin \frac{\pi t}{T} & 0 \le t \le T \\ 0 & \text{elsewhere} \end{cases} \tag{2.4}$$

$$\varphi_2(t) = \begin{cases} \sqrt{\frac{2}{T}} \sin \frac{2\pi t}{T} & 0 \le t \le T \\ 0 & \text{elsewhere} \end{cases} \tag{2.5}$$

The information bits are transmitted in two different frequencies, $1/(2T)$ and $1/T$. FSK can be extended if the number of basis functions N is increased at the cost of linear bandwidth growing with N.

2.4 Circular Constellations

The main characteristic of circular constellations is equal phase spacing of symbols while the amplitude is constant and identical. This sort of constellation is called Phase Shift Keying (PSK) and the information bits are conveyed in the phase of the transmitted signal. Two-dimensional signal space is needed for the transmitted signal, identical to the QPSK case. The basis functions are the same as for QPSK. Although any number of phases can be used, 8PSK (8 angles) is usually the highest order used. The error-rate for higher order constellations is considerably increased with respect to other types, e.g., QAM.

Satellite communication systems such as DVB-S2 make use of QPSK and 8PSK constellations due to their low PAPR. While PSK is less susceptible to errors than PAM/ASK occupying the same bandwidth and higher data rate than FSK is possible. Nevertheless, the signal detection and recovery process are more complex.

2.5 Rectangular Constellations

Rectangular constellations are characterized by the equally spaced constellation symbols, independently of the dimensionality of the signal space. Two main types of rectangular constellations exist depending of the number of basis functions. For one dimensional signal constellation, pulse amplitude modulation (PAM) is the most popular scheme while for two-dimensional signal constellation, quadrature amplitude modulation (QAM) is widely known.

2.5.1 Pulse Amplitude Modulation (PAM)

The simplest form of linear modulation is the PAM, which is a one-dimensional constellation scheme with a constellation order of $M = 2b$. No quadrature component is found in this sort of constellation and the information bits are transmitted in the signal amplitude component. The transmitted signal is made of one basis function with unit-energy which often is

$$\varphi_1(t) = \frac{1}{\sqrt{T}} \operatorname{sinc}\left(\frac{t}{T}\right) \tag{2.6}$$

The main advantage of PAM is the simple receiver and transmitter schemes. PAM is not a practical standalone modulation but a powerful scheme that enables the construction of the most commonly used constellations such as QAM.

2.5.2 Quadrature Amplitude Modulation (QAM)

The construction of the QAM constellation comes from the two-dimensional generalization of the PAM. The main difference with respect to PAM is that QAM provides two degrees of freedom to encode the information bits, i.e., amplitude and phase components of the transmitted signal. In order to transmit the information bits, two orthonormal basis functions are used in the same symbol period

$$\varphi_1(t) = \frac{1}{\sqrt{T}} \operatorname{sinc}\left(\frac{t}{T}\right) \cos 2\pi f_c t \tag{2.7}$$

$$\varphi_2(t) = \frac{1}{\sqrt{T}} \operatorname{sinc}\left(\frac{t}{T}\right) \sin 2\pi f_c t \tag{2.8}$$

Where f_c is the carrier frequency. QAM is widely used in current communication systems such as LTE and DVB-T2 as it is more spectrally efficient than PAM and PSK constellations with low transmitting and receiving complexity. One of the main advantages of QAM constellations is their low demapping complexity, exploiting the characteristics of the PAM.

2.6 Combination of Circular and Rectangular Constellations

The combination of the PSK and PAM schemes allows the construction of Amplitude Phase Shift Keying (APSK) constellations. APSK is composed of several concentric circles of different radius. The constellation symbols are placed

in different circles with equally spaced angles. The basis functions are identical to the QAM case.

APSK constellations are commonly used in satellite communication systems, providing higher spectral-efficiency than QAM with low PAPR. In the receiver, the system complexity is increased with respect to QAM as a two-dimensional demapper is needed.

2.7 Geometrically Shaped Non-Uniform Constellations

Constellations with non-uniformly spaced and equiprobable points are known as geometrically shaped constellations. The construction of these signal sets is based on several metrics depending on the objective of the communication systems, i.e., maximization of channel capacity, minimization of bit error probability, robustness against a determined type of fading channel, etc.

Based on the restrictions applied to the constellation shape (namely Degrees of Freedom - DoF), different schemes can be designed. The most widely known are the Non-Uniform APSK (NU-APSK) and Non-Uniform QAM (NU-QAM). In NU-APSK, the constellation points are non-uniformly spaced across circles of different radius. This solution provides higher spectral efficiency than APSK with no PAPR increase. For NU-QAM, there are two main types of schemes depending on the number of DoF: One-Dimensional NU-QAM (1D-NU-QAM) and Two-Dimensional NU-QAM (2D-NU-QAM). 1D-NU-QAM is equivalent to two non-uniform PAM signals. 1D-NU-QAM are characterized by their square shape and their design is limited by the possible DoF of each constellation point of each of the PAM signals. The advantage of 1D-NU-QAM is their higher gain if compared with uniform QAM constellations and the negligible demapping complexity increase.

On the other hand, in 2D-NU-QAM all the constellation points have full freedom of mobility at the optimization stage and they are circularly shaped for low and mid SNR ranges. Besides, they present more gain than 1D-NU-QAM at the cost of complexity at the demapping (stage since a two dimensional demapper is needed).

2.8 **Hexagonal Constellations**

Hexagonal constellation is a type of irregular constellations where the number of constellation symbols is not a power of 2 of the number of information bits. Another type of irregular constellations is the non-square QAM constellation shown in [54]. The main characteristic of hexagonal constellations is the hexagonal lattice at which each constellation symbol is placed. In two-dimensional signal sets, the hexagonal scheme is the densest packing of regularly spaced points, providing low PAPR with comparable bandwidth efficiency and minimum ED to QAM [55]. However, the encoder and detector for hexagonal lattice constellations and the assignment of binary information are more complex than the ones used in QAM. The number of constellation points is not a power of two and this fact increases the system implementation complexity.

2.9 **Key Characteristics**

For illustration purposes this sub-section shows the different system models included in the existing DTT broadcast systems. The BICM system model has been included in the latest designed DTT broadcast standards, i.e., DVB-T2 and ATSC 3.0 which include a bit interleaver. QPSK and QAM constellation schemes are mainly used in these standards. FEC encoder based on LDPC coding is used in ATSC 3.0, DTMB and DVB-T2 systems whereas previous systems make use of convolutional (DVB-T and ISDB-T) and Trellis coding (ATSC 1.0).

Table 2.1 gathers the different system models and techniques defined for the existing DTT standards.

Table 2.1. Comparison of different DTT standards

Characteristics	ATSC 1.0	ATSC 3.0	DTMB	DVB-T, DVB-H	DVB-T2	ISDB-T
Outer FEC	RS and concatenated RS	BCH, CRC or none	BCH	RS	BCH	RS
Inner FEC	Trellis	LDPC	LDPC	Conv. code	LDPC	Conv. code
Inner interleaving	Independent encoded stream interleaved in time	Cell, time and frequency	Freq.	Bit and symbol	Cell, time and freq.	Frequency and time interleaving
Outer interleaving	Byte-wise conv. interleaver	Parity, group-wise and block interleaver	Conv. interleav.	Byte-wise conv. interleaver	Bit (parity and column twist)	Byte-wise conv. interleaver
Constellation	8-VSB	QPSK 2D-16QAM 2D-64QAM 2D-256QAM 1D-1024QAM 1D-4096QAM	4QAM-NR 4QAM 16QAM 32QAM 64QAM	QPSK 16QAM 64QAM MR-16QAM MR-64QAM	QPSK 16QAM 64QAM 256QAM	DQPSK QPSK 16QAM 64QAM

3. CONSTELLATION DESIGN METHODOLOGIES

During the last decades, an intense effort has been carried out in order to design the most efficient constellation schemes with high spectral efficiency in terms of bit/s/Hz for a wide variety of SNR values. This section analyzes the state of art in terms of constellation design methodologies.

There are two main families of constellation design techniques: 1) constellation design based on the geometrical shaping (GS) variation of the constellation scheme and 2) constellation design with probabilistic shaping (PS) of the constellation points. Finally, additional approaches to constellation design, based on other criteria are shown.

3.1 Geometrical Shaping (GS)

The case of non-uniformly spaced and equiprobable symbols is known as Geometrical Shaping constellation. The probability of transmitting one constellation symbol is $\frac{1}{M}$, where M is the number of total constellation points. The constellation points are non-uniformly distributed alongside the diagram. This structure allows modifying different parameters of a communication system such as the Bit Error Rate (BER) or channel capacity.

Constellation design based on geometrical shaping uses two criteria: minimization of the error probability and maximization of the channel capacity. In [56] and [65] an error probability metric is considered to design efficient constellation schemes. Works in [57], [59], [61], [62] and [66] focus on maximizing the channel capacity of different system models in order to approach Shannon's limit. They make use of the same solution to increase the channel capacity, i.e., approximate the probability density function (pdf) of the transmitted signal to a Gaussian one. As Shannon stated in his seminal work, the highest capacity for an AWGN channel is obtained when the transmitted signal presents a Gaussian distribution. In the case of non-Gaussian noise scenarios, such as phase noise or iid noise process and independent of the symbol being transmitted, works in [66] and [60] present a solution for each case, respectively. In [65], authors design constellations via GS using several cost functions: minimum symbol error rate, BICM capacity, signal set capacity and exploitation of perfect a priori information. The studies presented in [63], [64] evaluate theoretically the feasibility of such designs in terms of system capacity gain and compares GS with PS.

Finally, the authors in [58] prove that for low SNRs, the warping technique provides efficient constellation schemes in terms of channel capacity. For high SNR values, the authors conclude that uniformly spaced constellations are recommended. The following paragraphs describe in detail the works referenced above.

Foschini et al. (1974) [56] study the GS approach to design constellation schemes with $M > 2$ to minimize the probability of error in Gaussian noise under an average power constraint. The authors derive an asymptotic expression of the minimum distance for large SNR to calculate the error rate. With this expression, they design locally optimum constellations using a gradient-search procedure. The initial conditions are chosen from several random *M*-point arrays. The gradient-search algorithm is tested for $M = 4$, 7, 8, 16 and 19 for a single value of SNR associated to an error rate of approximately 10^{-6}. The results show that the gain of the optimization is negligible for $M = 8$. However, for $M = 16$ there is 0.5 dB power saving over 16-QAM. In conclusion, for the GS approach there is a minimum value of $M = 8$ in order to obtain power saving with respect to standard QAM schemes.

Sun et al. (1993) [57] propose to approach channel capacity via equiprobable signalling and GS imposing signal points to have a Gaussian probability distribution. The authors in this work demonstrate theoretically that equiprobable signaling in low dimension space achieves channel capacity for the memoryless Gaussian channel. It is also shown that the designed signal set is related to the input power, i.e., different signal sets should be used depending of the SNR value. Furthermore, the coding scheme should be taken into account. However, the main drawback of this work is that the proposed signal sets have a very high PAPR value.

Betts et al. (1994) [58] show that if the constellation points near the perimeter are spaced further apart than points close to the center (warping technique), then the Gaussian noise immunity of the perimeter points increases. For communication systems that use pulse code modulation the noise immunity is of special interest for points near the constellation perimeter as they are more coarsely quantized. However, the warping technique reduces the immunity to Gaussian noise for low values of Gaussian noise as points near the center are closer together than in a uniformly spaced constellation with the same average power, e.g., QAM constellation. The main conclusion of this work is that for low SNR values, warping technique is appropriate for approaching channel capacity while for high SNR values, uniformly spaced constellation points should be considered.

Sommer et al. (2000) [59] designed equiprobable non-uniformly spaced ASK constellations for AWGN channels. Besides, the design of the constellations is considered for the BICM system model. The objective is that the designed ASK constellations should have an approximately Gaussian distribution in order to reduce the existing gap to the Shannon's limit. Parallel decoding capacity is considered (each bit-level is considered separately) in order to reduce the designing complexity. It is shown that the use of Non-Uniform ASK (NU-ASK) provides higher capacity gains than uniform ASK for high order modulation schemes for BICM systems. However, the shaping gain with the method proposed in this work is lower than other proposed shaping methods and, for higher order modulation schemes the ultimate gain of 1.53 dB is not achieved. The main advantage of the work is the simplicity of the method proposed.

Kearsley (2001) [60] proposes different global and local optimization algorithms for optimal signal set design under non-Gaussian noise. The author studies the optimization problem considering that the noise process is iid and independent of the symbol being transmitted. In the field of local algorithms, the Sequencial Quadratic Programming (SQP) is considered because a feasible solution always exists and the objective function may be used directly as a merit function. For the global solution, the stochastic approach based on Multi-Level Single Linkage (MLSL) algorithm is used as it is a smart way of generating initial points for the local algorithm. The results show that the methodology proposed in this work can overcome the performance of the standard SQP method.

Fragouli et al. (2001) [61] use non-uniform constellations to achieve shaping gain for parallel concatenated turbo codes. The approach considered is to approximate the output signal to a Gaussian distribution. However, as the points near the center are closely spaced there is a high error floor for turbo codes. The authors design a two-step process to avoid this situation. First, a semi-random interleaver is used in order to lower the error floor. Then, they select the encoder that leads to a higher overall free distance with the selected interleaver. The simulation results show that for 4 bit/s/Hz the designed non-uniform 64QAM via GS offers an improvement of 0.2 dB if turbo codes are used with respect to the 64QAM under Gaussian noise.

Zesong et al. (2003) [62] consider GS design for Binary Turbo Coded Modulation (BTCM). The authors propose to modify the criteria considered in previous works. The output signal does not follow a Gaussian distribution. In Turbo decoding the information bits are usually more important than the parity bits for decoding BER performance. Therefore, the authors divide the output

coded bits into at least two sub-flows. Based on this consideration, the mapping rule is optimized and gains from 0.5 to 1 dB are achieved for high order modulations and low and middle SNR values.

Barsoum et al. (2007) [63] and [64] discuss the constellation design via capacity maximization and compared the GS and PS design. The authors design non-uniformly spaced constellations taking into account the joint and parallel decoding capacities for Gaussian noise. Non-uniform PAM and PSK constellation schemes are obtained and their system performance is analyzed using LDPC codes. The results show that for 32-PAM, the non-uniform 32-PAM provides 1.2 dB performance gain if compared with conventional uniform 32-PAM. Furthermore, the results show that performance does not considerably improve if iterative decoding is considered. The most important outcome of the work is that they prove theoretically that any gain in capacity that can be achieved by PS can be also achieved or exceeded by equiprobable and non-uniformly spaced signaling, i.e., GS.

Muhammad (2010) [65] proposes different constellation schemes using GS with different metrics and system models. The author considers cost functions such as optimization for minimum symbol error rate, maximum BICM capacity, maximum signal set capacity and maximum exploitation of perfect a priori information. Constellations up to 32 points are designed with respect to both bit labelling and symbol constellation showing that gains in the order of several tenths of a dB are achievable.

Kayhan et al. (2014) [66] optimize the constellation sets considering that the communication system is affected by phase noise. The authors focus on maximizing the channel mutual information via GS for 8, 16, 64 and 256 constellation points. The channel model is a complex AWGN channel with phase jitter and simulated annealing algorithm is used for jointly optimizing the signal and labelling of the constellation points. The authors also propose a computationally efficient approximation of the Average Mutual Information (AMI) and Pragmatic Average Mutual Information (PAMI) for channels with memoryless thermal and phase noises. The results conclude that if the constellation optimization is focused on AWGN channels then the signal sets are very sensitive to phase noise. The system performance showed that AMI and PAMI are the most adequate objective functions to design constellations in systems that make use of capacity-approaching codes.

Table 2.2. State-of-the-art of GS constellations

Authors	Title	Year	Design Target	Contribution
[56] Foschini et al.	Optimization of Two-Dimensional Signal-Constellations in the Presence of Gaussian Noise	1974	Minimize the error probability in Gaussian noise	GS to minimize error probability with 0.5 dB of power saving for M=16
[57] Sun et al.	Approaching Capacity by Equiprobable Signaling on the Gaussian Channel	1993	Maximize channel capacity in AWGN	GS achieves channel capacity in low dimension space
[58] Betts et al.	Performance of Nonuniform Constellations on the Gaussian Channel	1994	Geometrical characteristics of constellation schemes for low and high SNR	GS with warping technique approaches channel capacity at low SNR values
[59] Sommer et al.	Signal Shaping by Non-Uniform QAM for AWGN Channels and Applications Using Turbo Coding	2000	Maximize channel capacity in BICM systems	GS NU-ASK provides higher capacity than ASK for high order constellation in BICM systems
[60] Kearsley et al.	Global and Local Optimization Algorithms for Optimal Signal Set Design	2001	Constellation design for non-Gaussian noise	Improved optimization methodology to design GS constellations
[61] Fragouli et al.	Turbo Codes with Non-Uniform Constellations	2001	Constellation design for parallel concatenated turbo coded	GS to achieve shaping gain for parallel concatenated turbo codes
[62] Zesong et al.	Shaping Gain by Non-Uniform QAM Constellation with Binary Turbo Coded Modulation	2003	Constellation design for BTCM	GS design for binary turbo coded modulation (BTCM)
[63] and [64] Barsoum et al.	Constellation Design via Capacity Maximization / On Constellation Design and Iterative Codes	2007	Comparison of GS and PS	GS can achieve or exceed any capacity gain than can be achieved by PS
[65] Muhammad	Coding and Modulation for Spectral Efficient Transmission	2010	Constellation design via several cost functions	Different metrics to design constellations via GS
[66] Kayhan et al.	Constellation Design for Memoryless Phase Noise Channels	2014	Maximize channel capacity in phase noise systems	GS constellations for communication systems affected by phase noise

3.2 **Probabilistic Shaping (PS)**

Probabilistic shaping imposes a non-equiprobable distribution of the constellation points while maintaining the set of constellation points equidistant. There are two different approaches: 1) perform the shaping operation after encoding which usually requires iterative processing in the receiver, 2) concatenate encoding and shaping in the same operation, simplifying the receiver scheme.

For constellation design via probabilistic shaping, there are five main design criteria.

1) Authors in [68] propose to approximate the distribution of the constellation points to have a Gaussian pdf via non-uniform distribution. However, this solution presents problems of buffering delays.
2) Sub-constellation selection is presented in [69] jointly with shaping codes to reduce the PAPR of the system.
3) Authors in [70] introduce prefix codes applied to non-equiprobable constellation schemes.
4) Mapping of equiprobable input words into non-equiprobable bits of the constellation scheme via Look-Up-Table (LUT) is considered in [71], [72].
5) Authors in [78] present Probabilistic Amplitude Shaping (PAS) in order to increase the spectral efficiency.

For BICM-ID systems, works in [73] and [76] make use of shaping coding. In the case of BTCM systems, criterion 4) is used in [71], [72]. Finally, if a bit interleaver is added to BTCM system model, i.e., BITCM criterion 2) is considered in [74] and [77]. The following paragraphs describe in detail the works referenced above.

Forney et al. (1984) [68] introduce the non-uniform distribution to constellation points in order to have a Gaussian probability distribution. Although the gains achieved for uncoded schemes in higher dimensions or source coding with non-uniform probabilities of the signal points are more than 1 dB, the authors foresee some practical problems. One way to achieve potential gain is to divide the input data bits into words of non-uniform length and map the words into signal points. However, this solution requires that the number of data bits transmitted per unit time is a random variable which leads to implementation problems such as buffering delays.

Calderbank et al. (1990) [69] propose a technique based on probabilistic shaping in order to approach the full asymptotic gain of *N*-sphere over *N*-cube in the limit $N \to \infty$. The signal constellation is divided into different subconstellations of equal size. The points inside each subconstellation are of equal probability. The selection of the subconstellation is carried out at a determined frequency using a shaping code. The designed scheme is compared with equiprobable signalling schemes of multidimensional lattices based on Voronoi regions [67]. The results show that superior PAPR is achieved with the non-equiprobable scheme.

Kschischang et al. (1993) [70] study prefix codes in order to approach the optimal performance of non-equiprobable constellation schemes. The shaping schemes designed by the authors approximate to the ultimate shaping gain performance given by the Maxwell-Boltzman probabilities applied to the constellation points. Huffman procedure is proposed to design prefix codes approaching the optimal performance. Two different channels are provided by these schemes: 1) fixed-rate primary channel, and 2) variable-rate secondary channel. As pointed out in previous works, the main drawback is the variable bit rate which limits the broad applicability of non-uniform signaling.

Raphaeli et al. (2002) [71] and (2004) [72] show how to create non-uniform constellation sets in the pragmatic binary turbo coded modulation system. Their proposal makes use of a table that maps equiprobable input words into non-equiprobable bits of an *M*-ary PAM. The results show that that the proposed scheme provides shaping gains of 0.6 and 0.93 dB at rates of 2 and 3 bit/dimension. This means that for a 6 bit/QAM symbol a gain of 0.93 dB is achieved.

Khoo et al. (2006) [73] investigate the insertion of non-equiprobable signaling in BICM-ID systems. In the transmitter, a shaping code block is inserted after the convolutional encoder and before the mapper. In the receiver, the demapper calculates the extrinsic LLR value based on a priori LLRs generated by both shaping and convolutional decoders. The results show that the error performance of a 2 bit/s/Hz 16QAM convolutional coding scheme is improved by 0.7 dB at BER = 10^{-3} and 0.35 dB at BER = 10^{-5} selecting the adequate shaping codes.

Le Goff et al. (2007) [74] introduce a new probabilistic shaping technique for improving the performance of Bit-Interleaved Turbo-Coded Modulation (BITCM) over AWGN channels. The authors propose to partition the basic constellation into several equal-sized sub-constellations of increasing average energy. The sequence of sub-constellations is specified using a shaping code. In this way, low-

energy signals are transmitted more often than high-energy signals. The constellation set is labelled using Gray code and PAM constellations are taken into account. The technique consists of inserting a single short-length binary shaping code between turbo code and modulation blocks. The simulation results show that gains of up to 0.8 dB are achieved using 16PAM signal sets. The results also demonstrate that if the demapper is removed from the iterative decoding process, the results remain unaltered while the receiver complexity is reduced.

Mheich et al. (2011) [75] analyze the problem of PS in degraded broadcast channels. The authors investigate if higher achievable bit rates than those for Hierarchical Modulation (HM) are possible. The design of the constellation is carried out maximizing the multidimensional AMI of the system. Simulated annealing is used to solve the optimization problem as it provides a good approximation to the global optimum. The results show that if joint optimization of probability density and constellation symbols positions are included in broadcast transmission, higher achievable rates than for HM are generated in 4PAM. This gain is translated into SNR gains of up to 2 dB.

Valenti et al. (2012) [76] consider the use of PS for BICM-ID LDPC coded systems using APSK constellations. The authors propose the use of a non-linear shaping encoder in which the output is more likely to be zero than one, dividing the basic constellation into several subsets. The shaped bits are used to select one subconstellation and the unshaped bits are used to select the constellation point inside the subconstellation. The system is designed in a way that the CM capacity of the system is used in order to optimize the ring of the APSK modulation and the probability distribution of the shaping code. Then, the LDPC code is optimized using Extrinsic Information Transfer Charts (EXIT) to select the most adequate variable-node degree distributions. With the shaping and LPDC codes correctly optimized, the iterative system outperforms a standard DVB-S2 system by over 1 dB in AWGN channel with 32APSK at a rate of 3 bit/symbol. The main drawback of the solution proposed is the iterative receiver complexity.

Yankov et al. (2014) [77] study a rate-adaptive constellation shaping technique to approach capacity in Turbo Coded BICM. A family of mapping functions are designed using many-to-one constellation shaping based on Huffman code with binary-reflected Gray code. The results of this work are provided for a wide range of SNR values and AWGN and Rayleigh iid channels are considered. The optimal code rate, constellation and mapping are dynamically selected based on the operating SNR. The results show that this approach reduces the gap to channel capacity, outperforming state of art TTCM schemes.

Böcherer et al. (2015) [78] propose a new CM scheme making use of PS without iterative demapping applied to ASK constellations. The authors introduce the Probabilstic Amplitude Shaping (PAS) technique, concatenating a distribution matcher and a systematic binary encoder for FEC in order to get rid of the iterative decoder. Various orders of ASK (4, 8, 16, 32 and 64) are considered and only one LDPC code rate per constellation size. This CM scheme achieves any spectral efficiency between 2-10 bit/s/Hz within 1.1 dB of capacity for the AWGN channel.

Table 2.3. State-of-the-art of PS constellations

Authors	Title	Year	Design Target	Contribution
[68] Forney et al.	Efficient ModuIation for Band-Limited Channels	1984	Maximize channel capacity	PS to provide signal set to have a Gaussian probability distribution
[69] Calderbank et al.	Nonequiprobable Signaling on the Gaussian Channel	1990	PAPR improvement via PS constellation design	PS with subconstellation partition to approach the full asymptotic gain
[70] Kschischang et al.	Optimal Nonuniform Signaling for Gaussian Channels	1993	Approach the optimal performance of non-equiprobable constellation schemes	Prefix codes to approach the optimal performance of PS constellation schemes
[71] and [72] Raphaeli et al.	Constellation shaping for pragmatic turbo coded modulation / Constellation Shaping for Pragmatic Turbo-Coded Modulation With High Spectral Efficiency	2002 and 2004	Constellation design for BTCM system	Constellation design via PS for the pragmatic binary turbo coded modulation
[73] Khoo et al.	Bit-interleaved Coded Modulation with Iterative Decoding Using Constellation Shaping	2006	Constellation design for BICM-ID system	PS in BICM-ID systems
[74] Le Goff et al.	Constellation Shaping for Bandwidth-Efficient Turbo-Coded Modulation With Iterative Receiver	2007	Constellation design for BITCM system	PS technique for BITCM systems
[75] Mheich et al.	Constellation Shaping for Broadcast Channels in Practical Situations	2011	Constellation design for broadcast channels	PS technique in degraded broadcast channels
[76] Valenti et al.	Constellation Shaping for Bit-Interleaved LDPC Coded APSK	2012	Constellation design for BICM-ID system	PS for BICM-ID LDPC coded systems using APSK constellations
[77] Yankov et al.	Rate-adaptive Constellation Shaping for Near-capacity Achieving Turbo Coded BICM	2014	Constellation design for BITCM system	Rate-adaptive constellation PS technique to approach capacity in Turbo coded BICM
[78] Böcherer et al.	Bandwidth Efficient and Rate-Matched Low-Density Parity-Check Coded Modulation	2015	Design of a new CM scheme with ASK constellations	PAS without iterative demapping applied to ASK constellations

3.3 Other Constellation Design Techniques

Constellation design is not only restricted to probabilistic or geometrical shaping methodologies. Depending on the characteristics of the system, constellation schemes that adapt to the requirements have been proposed in the literature, e.g., reduction of PAPR, maximization of the channel capacity for multilayer systems, constellation optimization for multi-antenna systems. Several examples can be found for Multiple-Input Multiple-Output (MIMO), LDM, PAPR reduction and signal space diversity.

3.3.1 MIMO

In the case of MIMO systems, several design procedures have been published. Most of those works address optimization as a function of the channel state information and the channel matrix.

Srinivasan et al. (2007) [79] designed constellation schemes for the noncoherent MIMO Rayleigh fading channel. The authors consider the cutoff rate expression as the design criterion and the mutual information as the performance metric. The design is based on convex programming, where the optimization variables are the input probabilities and per-antenna amplitudes for the constellation points. The results show significant to moderate capacity increase in the low-medium SNR regime.

Maleki et al. (2013) [80] introduced a novel constellation design for spatial modulation (a class of MIMO system) taking into account the effect of Channel State Information at the Transmitter (CSIT). Considering full and imperfect CSIT, the authors propose two different constellation schemes to increase the distance among the received constellation vectors. The first solution, called Multi-antenna Spatial Modulation (MSMod) makes use of all the transmit antennas per transmit interval. The second solution, called Modified Space Shift Keying (MSSK) employs only one transmit antenna scheme in order to avoid that all transmit antennas should be active simultaneously. The results show that MSMod provides better system performance than MSSK, the transmit complexity is higher as Inter-Antenna Synchronization (IAS) is needed.

Cai et al. (2016) [81] create an optimal constellation scheme for indoor 2x2 MIMO Visible Light Communications (VLC). Perfect Channel State Information (CSI) at the transmitter and receiver site is considered. The goal is to maximize the

ED between different received signal vectors under a total optical transmission power constraint. The simulation results show that when compared to conventional MIMO-VLC solutions, the proposed scheme offers the largest minimum ED.

3.3.2 PAPR

Another field of research is the search of PAPR reduction techniques for OFDM systems making use of constellation shaping. The works described below show several solutions created considering constellation-shaping methods, e.g., selective and shell mapping without any loss in spectral efficiency.

Mobasher et al. (2006) [82] propose a constellation-shaping method to reduce the PAPR in OFDM systems. The authors propose to use a cubic constellation alongside selective mapping in order to reduce the PAPR of an OFDM system. The cubic constellation is based on the Hadamard matrix which provides reduced PAPR. This solution reduces the average energy, i.e., achieves small but positive shaping gain. Furthermore, PAPR reduction techniques can be applied to the constellation scheme proposed, further reducing the PAPR. The results show that the proposed scheme outperforms existing PAPR reduction techniques with no losses in terms of energy or spectral efficiency.

Sterian et al. (2010) [83] designed QAM constellation schemes via constellation shaping to reduce the PAPR of OFDM systems. The authors adapt constellation shaping by shell mapping to OFDM signals, designing the encoding and decoding algorithms. Simulation results for different values of subcarriers (16, 32 and 128) are obtained for the proposed constellation shaping scheme, showing significant PAPR reduction for the OFDM system. Furthermore, the proposed scheme does not require additional side information to be transmitted to the receiver and does not increase the average power of OFDM.

3.3.3 RC

In order to cope with fading channels, the rotated RC technique (a special case of SSD) is adopted in DVB-T2 and DVB-NGH. RC provides better system performance than standard constellation schemes such as QAM. The uniformly spaced and equiprobable QAM schemes are rotated a given angle (optimized for each operating waterfall SNR) and then, an interleaving process (different for DVB-T2 and DVB-NGH) is applied.

Polak et al. (2012) [84] compare the system performance of non-rotated and rotated constellations in DVB-T2. Using a DVB-T2 OFDM compliant system, the authors conclude that the maximum gain is achieved when using QPSK modulation with RC for 0 dB Echo channel. Authors do not include other types of fading scenarios such as Rayleigh. A wider range of code rates and higher order modulations should be considered compare fairly rotated and non-rotated constellations.

Gonzalvez et al. (2013) [85] study the use of rotated constellation in DVB-NGH to get improved time and frequency diversity. The authors consider the joint use of the long time interleaver and Time-Frequency Slicing (TFS) defined in DVB-NGH with RC. The study carried out from the information-theoretic approach reveals that RC technique improves the performance for high code rates. Moreover, the gain obtained with RC is higher with interleaving durations up to several seconds and with TFS as large signal variations are compensated.

3.3.4 LDM

ATSC 3.0 incorporates a Non-Orthogonal Multiple Access (NOMA) technique known as Layered Division Multiplexing (LDM). LDM delivers two independent services on the same frequency channel. As this technique is of recent creation, there is only one work related to constellation design for LDM.

Mouhouche et al. (2015) [86] extend the use of non-uniform constellation design via GS to LDM systems. The authors consider to take into account more than one SNR in order to optimize the sum BICM capacity (sum of the BICM capacity at the waterfall SNR of LDM and the BICM capacity at the waterfall SNR without LDM). For 64 constellation points, non-uniform constellations provide SNR gain about 0.55 dB. For 256 constellation points, system performance gains of up to 0.85 dB are obtained.

Table 2.4. State-of-the-art of other constellation design techniques

Authors	**Title**	**Year**	**Design Target**	**Contribution**
[79] Srinivasan et al.	Constellation Design for the Noncoherent MIMO Rayleigh-Fading Channel at General SNR	2007	MIMO systems	Design of constellation schemes for the noncoherent MIMO Rayleigh fading channel
[80] Maleki et al.	Space Modulation With CSI: Constellation Design and Performance Evaluation	2013		Constellation design based on CSIT for Spatial Modulation
[81] Cai et al.	Optimal Constellation Design for Indoor 2×2 MIMO Visible Light Communications	2016		Optimal constellation for indoor 2x2 MIMO VLC
[82] Mobasher et al.	Integer-Based Constellation-Shaping Method for PAPR Reduction in OFDM Systems	2006	PAPR reduction	Cubic constellation shaping with selective mapping
[83] Sterian et al.	Reducing the Peak and Average Power for OFDM Systems Using QAM by Constellation Shaping	2010		Constellation shaping with sell mapping
[84] Polak et al.	Comparison of the Non-rotated and Rotated Constellations Used in DVB-T2 Standard	2012	Robustness in fading channels	System performance of RC technique
[85] Gonzalvez et al.	Rotated Constellations for Improved Time and Frequency Diversity in DVB-NGH	2013		Improve performance of DVB-NGH using RCs with long TI and TFS
[86] Mouhouche et al.	Design of Non Uniform Constellations for Layered Division Multiplexing	2015	LDM systems	Constellation design via GS for LDM systems

4. DISCRETE DATA DETECTION

4.1 Overview

The necessary technical background of the transmitter stages is covered in sections 1 and 2 showing the main modulations, system models and the techniques used in DTT systems. This section is focused on technical aspects associated to the receiver, in particular the detection/demapper. Sections 4.2 - 4.5 describe the basis of the optimal detection of a digital signal. The optimal detector and some approximations are explained in order to set the basis for the design of advanced detection algorithms. Figure 2.6 depicts the main low complexity detection schemes classified by the number of antennas of the communication system. In Single-Input Single-Output (SISO) systems, there are five main detection schemes:

- One-dimensional: Considers that the constellation points are distributed uniformly inside a rectangular region of the constellation diagram. In this way, taking into account that In-phase (I) and Quadrature (Q) components of each constellation symbol are independent, the LLR soft metric of each symbol bit can be obtained from a determined constellation point of the PAM scheme.

- Sub-region: The constellation diagram is divided into a number of sub-regions. This number depends on the technique used as explained in Section 6.1.2. Depending on the code rate used a specific region is selected. The constellation symbols inside the sub-region are decoded.

- Product constellation labelling: An APSK scheme based on a Gray labelled PSK constellation and a Gray labelled PAM constellation is created. In this way, the APSK constellation can be viewed as the Cartesian product of the PSK and PAM sets. At the demapping stage the APSK constellation can be composed in PSK and PAM sets and one-dimensional demapping can be applied to each one.

- Per-dimension: the constellation diagram is divided into sectors that are limited by parallel lines along the imaginary axis and there are calculated the EDs of the received symbol and the constellation points within the two sectors closest to the received observation.

- Condensed: Exploits the low EDs between constellation points near the center of the constellation diagram for low SNR values and gathers very close points in order to get rid of the LLR calculation of the Least Significant Bits (LSBs).

For MIMO systems, there are two main detection techniques:

- Lattice: Reduces the number of lattices of the constellation diagram based on the geometrical characteristics of the constellation and tries to find out the closest point to the received observation.

- Sphere: The Sphere Decoder (SD) is a type of lattice reduction decoder which reduces the complexity considering only the constellation points that are inside a sphere of a determined radius.

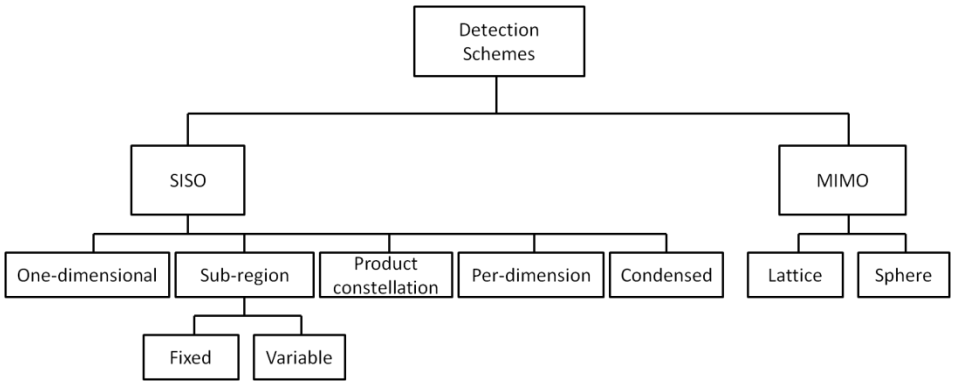

Figure 2.6. Diagram of basic detection schemes.

4.2 **Discrete Channel Model**

During the symbol period $0 \leq t \leq T$, the channel output is $x(t) = s_i(t) + n(t)$ where $s_i(t)$ is the transmitted signal, i is the number of the symbol transmitted and $n(t)$ is a Gaussian random process. The goal is to determine the transmitted constellation point s_i. A similar procedure is carried out for each time interval. In order to work in finite-dimensional vector space for estimating the transmitted signal, the purpose is to convert the received signal $x(t)$ over each time interval into a vector. This process is detailed in [50]. Without loss of generality we can express $x(t)$ as the real vector $\mathbf{x} = (x_1, \ldots, x_N)$ where $x_i = s_i + n_i$.

4.3 **Maximum Likelihood Detector**

Given a transmitted message m and a decoded message $\hat{m}$, the goal of the detector is to minimize the error probability $\mathrm{P_e}$, i.e., the probability that the decoded message is not equal to the transmitted message. Given a received vector $\mathbf{x}$, the optimal receiver selects $\hat{m} = m_i$ corresponding to the constellation s_i that satisfies $\mathrm{p}(s_i \text{ sent}|\mathbf{x}) > p(s_j \text{ sent}|\mathbf{x})\ \forall\ j \neq i$.

As the probability $\mathrm{p}(s_i \text{ sent}|\mathbf{x})$ is unknown, we apply Bayes' rule in order to convert the expression into known probabilistic:

$$\mathrm{p}(s_i \text{ sent}|\mathbf{x}) = \frac{\mathrm{p}(\mathbf{x}|s_i)\mathrm{p}(s_i)}{\mathrm{p}(\mathbf{x})} \tag{2.9}$$

In order to minimize the $\mathrm{P_e}$, the detector looks for the constellation symbol s_i that maximizes $\mathrm{p}(s_i \text{ sent}|\mathbf{x})$. In other words, s_i must fulfil the next condition:

$$\arg\max_{s_i} \frac{\mathrm{p}(\mathbf{x}|s_i)\mathrm{p}(\mathrm{s_i})}{\mathrm{p}(\mathbf{x})} = \arg\max_{s_i} \mathrm{p}(\mathbf{x}|s_i)\mathrm{p}(s_i)\,, i = 1, \dots, M. \tag{2.10}$$

As $\mathrm{p}(\mathbf{x})$ is not a function of s_i, it is suppressed in the second equality. If all the messages are of equal probability then, $\mathrm{p}(s_i) = \mathrm{p}(\frac{1}{M})$ and Equation 2.10 can be expressed as:

$$\arg\max_{s_i} \mathrm{p}(\mathbf{x}|s_i), i = 1, \dots M. \tag{2.11}$$

The likelihood function is defined as:

$$\mathrm{L}(s_i) = \mathrm{p}(\mathbf{x}|s_i) \tag{2.12}$$

Considering that the log function is increasing in its argument, we can equivalently maximize the log likelihood function as $\mathrm{l}(s_i) = \log \mathrm{L}(s_i)$:

$$\mathrm{l}(s_i) = -\frac{1}{\mathrm{N_0}} \sum_{\mathrm{j}=1}^{N} (x_j - s_{ij})^2 = \|\mathbf{x} - s_i\|^2 \tag{2.13}$$

Therefore, the log likelihood function of the optimal detector depends on the EDs between the received observation and all the constellation symbols.

This approach is valid for CM system models. For BICM systems, the possible bit values of the transmitted symbols are taken into account and the detector calculates the Log-Likelihood Ratio (LLR) values.

The LLR for the bit $\mathrm{b_i}$ (where i = 1,...,m being $m = \log_2 M$) considering that the received observation $\mathbf{x}$ is composed by the In-phase (I) and Quadrature (Q) components is expressed as:

$$\mathrm{LLR}(b_i) = \ln\left(\frac{\Pr(b_i=1 \mid I,Q)}{\Pr(b_i=0 \mid I,Q)}\right) \tag{2.14}$$

A positive LLR would indicate that b_i was more probably transmitted as a 1, a negative value that b_i was more probably transmitted as a 0.

A particular constellation point, s_i, is transmitted with coordinates I_s, Q_s. Ideally the received constellation I, Q would be identical. In practice, it differs for two reasons: the cells in which I and Q travelled have been subjected to amplitude-fading factors (ϱ_I , ϱ_Q), and furthermore, noise has been added. We can therefore write the following for the conditional probability distribution function (pdf) of receiving particular I, Q, given that we know point s_i was transmitted:

$$\mathrm{p}(I, Q \mid s_i \text{ was transmitted}) = \frac{1}{2\pi\sigma^2} \mathrm{e}^{-\frac{\left(I-\rho_I I_{s_i}\right)^2+\left(Q-\rho_Q Q_{s_i}\right)^2}{2\sigma^2}} \tag{2.15}$$

Now, let's consider reception of a particular bit $\mathrm{b_i}$. If it was transmitted as a 1, then that implies that any of 2m-1 possible states was transmitted, each one depending of course on the state of the other (m - 1) bits. If it was a 0, then one of the other 2m-1 possible states would be transmitted. Let C_i^j denote the set of constellation points s_i for which the bit $\mathrm{b_i}$ takes the value j (0 or 1).

The conditional pdf for the received values I, Q, given that $\mathrm{b_i}$ was transmitted as a 1 is thus given by the following expression, under the assumption that all of the 2m-1 possible transmitted states for which $b_i = 1$ are transmitted with equal probability. (In other words, each of the other (m - 1) bits takes the values 0 and 1 with equal frequency).

$$\mathrm{p}(I, Q \mid b_i = 1) = \frac{1}{2^{\mathrm{m}}\pi\sigma^2} \sum_{s_i \in C_i^1} \mathrm{e}^{-\frac{\left(I-\rho_I I_{s_i}\right)^2+\left(Q-\rho_Q Q_{s_i}\right)^2}{2\sigma^2}} \tag{2.16}$$

The conditional pdf for receiving I, Q, given that b_i was transmitted as a 0 is the same except that the summation is taken over points $s_i \in C_i^0$. Now if we invoke Bayes' theorem, and make the further assumption that the transmitted bit b_i is itself equally likely to be 0 or 1, then we can obtain the LLR as required:

$$\mathrm{LLR}(b_i) = \ln\left(\frac{Pr(b_i=1 \mid I,Q)}{Pr(b_i=0 \mid I,Q)}\right) = \ln\left(\frac{p(I,Q|b_i=1)}{p(I,Q|b_i=0)}\right) = \ln\left(\frac{\sum_{\mathbf{s}_i \in \mathbf{C}_i^1} e^{-\frac{(I-\rho_I I_s)^2+\left(Q-\rho_Q Q_s\right)^2}{2\sigma^2}}}{\sum_{\mathbf{s}_i \in \mathbf{C}_i^0} e^{-\frac{(I-\rho_I I_s)^2+\left(Q-\rho_Q Q_s\right)^2}{2\sigma^2}}}\right) \quad (2.17)$$

4.4 Maximum a Posteriori (MAP) Detector

The main difference between the ML and the Maximum A Posteriori (MAP) detector is that the MAP assumes some probability distribution on the transmitted signal $\mathrm{p(s)}$ and selects the estimate $\hat{s}$ that maximizes $\mathrm{p}(s|\mathbf{x})$. If it is assumed that there is no prior knowledge of $\hat{s}$, then $\mathrm{p(s)}$ is uniform and the MAP and ML criteria are equivalent. This case occurs in BICM systems where there is no prior information about the transmitted signal. However, in iterative decoding systems such as BICM-ID, the MAP detector is widely used [87], [88].

4.5 Max-Log Detector

The Max-Log detector reduces the number of mathematical computations with respect to the ML detector while the number of EDs is unaltered. Taking the Jacobian Logarithm we can express

$$\ln(\mathrm{e}^{\mathrm{a}} + \mathrm{e}^{\mathrm{b}}) = \max(\mathrm{a}, \mathrm{b}) + \ln(1 + \mathrm{e}^{-|\mathrm{a}-\mathrm{b}|}) \quad (2.18)$$

Then, the Max-Log algorithm basically ignores the second term on the right

$$\ln(\mathrm{e}^{\mathrm{a}} + \mathrm{e}^{\mathrm{b}}) \approx \max(\mathrm{a}, \mathrm{b}) \quad (2.19)$$

The LLR computation can be simplified by applying the Max-Log approximation:

$$\ln(\mathrm{e}^{\mathrm{a}_1} + \cdots + \mathrm{e}^{\mathrm{a}_\mathrm{k}}) \approx \max_{\mathrm{i}=1\ldots\mathrm{k}}(\mathrm{a}_\mathrm{i}) \quad (2.20)$$

The LLR becomes:

$$\mathrm{LLR}(b_i) \approx \frac{1}{2\sigma^2}\left[\min_{s_i \in C_i^0}\left((I-\rho_I I_s)^2 + \left(Q-\rho_Q Q_s\right)^2\right) - \min_{s_i \in C_i^1}\left((I-\rho_I I_s)^2 + \left(Q-\rho_Q Q_s\right)^2\right)\right] \quad (2.21)$$

5. Demapper Design Techniques

In this section, works related with low complexity demapping techniques are discussed. Two major areas are distinguished: 1) multidimensional constellation schemes in MIMO systems and 2) shaping characteristics of the constellation schemes.

5.1 Demapping Solutions in MIMO Systems

Multi-antenna systems are known to increase the capacity of a communication system using multiple transmit and receive antennas in order to exploit multipath propagation. At the receiver side, the detectors make use of the computation of the EDs between the received and all the possible transmitted constellation symbols. The problem in MIMO systems is that the complexity associated to the demapping of the received symbols depends both on the dimension of the constellation scheme and on the number of transmit and receive antennas n_t. Therefore the complexity of a MIMO receiver based on ML detection is ~O(M^{n_t}) while for a SISO system is ~O(M). Two main techniques are considered for lowering the demapping complexity in MIMO systems: 1) Lattice Reduction (LR) decoder, and 2) Sphere decoder (SD).

5.1.1 Lattice Reduction Decoder (LR)

The LR decoder reduces the number of lattices of the constellation diagram based on the geometrical characteristics of the constellation and tries to find out the closest point to the received observation, lowering the complexity of the receiver.

The key is to select a minimum number of lattices in the constellation scheme that reduces the number of computations associated to the calculation of the EDs with negligible system performance losses. The main methodology used to fulfil the above mentioned objective is via radius calculation. The existing lattices inside the region covered by the radius value starting from the received observation are considered in ED calculation. In [89], search restriction of constellation points via radius value is proposed. The next advance is the definition of the radius value for fading scenarios. In this way, authors in [90] consider to calculate the radius value taking into account the fading coefficient. In [92] a further step is considered, recalculating the radius value iteratively in order to reduce the number of lattices considered at demapping stage. Finally, joint lattice reduction and conditioned

detection is proposed in [94] to reduce the number of multiplications associated to ED calculation.

Viterbo et al. (1993) [89] introduce a universal decoding algorithm for lattice codes that solves the decoding problem for any lattice, independent of its algebraic structure. The idea is to restrict the search to a finite number of lattice points that lie within a bounded region of the constellation diagram. The authors propose a radius value in order to define the search region. The bounds of the region can be adaptively adjusted according to the noise level. The advantage of this method is that vectors with a norm greater than the given radius are never tested.

Viterbo et al. (1999) [90] extend their prior work on lattice decoding to fading channels. In this work the authors consider a sphere centered at the received point in order to determine the bounded distance search. The lattice points falling inside the sphere are considered in the decoding process. The choice of the radius is critical in fading scenarios and the authors overcome this problem by adapting the radius to the values of the fading coefficients. Results show that the sphere decoder can decode lattice codes of dimensions up to 32 in fading environments.

Agrell et al. (2002) [91] make a survey of closest point search methods for lattices without a regular structure. The authors review the Babai nearest plane algorithm, the Kannan strategy, the Pohst strategy, and the Schnorr-Euchner refinement of the Posht strategy. A detailed pseudocode implementation of a closest point search algorithm based on the Schnorr-Euchner strategy is presented. The solution is faster than Kannan and Viterbo-Boutros algorithms.

Yao et al. (2002) [92] propose to use lattice reduction in conjuction with traditional detectors in 2 x 2 coherent MIMO systems. The authors design a new iterative detector where a reduction algorithm is introduced in order to search the closest point to the received observation. The complexity of the algorithm for optimal decoding is tipically low. Simulation results for both Gaussian and Rayleigh fading channels are carried out. For Gaussian channels, LR techniques are within 3 dB to the ML bound. In the case of Rayleigh fading channels, for large constellations the same diversity is achieved.

Damen et al. (2003) [93] propose to use number-theoretic tools for searching the closest lattice point. The authors develop two algorithms. One is inspired by the Pohst enumeration strategy, which provides significant complexity reduction compared to Viterbo-Boutros decoder. The second one is an application of the Schnorr-Euchner strategy to ML decoding. The combination of the second

algorithm with an efficient preprocessing stage provides significant reductions in computational complexity and its performance is close to the ML decoder.

Haroun et al. (2016) [94] designed a detection algorithm for QAM constellations in 2 x 2 MIMO systems based on lattice reduction and conditioned detection. The authors propose to estimate the I and Q components of the received symbol applying conditional detection on the second symbol received corresponding to the second antenna. Then, the local minimum is calculated making use of the geometrical shape of the QAM constellation. This detector provides a reduction of 95% of the number of multiplications required to estimate the EDs. The system performance is not degraded if compared to Belief Propagation (BP) detection.

5.1.2 Sphere Decoder

The exponential complexity of the ML detector in MIMO systems makes it unfeasible in a practical system with a large number of antennas and high order constellations. The Sphere Decoder (SD) is a type of lattice reduction decoder which reduces the complexity considering only the constellation points that are inside a sphere of a determined radius.

In the literature, different variants of sphere decoders can be found with the same objective: reduce the number of constellation points considered at the demapping stage. Authors in [95], [96] propose the joint maximum-likelihood detection and decoding in order to improve the system performance. Another type of sphere decoder is designed in [97]. Sphere iterative decoder is proposed using a list of candidate points. One step forward is considered in [98], [101] and [103] where list sphere decoding is proposed in order to reduce the computational complexity associated to the standard sphere decoder. Finally, authors in [99] propose the hard sphere decoding in order to reduce the running-time of the soft sphere decoding.

Vïkalo et al. (2002) [95] and (2005) [96] propose several sphere decoding algorithms and study their complexity for MIMO systems. The authors consider the problem of joint detection and decoding in MIMO systems and developed the Joint Maximum-Likelihood Detection and Decoding (JDD-ML) algorithm. If detection and decoding are jointly considered, the system performance is better than if they were considered separately. The expected complexity is a polynomial in the length of the uncoded information word over a wide range of SNRs and the authors derive the bound on the expected computational complexity.

Boutros et al. (2003) [97] design a sphere iterative decoder for coded transmission. The authors evaluate the a posteriori information at the detector output using a shifted spherical list of candidate points. The radius of the sphere is chosen to control the list size. The results show a BER of 10^{-5} at 1.25 dB from capacity limit for 16-QAM constellation.

Hochwald et al. (2003) [98] introduce the so-called List Sphere Decoding (LSD) algorithm. This solution avoids the exhaustive search by restricting the search inside a preset sphere. The authors demonstrate that LSD achieves capacity-approaching performance in coded Layered Space-Time (LST) systems. Some guidelines for choosing the number of constellation points candidates are given, remarking that the size of the list determines the running time and closeness to capacity. In future works, the performance of LSD should be examined on static channels.

Wang et al. (2006) [99] propose a bit-level multi-stream coded LST transmitter with soft-to-hard conversion at the decoder for MIMO channels. The authors convert the Max-Log-based MAP (Max-MAP) problem to a set of Hard Sphere Decoding (HSD) problems using soft-to-hard transformation for binary constellations. The simulations conclude that the proposed solution has almost identical performance for QPSK as LSD while for 16-QAM and 64-QAM gains up to 0.5 dB are achieved. In terms of running-time, for a small number of antennas and/or constellation size, the proposed solution and LSD have comparable running-time. If the number of antennas and/or constellation size increases, the HSD becomes faster than LSD.

Guo et al. (2006) [100] propose a low complexity decoding algorithm based on the Schnorr-Euchner (SE) strategy called (KSE). The objective is to search the lowest possible squared distance between k-dimensional and 1-dimensional sublattice. The advantage of the method proposed is that several computations can be carried out in a preprocessing unit, resulting in lower complexity in the decoding process. The KSE algorithm approaches near-ML performance for MIMO detection with low complexity. The authors also propose the Modified KSE (MKSE) in order to improve the performance of KSE. As an additional contribution, the authors propose VLSI architecture for both algorithms.

Barbero et al. (2008) [101] design a fixed-complexity SD in order to overcome the two problems of LSD, i.e., its variable complexity and the sequential nature of its tree search. The authors designed a Soft-output Fixed-complexity Sphere Decoder (SFSD) for turbo-MIMO systems. The list of candidates is fixed for each

iteration in the decoding process, independently of the noise level and channel conditions.

Azzam et al. (2009) [102] reduce the complexity of the conventional SD via a reordering of the channel representation adding rounding and adaptive K-best techniques. The authors reorder the channel matrix and define each pair of columns as one set in order to get orthogonal columns in each set. The results show that for 2 x 2 systems, there is no performance loss with respect to the conventional SD while a complexity reduction of 80% is achieved. The system losses are below 1 dB with a complexity reduction of more than 50% in 4 x 4 and 6 x 6 cases.

Wang et al. (2011) [103] study several approaches to improve the radius at the initialization and reduction steps in the original LSD algorithm. The authors propose an iterative method that updates the value of the radius depending of the value of the previous iteration. If the new candidate point has smaller radius than the one with maximum radius in storage list, then the radius is updated to the smaller value. The simulation results indicate that the proposed solution can significantly speed up the LSD algorithm.

Table 2.5. State-of-the-art of lattice reduction decoders

Authors	Title	Year	Decoder	Design Target	Contribution
[89] Viterbo et al.	A Universal Decoding Algorithm for Lattice Codes	1993	Lattice reduction	Restriction of the search of constellation points	Universal low complexity lattice decoder independent of lattice algebraic structure
[90] Viterbo et al.	A Universal Lattice Code Decoder for Fading Channels	1999		Radius calculation for fading channels	Lattice decoder based on sphere region for fading channels
[91] Agrell et al.	Closest Point Search in Lattices	2002		Lattice reduction for non-regular structures	Survey of closest point search methods for lattices without regular structure
[92] Yao et al.	Lattice-Reduction-Aided Detectors for MIMO Communication Systems	2002		Improvement in radius calculation	Iterative lattice reduction decoder for 2 x 2 MIMO systems
[93] Damen et al.	On Maximum-Likelihood Detection and the Search for the Closest Lattice Point	2003		Computational complexity reduction of lattice decoder	Searching of closest lattice point based on number-theoretic tools
[94] Haroun et al.	Low-Complexity Soft Detection of QAM Demapper for a MIMO System	2016		Computational complexity reduction of lattice decoder	Lattice reduction and conditioned detection algorithm for QAM constellations in 2 x 2 MIMO systems

Table 2.6. State-of-the-art of sphere decoders

Authors	Title	Year	Decoder	Design Target	Contribution
[95] and [96] Vikalo et al.	Sphere Decoding Algorithms for Digital Communications / On the Sphere-Decoding Algorithm I. Expected Complexity	2002 and 2005	Sphere	Improve the system performance of separate detection and decoding processes	Joint maximum-likelihood detection and decoding algorithm for MIMO systems
[97] Boutros et al.	Soft-input soft-output Lattice Sphere Decoder for Linear Channels	2003		Improve radius calculation	Sphere iterative decoder for coded transmission
[98] Hochwald et al.	Achieving Near-Capacity on a Multiple-Antenna Channel	2003		Avoid the exhaustive search in LST systems	List Sphere Decoding algorithm
[99] Wang et al.	Approaching MIMO Channel Capacity With Soft Detection Based on Hard Sphere Decoding	2006		Reduce the running-time associated to sphere decoding	Hard sphere decoding using soft-to-hard conversion for MIMO channels
[100] Guo et al.	Algorithm and Implementation of the K-Best Sphere Decoding for MIMO Detection	2006		Translate computations to the preprocessing unit	Low complexity decoding algorithm based on the Schnorr-Euchner strategy
[101] Barbero et al.	A Low-Complexity Soft-MIMO Detector Based on the Fixed-Complexity Sphere Decoder	2008		Overcome the variable complexity of tree search in LSD	Fixed-complexity sphere decoder for turbo-MIMO systems
[102] Azzam et al.	Reduced Complexity Sphere Decoding via a Reordered Lattice Representation	2009		Complexity reduction of conventional sphere decoder	Rounding and adaptive K-best techniques to reduce the complexity of the sphere decoder
[103] Wang et al.	A List Sphere Decoding Algorithm with Improved Radius Setting Strategies	2011		Improve the performance of LSD	Techniques to improve radius selection for the list sphere decoder

5.2 Demapping Solutions in Single-Input Single-Output (SISO) Systems

In SISO systems, the geometrical shape of the transmitted constellation scheme can be exploited at the demapping process to reduce the complexity associated to the exhaustive search method. The demapping strategies shown in section 4.1 have been applied in several works focusing on specific constellation schemes such as QAM, APSK and NUCs, fitting the demapper to their geometrical characteristics.

The one-dimensional demapper is proposed in the literature for several constellation schemes. In [106], the one-dimensional demapper is applied to *M*-APSK with the objective of reducing the computational complexity of the exhaustive method. For QAM constellations, this demapper is considered in [107] and [108], reducing the demapping complexity with negligible system performance losses. Its usability is extended to non-uniform constellations in [111] with system degradation below 0.4 dB.

Although the one-dimensional demapper is extensively used in the literature, product constellation mapping is also used for APSK constellations [138] and QAM constellations [110] in order to reduce the complixity for ML decoder. Sub-region, condensed and per-dimension demappers are commonly used in terrestrial broadcast applications and, thus, they are detailed in section 6.1.

5.2.1 Amplitude Phase Shift Keying (APSK)

Park et al. (2008) [104] propose a low complexity Max-Log demapper and efficient parallel to serial converter for high order APSK constellations. First, a soft-decision demapper interface is designed in order to get rid of the parallel to serial converter before LDPC decoding. The interface consists of two First-In First-Out (FIFO) memories, counter and controller where each FIFO stores the input data and the controller transfers the stored data to the soft decision demapper. The soft decision demapper reuses the controller structure in order to compute the EDs and reduce the number of multipliers needed. In this way, the proposed architecture can reduce 91% of the multipliers used by the max-log demapper.

Lee et al. (2010) [105] present a simple bit-to-symbol mapping scheme with better BER performance than state-of-the-art mappings for 4+12+16 APSK. The

authors develop a low complexity detection algorithm for the non-linear AWGN channel applicable to a specific mapping scheme. The mapping consists of assigning bits to symbols for which the signal points can have smaller Hamming distance. The constellation diagram is divided into several decision boundaries depending of the nonlinearities of the High Power Amplifier (HPA). These boundaries are used in the bit detection algorithm dividing the whole constellation diagram into 3 different subregions, with different bit assignation to each one. The region of the received observation is calculated and the values of the associated bits are obtained. The proposed decoder requires less processing time than ML detection with negligible system performance losses.

Zhang et al. (2011) [106] apply the one-dimensional demapping method to M-APSK schemes to reduce the computational complexity. Not as in the case of uniform QAM constellations which are constructed from a PAM scheme, the constellation points of APSK are situated in different rings. Therefore, if one-dimensional demapping is considered there exists a mismatch in the ED calculation. The authors study the impact of this mismatch for 16-APSK and 32-APSK and obtain a BER performance similar to that of the ML decoder with high computational reduction.

5.2.2 Quadrature Amplitude Modulation (QAM)

Tosato et al. (2002) [107] introduce the one-dimensional demapper for QAM constellations. The authors study the geometrical characteristics of the QAM scheme and exploit the construction of QAM from the PAM constellation. In this way, taking into account that I and Q components are independent, the LLR soft metric of each symbol bit can be obtained from a determined constellation point of the PAM scheme. Then, several decision thresholds depending of the value of the received observation are calculated in order to compute the LLR values of each bit. This solution reduces the demapping complexity with negligible system performance losses when compared to conventional ML demapper.

Akay et al. (2004) [108] design a low complexity decoding scheme for M-ary QAM constellations in BICM systems. The authors propose to apply Gray labeling to the I and Q components of the QAM signal separately. Then, the soft-decision metrics can be simplified computing only $\sqrt{M}/2$ real EDs instead of $M/2$ complex EDs for ML detection with the same system performance.

Sherratt et al. (2007) [109] proposed a dual soft-output QPSK demapper that merges demapping Time Domain Spreading (TDS) and guard carrier diversity into

a single instance. The authors propose a parallel architecture to process the main and spread OFDM symbols where the main and spread symbols have their own FFT and equalizer. This scheme minimizes the CPU cycles and the required memory access is reduced a 40%.

Wang et al. (2014) [110] present a low complexity demapper based on product constellation labelling. The authors demonstrate that for Gray-labelled constellations, the nearest constellation point can be determined by using simple comparison and addition operations. The computational complexity is reduced from O(2*m*) (the case of ML decoder) down to O(*m*), where *m* is the number of bits per constellation point. The designed demapper has similar performance to ML for Gray-labelled PAM, PSK and QAM schemes. In the case of Gray-labeled product APSK, negligible performance degradation is achieved compared to ML decoder.

5.2.3 Non-Uniform Constellation (NUC)

Shitomi et al. (2016) [111] propose to extend the demapper shown in [107] to 1D-NUCs. The influence of the non-equidistant distances between adjacent constellation points is evaluated in dual-polarized MIMO channels captured in urban area. The simplified demapping scheme mitigates the degradation in the required CNR by no more than 0.4 dB when using 4096 NUQAM while greatly reducing the computation complexity in comparison to ML decoder.

Barjau et al. (2017) [112] present a MIMO sphere decoder with Successive Interference Cancelation (SIC) for 2D-NUCs. The main idea of this work is to select the most appropriate Voronoi regions adapted to the geometry of the NUC. This solution presents complexity reductions of 87.5%. 97.5%, 99.5%, 99.8% and 99.9%, for 16NUC, 64NUC, 256NUC, 1024NUC and 4096NUC, respectively. The system performance carried out in a 2 x 2 MIMO system reflects a maximum performance loss of 0.1 dB compared to max-log and 0.7 dB compared to ML demappers.

Table 2.7. State-of-the-art of demappers for SISO systems.

Authors	Title	Year	Constellation	Design Target	Contribution
[104] Park et al.	Low Complexity Soft-Decision Demapper for High Order Modulation of DVB-S2 system	2008	APSK	Reduce the number of multipliers	Joint Max-log demapper and parallel to serial converter for high order APSK
[105] Lee et al.	Simple Signal Detection Algorithm for 4+12+16 APSK in Satellite and Space Communications	2010		Processing time reduction with negligible system performance losses	Simple bit-to-symbol mapping scheme for efficient decoding of 4+12+16 APSK
[106] Zhang et al.	Efficient Soft Demapping for M-ary APSK	2011		Processing time reduction with negligible system performance losses	Extension of one-dimensional demapper to APSK
[107] Tosato et al.	Simplified Soft-Output Demapper for Binary Interleaved COFDM with Application to HIPERLAN/2	2002	QAM	Reduce the demapping complexity with negligible system performance losses	One-dimensional decision threshold (DT) demapper for QAM
[108] Akay et al.	Low Complexity Decoding of Bit-Interleaved Coded Modulation for M-ary QAM	2004		Reduce the demapping complexity in BICM systems	Low complexity decoder based on separate I/Q Gray labelling for QAM
[109] Sherratt et al.	A Dual QPSK Soft-demapper for Multiband OFDM Exploiting Time-Domain Spreading and Guard Interval Diversity	2007		Minimize the CPU cycles and the required memory access	Single instance TDS, guard carrier diversity and QAM demapper
[110] Wang et al.	A Universal Low-Complexity Symbol-to-Bit Soft Demapper	2014		Reduce the demapping complexity with negligible system performance losses	QAM demapper based on product constellation labelling
[111] Shitomi et al.	Evaluation of Simplified Demapping Algorithm for NUQAMs Using Urban MIMO Channel Response	2016	NUC	Extend one-dimensional demapper to non-uniform constellations	Decision threshold (DT) demapping algorithm for 1D-NUCs
[112] Barjau et al.	MIMO Sphere Decoding With Successive Interference Cancellation for 2D-NUCs	2017		Sphere decoder applied to non-uniform constellations in MIMO systems	MIMO decoder based on successive interference cancelation for 2D-NUCs

6. Use Cases

The constellation design and demapping techniques detailed in the previous sections are used in several communication systems. The design of constellations via GS and NUC and APSK detection techniques shown above are implemented in terrestrial and satellite broadcasting systems. MIMO detection schemes shown in Section 5.1 are used in broadband systems such as LTE and 5G system (5G-NR, Release 15). LTE/4G and 5G-NR make use of QPSK and QAM constellations, up to 256 constellation points in some cases. PS is widely used in fiber optic systems.

This section gathers the most important contributions related with constellation design and detection techniques used in the aforementioned communication systems.

6.1 Terrestrial Broadcasting

6.1.1 Constellation Design

The latest designed broadcast communication systems, i.e., DVB-NGH and ATSC 3.0, make use of the GS design of constellation signals to approach channel capacity. GS provides capacity-approaching constellation schemes with no further increase in system complexity. Several works have been carried out to validate the use of non-uniformly spaced constellations in terrestrial broadcasting.

In [113] a first attempt to design optimal constellations for BICM systems is presented based on their probability density function for the AWGN channel. Further improvement is possible for a BICM system if the capacity for this system is maximized. With this objective, in [113] and [63] presented optimized one-dimensional constellations for a BICM system. The results show that the designed constellations achieve a smaller gap to the Shannon limit. In [65], those results are extended to two-dimensional constellation sets for configurations up to 32 constellation points. In [117] 1D-NUCs and 2D-NUCs are analyzed in order to check the BICM system performance, showing a system gain of more than 1.5 dB. In [115] both high order 1D-NUCs and 2D-NUCs are designed. These constellations present a shortcoming of only 0.036 b/s/Hz from the Shannon limit at 29 dB SNR. Zoellner *et al.* [115] use the interior point optimization algorithm [116] to design these high order constellations.

Finally, the authors in [118] study the joint design of constellation schemes via GS for BICM systems with RC and multi-RF techniques. In [119] probabilistic

shaping is proposed as a way to outperform the constellations designed for broadcast applications via geometrical shaping.

In the **Digital Video Broadcasting Next Generation Handheld** (DVB-NGH) system (2012), 1D-NUCs were included. 64 and 256 constellation orders are defined for each code rate.

Stott (2013) [113] and (2014) [114] makes a deep study of constellation design for BICM systems focused on terrestrial applications. The author proposes a GS approach in order to design capacity-approach constellation sets. A low-complexity design methodology for 1D-NUC is shown and the condensation technique is presented for low SNR values. The results show that NUCs provide significant system gains compared with conventional QAM schemes with very little impact on the implementation of transmitters and receivers.

Zoellner et al. (2013) [115] study the optimization of high order NUCs. High order 1D-NUCs and 2D-NUCs are designed. These constellations present a shortcoming of only 0.036 b/s/Hz from the Shannon limit at 29 dB SNR. The authors use the interior point optimization algorithm [116] to design these high order constellations. This technique is both too complex and computationally expensive and, what is more, the importance of initial conditions is not highlighted and some of the post processing steps are not included.

Loghin et al. (2016) [117] revise the NUCs included in ATSC 3.0. The authors review the performance of the NUCs taking into account different channel realizations with the combination of LDPC code and bit interleaver. The results show shaping gains of more than 1.5 dB with respect to standard QAM schemes from 16 to 4096 constellation orders.

Fuentes et al. (2016) [118] study the optimization of NUCs taking into account the RC and multi-RF transmission techniques included in ATSC 3.0. The authors propose the use of RC and multi-RF jointly with NUCs for high SNR values to increase the spectral efficiency of the system. Channel Bonding (CB) and Time-Frequency Slicing (TFS) are the multi-RF techniques considered. The rotation angle is included as an additional variable in the design of geometrical shaped NUCs. The highest rotation gain is obtained for low-order constellations and high code rates, with a maximum gain of 1.7 dB for QPSK 13/15 code rate. Considering the Power Imbalance (PI) of multi-RF techniques, for a PI of 9 dB the SNR gain obtained is up to 6.7 dB for the largest possible code rate and QPSK constellation.

Steiner et al. (2016) [119] compare the GS and PS approaches applied to ATSC 3.0. The authors provide a comprehensive comparison of both geometric and probabilistic shaping considering the information theoretic achievable rates for Symbol-Metric Decoding (SMD) and Bit-Metric Decoding (BMD). The optimization problem for geometric approach is carried out using differential evolution. In the case of probabilistic shaping, the authors use the Maxwell-Boltzmann distribution family alongside Blahut-Arimoto and Cutting-Edge approaches. System performance analysis is obtained for M-ary ASK (for M = 4, 8, 16, 32) and AWGN channel. The results show that PAS with BMD is able to close the gap of BMD to approach AWGN capacity. For GS, a gap of 0.4 dB exists for low order modulations. However, as it is already demonstrated in [63] and [64] GS outperforms PS for high order modulations. Furthermore, the results should be extended to Rayleigh fading channels and the system complexity of PS should be analyzed.

6.1.2 Demapping Technique

There are two main demapping techniques in terrestrial broadcasting systems: RC and NUC demapping. Since the introduction of RC in DVB-T2 and DVB-NGH, several works have been carried out in order to reduce the demapping complexity.

The main demapping technique used to reduce the complexity associated to RC demapping is the sub-region demapper. This technique is based on creating sub-regions of constellation points inside the constellation diagram as a function of different metrics: sign of the received observation [120] and statistics of the received observation for a determined code rate [121], [122] and [129] (for NUCs). Apart from sub-region demapper, the per-demapper technique is also considered in [123] for RC to achieve the best trade-off between complexity and system performance.

Li et al. (2009) [120] propose a detection algorithm based on sub-region computation. The authors divide the constellation diagram into four sub-regions with the same number of constellation points. According to the sign of the received observation, the constellation diagram is divided into subregions including the two closest points with values 0 and 1 for every LLR computation. The solution has no impact on the performance compared to the Max-Log detector and complexity reduction up to 69% can be achieved for 256-QAM.

Calderon et al. (2011) [121] and (2013) [122] design a simplified rotated constellation demapper based on statistical sub-region partitions. The sub-regions are designed via statistical analysis of the minimum 2-D distances simulating the DVB-T2 standard. For all the points received in a particular quadrant, the constellation symbols that are more likely to be at the minimum distance are determined. Then, the subset for this particular quadrant is composed of the symbols with greater occurrence probability. Results show that 78% of complexity reduction compared to ML detector is achieved with no performance degradation.

Tomasin et al. (2012) [123] design a fixed sub-region demapper called Per-Dimension Demapper (PD-DEM) for rotated constellations in DVB-T2. The idea is based on dividing the constellation diagram into sectors that are limited by parallel lines along the imaginary axis. The EDs of the received symbol and the constellation points within the two sectors closest to the received observation are then calculated. Numerical results show that PD-DEM provides the best trade-off between complexity and system performance when compared to state of art demappers for RCs.

Kim et al. (2013) [124] reformulate the received rotated QAM as two PAM signals applying Minimum Mean Square Error (MMSE) decorrelation in order to simplify the demapping process of RCs. The residual interference caused by the decorrelation is tackled using interference cancellation techniques. The results indicate that for 256-QAM and 4/5 code rate, the performance losses of the proposed solution compared to exhaustive search are less than 0.15 dB in memoryless Rayleigh channels with and without erasures. The authors implemented the demapper on a Digital Signal Processor (DSP) achieving 73% less computations than the full search method.

Tao et al. (2014) [125] and (2016) [126] propose a switched soft demapper for RCs. The authors design different demapping algorithms with various complexities which can be selected depending of the I and Q channel fading conditions. The switch selects between the one-dimensional or two-dimensional demapper, depending of three different decision criteria developed in the work. The simulation results show that the proposed scheme reduces up to 77% the demapping complexity for rotated 64-QAM if compared to exhaustive search method with negligible system performance losses. In the case of rotated 256-QAM, up to 95% of complexity reduction can be achieved.

Jafri et al. (2017) [127] designed a high-throughput and area-efficient demapper for RCs. The authors propose the hardware architecture model that

exploits the solutions presented in previous works. The architecture of the demapper is designed using an Application-Specific Instruction-set Processor (ASIP). The structural mode presented in this work provides significant hardware reductions if compared to state-of-the-art implementations of RC demappers.

The inclusion of non-uniform QAM constellations in DVB-NGH and ATSC 3.0 communication systems has reinforced the research of advanced demapping techniques to reduce receiver complexity. Recently, several contributions have been presented to deal with the demapping complexity of such constellations in terrestrial broadcasting systems. Some techniques have already been shown in Section 5.2.3. Next, two more contributions are detailed. The first one is condensation demapping [128] which takes advantage of the wrapping of constellation points for low SNR values in order to get rid of the LLR computations of the LSBs. The second contribution presents a sub-region demapper for NUCs [129] which is based on the one already presented in [121] and [122].

Kwon et al. (2015) [128] propose a simplified demapper for NUC schemes. The authors exploit the low EDs between constellation points near the center of the constellation diagram for low SNR values and consider to gather very close points in order to get rid of the LLR calculation of the LSBs. The results show that NUCs designed for low code rates/SNR values present a significant reduction in computation complexity with negligible performance loss for the proposed solution if compared to ML decoder.

Fuentes et al. (2016) [129] designed a fixed sub-region demapper for 2D-NUCs. The idea is based on the demapper shown in [121] and [122], where a statistical analysis of the LDPC decoding capability is carried out in order to create a fixed set of constellation points to be demapped. This solution performs correctly for high code rates. For low code rates, the demapper proposed in [128] is used. The results show a reduction in the number of required operations from 69% to 93% depending on the code rate with performance losses below 0.1 dB.

Table 2.8. State-of.the-art of constellation design techniques for terrestrial broadcasting

Authors	**Title**	**Year**	**Design**	**Target**	**Contribution**
[113] and [114] Stott	CM and BICM Limits for Rectangular Constellations / Beyond NUQAM & ConQAM – Overcoming their Limitations, Especially at Lower SNRs	2013 and 2014	Constellation	Maximize BICM channel capacity	Design of NUCs via GS
[115] Zoellner et al.	Optimization of High-order Non-uniform QAM Constellations	2013		Maximize BICM channel capacity for high SNR values and Rayleigh channel	Design of high-order NUCs via GS using interior point optimization
[117] Loghin et al.	Non-Uniform Constellations for ATSC 3.0	2016		Evaluate the feasibility of ATSC 3.0 NUCs	Review of the NUCs included in ATSC 3.0
[118] Fuentes et al.	Optimization and Performance of Non-Uniform Rotated Constellations With Multi-RF Transmission Techniques	2016		Maximize BICM channel capacity for fading scenarios	Optimization of NUCs via GS with RC and multi-RF techniques
[119] Steiner et al.	Comparison of Geometric and Probabilistic Shaping with Application to ATSC 3.0	2016		Maximize BICM channel capacity via PS	Comparison of GS and PS approaches with application to ATSC 3.0

Table 2.9. State-of.the-art of demapping techniques for terrestrial broadcasting

Authors	Title	Year	Design	Target	Contribution
[120] Li et al.	Design of Rotated QAM Mapper/Demapper for the DVB-T2 Standard	2009	Demapper	Reduce the number of EDs with negligible system performance losses	Sub-region demapping algorithm for RC
[121] and [122] Calderon et al.	Rotated constellation demapper for DVB-T2 / Simplified Rotated Constellation Demapper for Second Generation Terrestrial Digital Video Broadcasting	2011 and 2013		Reduce the number of EDs to compute with negligible system performance losses	Statistical fixed sub-region demapper for DVB-T2 RC
[123] Tomasin et al.	Low Complexity Demapping of Rotated and Cyclic Q Delayed Constellations for DVB-T2	2012		Reduce the number of EDs to compute with negligible system performance losses	Per-dimension demapper based on sectorial division for DVB-T2 RC
[124] Kim et al.	One-Dimensional Soft-Demapping Algorithms for Rotated QAM and Software Implementation on DSP	2013		Simplify the demapping process of RC with negligible system performance losses	Low complexity RC demapper based on RC-QAM conversion to two PAM signals
[125] and [126] Tao et al.	Low-Complexity Switched Soft Demapper for Rotated Non-Uniform Constellation DVB-NGH Systems / Low Complexity Switched Soft Demapper for Rotated QAM Constellations	2014 and 2016		Efficient demapping technique for different types of constellations	Switched one-dimensional two-dimensional soft demapper for RC in fading channels
[127] Jafri et al.	High-Throughput and Area-Efficient Rotated and Cyclic Q Delayed Constellations Demapper for Future Wireless Standards	2017		Design the hardware architecture model of low complexity demapper for RC	Hardware architecture of a high-throughput and area-efficient RC demapper
[128] Kwon et al.	Simplified Non-uniform Constellation Demapping Scheme for the Next Broadcasting System	2015		Apply wrapping technique to NUCs for low SNR	Condensed demapper for NUCs at low SNR values
[129] Fuentes et al.	Low-Complexity Demapping Algorithm for Two-Dimensional Non-Uniform Constellations	2016		Apply fixed sub-region demapper to NUCs	Fixed sub-region demapper for 2D-NUCs

6.2 Satellite Communications

6.2.1 Constellation Design

QPSK is by far the most used scheme in satellite communication systems. With the development of DVB-S2 and DVB-S2X standards, *M*-ary APSK constellations with uniform and non-uniform geometrical shapes have been also included. Several authors hae proposed *M*-ary APSK constellations based on GS [130], [131], [133], [135], [136] and PS [130], [131], [132], [134]. Moreover, the design for different channel and system models has been also considered for satellite communications. In [132], the authors design 32-APSK for BICM-ID systems and in [133], the authors considered a non-linear satellite channel. Next, the above mentioned references are explained more in detail.

Liolis et al. (2008) [130] and (2010) [131] study the design of *M*-ary APSK constellations (M = 16, 32 and 64) for satellite applications considering two different approaches: GS and PS. For PS, the constellation points on each ring are assumed to be equiprobable but the a priori symbol probability per ring is considered different. The optimization problem consists of maximizing the average mutual information of the system. The channel considered is AWGN and phase and amplitude distortions are included. In the case of equiprobable constellation points (GS), the Gauss-Hermite quadrature rule is followed. The results show that the non-equiprobable constellations approach higher capacity than the equiprobable ones for relatively high SNR values.

Xiang et al. (2011) [132] improve the DVB-S2 system performance using constellation shaping and iterative demapping. The authors considered a 32-APSK constellation scheme to design the new signal set via PS. As PS requires a priori knowledge of the symbols transmitted in the design and receiver sides, the authors propose to incorporate the BICM-ID system for correct signal detection. This solution provides an additional 1 dB of coding gain at a rate of 3 symbols over an AWGN channel at the cost of increasing the receiver complexity.

Kayhan et al. (2012) [133] designed APSK constellation schemes via geometrical approach. The authors made use of the simulated annealing algorithm with a symmetry condition over the constellation points in order to speed up the computation for high order modulations. This algorithm allows to jointly optimize the constellation points and the bit labelling. 32-APSK is considered over nonlinear satellite channel under AWGN. The system performance is analyzed

with and without pre-distorters and the results of the designed constellations are compared with the APSK modulations used in DVB-S2. The simulation results show that the performance without pre-distortion techniques is improved about 0.4 dB and reduced to 0.2 dB if non-ideal HPA is considered. If pre-distortion techniques are enabled, gains slightly more than 0.3 dB are achieved with respect to the DVB-S2 standard.

Xiang et al. (2013) [134] extend their prior work proposing the optimization of codes for shaped modulation. In this way, the authors propose to change the variable degree distribution of the code in order to design a code whose EXIT curves are matched in a shaped modulation scheme. In the case of 32-APSK constellation using LDPC code with optimized degree distribution, additional gains of 0.44 and 0.43 dB for long (16,200 bits) and short (64,800 bits) length codes are achieved, respectively. If this solution is compared with a uniform system of the same rate, the shaping gain ranges from 0.6 to 0.73 dB, depending on the length of the code and the number of distinct variable node degrees. If shaping and coding are jointly considered, gains higher than 1 dB compared to the DVB-S2 standard are obtained.

Meloni et al. (2015) [135] and (2016) [136] propose the use of genetic algorithms in order to optimize APSK constellations and mapping using geometrical shaping. The objective function is the Minimum Square Error (MSE) between the symbol generated by the memoryless source and the one estimated at the receiver. The optimization problem aims to minimize the MSE designing new mapping techniques starting from conventional Consultative Committee for Space Data Systems (CCSDS) mapping and constellation points for different APSK configurations. The optimization results demonstrate that the use of modified mappings and unequally spaced symbols on the same circles improve the performance of conventional APSK in terms of MSE.

6.2.2 Detection Techniques

Contributions shown in Section 5.2.1 are applicable to satellite communication systems with APSK constellations such as DVB-S2. Two more works related with demapping techniques for APSK constellations in satellite communication systems are detailed below. The first one [137] deals with the improvement of system performance of the Max-Log-MAP for turbo decoding. The remaining one [138] considers product labelling demapper for APSK constellation to reduce the computational complexity with negligible degradation in system performance

Cho et al. (2007) [137] designed a soft decoding algorithm for 16-APSK constellations for DVB-S2 system. The authors employ pragmatic and statistical approaches in order to obtain the soft metrics as imperfect Gray mapping is used. The idea consists of finding the shapes of the bit region for each bit in a codeword and extract the metric via pragmatic and statistical approaches. The results show that if the proposed solution and the Max-Log-MAP decoder are compared using Turbo decoding, the proposed algorithm provides better system performance than Max-Log-MAP.

Xie et al. (2012) [138] propose the so-called product bit labelling for APSK constellations in order to reduce the demapping complexity. The authors create an APSK scheme based on a Gray labelled PSK constellation and a Gray labelled PAM constellation. In this way, the APSK constellation can be viewed as the Cartesian product of the PSK and PAM sets. At the demapping stage the APSK constellation can be decomposed in PSK and PAM sets and one-dimensional demapping can be applied to each one reducing the computational complexity with negligible degradation in system performance.

Table 2.10. State-of-the-art of constellation design and demapping techniques for satellite communications

Authors	Title	Year	Design	Target	Contribution
[130] and [131] Liolis et al.	On 64-APSK Constellation Design Optimization / Amplitude Phase Shift Keying Constellation Design and its Applications to Satellite Digital Video Broadcasting	2008 and 2010	Constellation	Maximize the average mutual information of the system for AWGN channel	Comparative study of APSK design via GS and PS
[132] Xiang et al.	Improving DVB-S2 Performance Through Constellation Shaping and Iterative Demapping	2011		Improve DVB-S2 system performance for BICM-ID system	PS with iterative demapping for DVB-S2
[133] Kayhan et al.	Constellation Design for Transmission over Nonlinear Satellite Channels	2012		Maximize the average mutual information of the nonlinear satellite channel under AWGN	APSK design via GS for DVB-S2
[134] Xiang et al.	Closing the Gap to the Capacity of APSK: Constellation Shaping and Degree Distributions	2013		Improve DVB-S2 system performance	Code optimization for PS APSK constellations
[135] and [136] Meloni et al.	On the Genetic Optimization of APSK Constellations for Satellite Broadcasting /64-APSK Constellation and Mapping Optimization for Satellite Broadcasting Using Genetic Algorithms	2015 and 2016		Minimize the minimum square error (MSE) in DVB-S2 system	APSK design via PS using genetic algorithm
[137] Cho et al.	An Approximated Soft Decoding Algorithm of 16-APSK Signal for DVB-S2	2007	Demapper	Improve system performance of max-log-MAP detector	Soft decoder for 16-APSK based on finding the shapes of the symbol bit region
[138] Xie et al.	Simplified Soft Demapper for APSK with Product Constellation Labeling	2012		Reduce the demapping complexity of APSK constellations	Product bit labelling APSK scheme to reduce demapping complexity

6.3 Fiber Optical Systems

6.3.1 Constellation Design

Constellation design techniques in fiber optical systems differs from the ones considered in terrestrial and satellite communications. In fiber optical systems, PS is considered as the input probabilities of the bits transmitted are not the same. Meanwhile all the works refer to PS, each reference design the constellation scheme for a determined objective function. Authors in [139] aim at maximizing the channel capacity. In [140] the objective is to minimize the energy of the transmitted signal via PS and the Vitervi algorithm. The authors in [142] propose to optimize the probability mass functions and in reference [143] error free decoding is imposed as the design objective.

Essiambre et al. (2010) [139] present constellation shaping as an option to provide efficient signal sets to optical fiber networks. The authors optimize the ring constellations by varying the ring spacing and the frequency of occupation on each ring. The capacity results of the designed constellations show that multi-ring constellations optimized via constellation shaping exceed the capacity values of one-ring. In the high SNR range, the capacity of one and multi-ring constellations becomes identical. For severe nonlinear distortions, the multi-ring constellation degenerates to a one-ring constellation. Maximum capacity is not achieved for more than two-ring constellations.

Smith et al. (2012) [140] design a pragmatic CM system incorporating signal shaping for high spectral efficiency fiber optic communications. The authors use a pseudo-MLC scheme in order to provide shaping through a bi-dimensional Gaussian distribution. The Viterbi algorithm is applied in order to minimize the energy of the transmitted signal. The results show that the system model proposed provides 0.62 bits/s/Hz per polarization of the estimated system capacity of length 2000 km.

Djordjevic et al. (2012) [141] use optimum signal constellations instead of QAM to facilitate the implementation of 400 GbE and 1 TbE technologies. The authors describe several optimum signal constellation designs such as: Iterative Polar Modulation (IPM), rotationally symmetric capacity achieving, energy-efficient signal constellation and feedback channel capacity inspired. If multidimensional systems, with dimension higher than 4, are considered few-mode fibers systems could enable multi-Tb/s serial optical transport at distances longer than 2000 km.

Yankov et al. (2014) [142] propose to optimize QAM constellation via PS for fiber optic channels. The authors optimized the Probability Mass Function (PMF) of a 1024QAM combining many-to-one mapping and turbo code. Spectral efficiency of up to 6.5 bits/s/Hz/polarization is achieved on a 800 km link.

Buchali et al. (2015) [143] design 64QAM constellation schemes via PS in order to provide adjustable data rate and capacity increase. PS is achieved via a distribution matcher which deliberately assigns different probabilities to the constellation symbols. Defining the reach as the maximum distance where error-free decoding is observed, the results show a 15% capacity increase and 43% reach increase if compared with 200 Gbit/s 16QAM. Arbitrary operation points can be chosen adjusting the shaping.

Fehenberger et al. (2016) [144] and (2016) [145] study the benefits of using PS QAM over uniform QAM carrying out back-to-back experiments. The experimental results are well aligned with simulations showing sensitivity gains of up to 0.8 dB over uniform input distributions. The authors also demonstrate that variations of the channel SNR of up to 11 dB in the low and medium SNR ranges do not require an adjustment of the input distribution if slightly reduced shaping gain is acceptable.

Table 2.11. State-of-the-art of demapping techniques for fiber optical systems

Authors	**Title**	**Year**	**Design Target**	**Contribution**
[139] Essiambre et al.	Capacity Limits of Optical Fiber Networks	2010	Maximum channel capacity	PS multi-ring constellation
[140] Smith et al.	A Pragmatic Coded Modulation Scheme for High-Spectral-Efficiency Fiber-Optic Communications	2012	Minimize the energy of the transmitted signal	Design of a pragmatic coded modulation with PS
[141] Djordjevic et al.	Optimum Signal Constellation Design for Ultra-High-Speed Optical Transport Networks	2012	facilitate the implementation of 400 GbE and 1 TbE technologies	Implementation of 400 GbE and 1 TbE technologies using PS
[142] Yankov et al.	Constellation Shaping for Fiber-Optic Channels with QAM and High Spectral Efficiency	2014	Optimize the probability mass function	Optimization of high order QAM via PS
[143] Buchali et al.	Experimental Demonstration of Capacity Increase and Rate-Adaptation by Probabilistically Shaped 64-QAM	2015	Achieve error free decoding	Design of PS 64QAM for adjustable data rate
[144] and [145] Fehenberger et al.	Sensitivity Gains by Mismatche Probabilistic Shaping for Optical Communication Systems / On Probabilistic Shaping of Quadrature Amplitude Modulation for the Nonlinear Fiber Channel	2016	Experimental analysis of PS QAM over uniform QAM	PS QAM schemes present gains of up to 0.8 dB over uniform input distributions

6.4 **Other Communication Systems**

6.4.1 Broadband

In the case of broadband systems such as 4G/LTE, the constellation schemes used are QPSK and QAM due to their simplicity and trade-off between throughput and robustness. 5G-NR systems use the same constellation schemes as 4G/LTE with higher constellation orders, i.e., up to 256QAM. Regarding the demapping stage, as MIMO is a technique used in this system, the contributions detailed in Section 5.1 are applicable to the demapper part. Another contribution related with the demapping of 256QAM constellations for 5G systems is found in [146].

Mao et al. (2016) [146] design a low complexity 256QAM soft demapper for 5G mobile system. In this work, in order to find the nearest points to the received observation, a piecewise function is generated and approximated as one linear function in order to simplify the soft detection. The demapper is evaluated in the context of an OFDM system and the results show similar performance between the proposed demapper and the Max-Log-MAP. The results show that the proposed demapper requires over 200 times less time than Max-Log-MAP to demap one bit.

6.4.2 Cable TV

Another use case of the constellation and demapper design presented in the previous sections can be found in systems that make use the Data Over Cable Service Interface Specification (DOCSIS). This standard is commonly used by cable TV operators and supports up to 8192 non-uniform QAM constellations. In order to cope with the demapping complexity associated to such high order modulations, in [147] a simplified non-square QAM demapper is proposed for DOCSIS 3.1 systems.

Lee et al. (2017) [147] propose a simplified demapper for the DOCSIS 3.1 system where non-square quadrature amplitude modulation schemes are used. In this case, independence between several bits of the symbol is exploited to simplify the demapping process using the fold-and-overlap approach on the Max-Log-MAP algorithm. Simulation results showe that the proposed method has negligible BER performance degradation with complexity reductions of up to 93% if compared to Max-Log MAP.

7. Analysis of Remaining Work

7.1 Constellation Design

Many references are available in the field of constellation design via Probabilistic (PS) and Geometrical Shaping (GS). GS demonstrates higher channel capacity than PS. Two main criteria for GS constellation design are considered in the bibliography, i.e., minimization of the error probability and maximization of the channel capacity. Several works focus on maximization of channel capacity by approximating the pdf of the transmitted signal to a Gaussian function. Further improvement is possible for a BICM system if the capacity for this system is maximized. 1D-NUCs are designed for a BICM system achieving a smaller gap to the ultimate Shannon limit. Next, 2D-NUCs constellations are proposed up to 32 constellation points. 1D-NUCs and 2D-NUCs are analyzed in order to check the BICM system performance, showing a system gain of more than 1.5 dB.

In conclusion, works related to the theory behind the two shaping approaches and the implementation of the designed constellations in different communication systems can be found. However, there is not any work in the state-of-the-art that assesses the optimization problem and establishes the most adequate optimization algorithm to design constellations in an efficient way for BICM system models. Furthermore, if the constellation set is optimized for fading channels such as Rayleigh, there is not any solution simplifying the optimization procedure for such channels. Finally, there is a lack of a work that encomprises the constellation design for a whole range of SNRs, defining in detail all the steps to be carried out in the optimization process.

Chapter 4 of this thesis focuses on the above mentioned points in order to create a reference work about the design of constellations via GS from theory to implementation for BICM system models.

7.2 Demapping Strategies

Two main areas are distinguished in the state of the art of demapping strategies, i.e., MIMO and SISO systems. For MIMO systems, there are two main demapping techniques: Lattice Reduction (LR) and Sphere Decoder (SD). For LR, the existing literature deals with the efficient calculation of the radius value in order to reduce the computational complexity at the demapping stage. For the SD, the contributions mostly try to replace the exhaustive search method with other

techniques. List sphere decoder is developed in several works as a way to reduce the computational complexity of sphere decoder.

For SISO systems, five main low complexity techniques can be found: one-dimensional, sub-region, product constellation, per-dimension and condensed demapper. One-dimensional and product constellation demappers are mainly used for QAM and APSK constellation schemes. Demapping complexity reduction for such constellation schemes has been a field of study in the last decade and many works deal with the complexity reduction associated to such constellation schemes. In the case of RC the main strategy is the sub-region demapper using fixed regions of constellation points. Per-dimension demapper is also proposed in RC applications.

Some 1D-NUCs and 2D-NUCs designed via GS for BICM system models are quite recent. In consequence, there is a research gap to develop low computational demappers for such constellation schemes. Although several studies have been recently carried out lowering demapping complexity there is still room for further improvement. The variable nature of the channel fading coefficients can be taken into account in order to design an adaptive sub-region demapper. The characteristics of the NUCs in the design procedure can be extrapolated to the demapping process in order to provide an efficient decoder algorithm. Finally, several characteristics of the demapper can be incorporated to the design of constellations as an input condition for the design process, constructing efficient NUCs that provide high spectral efficiency and low demapping complexity.

Chapter 5 of this thesis focuses on the above mentioned points and proposes low complexity demappers for 1D-NUCs and 2D-NUCs improving the performance of state-of-the-art demappers.

CHAPTER 3: **SYSTEM PERFORMANCE ANALYSIS OF ADVANCED MODULATION TECHNIQUES IN DTT BROADCAST SYSTEMS**

This chapter focuses on the analysis of two different constellation techniques: Non-uniform Constellation (NUC) and Rotated Constellation (RC). Lately, new LDPC codes with code rates from 2/15 to 13/15 and different structures of Parity Check Matrix (PCM) have been proposed for the next-generation DTT systems. The combination of NUCs and RC technique with the new LDPC codes is analyzed and compared with existing Modulation and Coding (ModCod) schemes to check out the feasibility of these proposals. The methodology to perform the study is derived in this chapter, detailing the metrics, evaluation cases and tools used.

The first analysis compares the system performance of NUC schemes and standard QAM schemes with the new LDPC codes in terms of BER versus SNR for AWGN and Rayleigh iid channels.

The second study compares the system performance of NUCs and new LDPC codes with and without RC technique. The study is carried out for three different channel models: Rayleigh iid, Rayleigh P1 and 0 dB Echo. The results are obtained via system performance simulation using the two simulation platforms (BICM and OFDM) designed in this thesis.

1. INTRODUCTION

One of the key factors for the successful deployment of the multimedia delivery platforms is closely related to its flexibility and efficiency, the latter measured in roll out and operational costs, carbon footprint as well as spectral resource consumption.

Current multimedia platforms are facing the challenge of satisfying the significantly increasing bitrate demands associated to Ultra-High Definition TV (UHDTV) content [148]–[150] and, in the midterm, they will need to deal with the augmented reality services. First generation UHDTV contents are either available in certain platforms [151] or expected in the short term [152], [153]. UHDTV will come not only with an increase in the number of pixels per frame [154] but also with "better pixels", featuring bit depth, High Dynamic Range (HDR), High Frame Rate (HFR), Wide Color Gamut (WCG). These advances imply a significant increase in bitrate requirements [155], from about 10 Mbps in the case of a simple 4K extension and up to 20 Mbps if all 4K+HFR+HDR+WCG are implemented.

There are two well known approaches that improve capacity and performance of DTT standards: video coding algorithms and physical layer efficiency optimization. Current video coding state-of-the-art products provide UHDTV output bitrates in the range from 15 to 20 Mbps, again depending on the UHDTV options used. The second approach is related to advanced radio interface design. This family includes better channel coding [156], smart spectral occupation options such as Channel Bonding (CB) in ATSC 3.0 [157], extended modes [158], optimized frequency utilization [159], MIMO [160], low complexity Non-Orthogonal Multiple Access (NOMA) technique such as Layered Division Multiplexing (LDM) [161] and advanced modulation techniques such as RC [85] and NUC [113], [114].

The efficiency increase in channel coding is related wih the development of very robust LDPC codes [162] with a new structure of the Parity Check Matrix (PCM) [163], [164]. These LDPC codes are able to perform at decoding thresholds below 1 dB of SNR solving the signalling issue of DVB-T2 [166]. However, there is still room for improvement in the modulation block where standard QAM schemes are still in use.

The main objective of this chapter is to evaluate and compare the performance of NUCs with RC technique against the existing modulation technique from the previous DTT broadcast standard DVB-T2. This chapter provides results of the system performance of NUCs with RC with the new LDPC codes. These results

are compared with the ones obtained from the previous modulation scheme, i.e., QAM in order to validate the new modulation proposal.

The new modulation technique and the evaluation methodology are detailed in Section 2. Next, the system performance of NUCs and RC technique is studied and compared with standard QAM schemes. Finally, the conclusions of the study carried out in this chapter are shown.

2. MODULATION TECHNIQUE FOR THE NEXT GENERATION DTT SYSTEM

This section presents the basis behind the NUCs, explaining where they come from and their geometrical characteristics. Next, the necessity and challenges associated to the evaluation of NUCs and RC technique is explained. Finally, the evaluation methodology carried out is detailed showing the metric, evaluation cases, and tools.

2.1 Characteristics of NUCs

Up to date, the most efficient system model for broadcast applications is the BICM [46] due to its performance under fading conditions. In order to design a spectrally efficient DTT broadcast communication system, the objective is to maximize the BICM channel capacity shown in [46].

Geometrically shaped NUCs are proposed as a solution to maximize the BICM capacity of a communication system in order to reduce the gap between QAM schemes and the capacity limit proposed by Shannon. The reasons for using geometrical and not probabilistical shaping were discussed in Chapter 2.

Analyzing the equation of the BICM channel capacity, given a SNR value and a concrete channel model, the only factor which affects the BICM channel capacity is the position and bit labelling of the constellation points. Therefore, for a given SNR value and channel model, there is only one set of positions and labelling of the constellation points that maximizes capacity.

The optimal shape of NUCs depends on the noise value, the channel model and the number of Degrees of Freedom (DoFs) in the design procedure.

For high noise values, the Least Significant Bits (LSBs) of each symbol are sacrificed in order to provide higher gain to the Most Significant Bits (MSBs). This is a consequence of the distortion, which prevents the detection of the LSBs. For low noise values, the optimum NUC is the one with the highest possible separation between the constellation points. In such case, the best option is to allocate the same capacity to each one of the bits. This sort of constellation is the standard uniform constellation, i.e., QPSK, *M*-ary QAM. In Figure 3.1 the shaping changes of optimized NUC for different noise values are shown.

The channel model is also a key parameter that will have a significant influence

on the BICM channel capacity. The optimum NUC for the same SNR value and the same DoFs is different if it is optimized for an AWGN or a Rayleigh iid channel.

The number of Degrees of Freedom (DoF) of the NUC also modifies the shape of the NUC, i.e., the number of constellation points to be optimized. Besides, this parameter not only identifies the number of constellation points to be moved but also the number of real and imaginary components of the whole constellation to be optimized.

In the design of NUCs, quadrant symmetry (one quadrant is designed and the remaining three quadrants are completed by symmetry) is used. This symmetry allows a reduction by a factor of four in the DoFs of NUCs without capacity loss. Taking into account the DoFs parameter, there are two main types of NUCs: One-Dimensional NUC (1D-NUC) and Two-Dimensional NUC (2D-NUC).

2.1.1 One-Dimensional Non-Uniform Constellations

1D-NUCs present a rectangular shape provided the I and Q components are two independent PAM components as shown in Figure 3.1. In this way, the number of DoFs is reduced and so does the complexity at design and demapping steps. Any *M*-ary constellation presents up to 2*M* DoFs. However, in the case of 1D-NUC considering quadrant symmetry, the number of DoFs at the design procedure is $\sqrt{M}$, where *M* is the number of symbols.

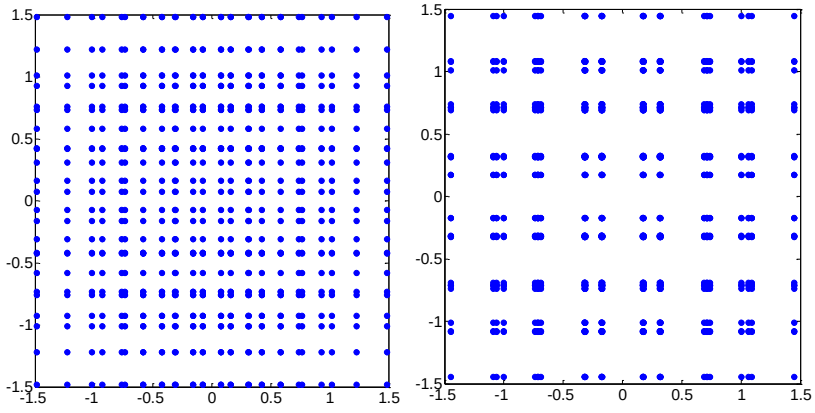

Figure 3.1. 1D-NUC for 1024 constellation points at 20 dB SNR (left) and 11 dB SNR (right)

One of the main advantages of 1D-NUC (if compared to 2D-NUC) is the complexity reduction at the demapping stage, where one dimensional demapper can be used with complexity $O(2\sqrt{M})$ at the cost of a loss in the system performance.

2.1.2 Two-Dimensional Non-Uniform Constellations

2D-NUCs are characterized by their circular shape given by a complete freedom of movement of all of the constellation points. The shape of 2D-NUCs is shown in Figure 3.2. Regarding the number DoFs of 2D-NUC is $\frac{M}{2}$ if quadrant symmetry is assumed, higher than for 1D-NUCs. However, this increase of the DoFs provides better performance at the cost of higher complexity at the demapping step, i.e., $O(2M)$.

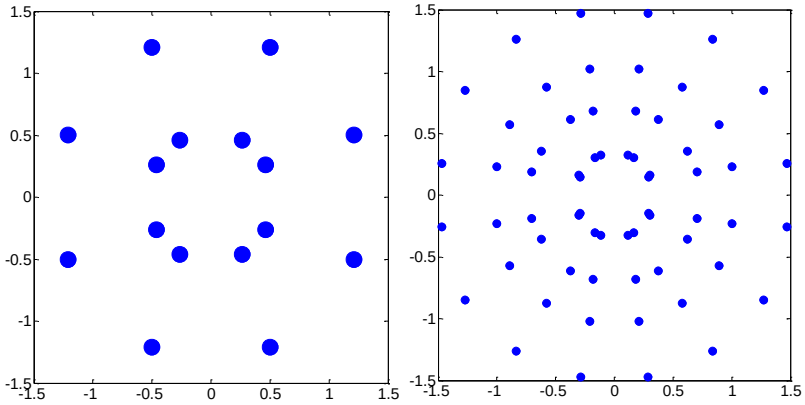

Figure 3.2. 2D-NUC for 16 constellation points at 6 dB SNR (left) 2D-NUC for 64 constellation points at 12 dB SNR (right)

NUCs based on non-uniform APSK constellations have already been tested in satellite applications. However, NUCs have not been evaluated under terrestrial channel models yet (at the time of realization of this thesis), e.g., Rayleigh channel. Besides, the design of new LDPC codes performing in the range of SNR below (1 dB) makes it necessary to test the combination of NUCs with the new codes under AWGN and fading scenarios.

2.2 Evaluation Methodology

This section describes the methodology used for evaluating NUC performance. The methodology is composed of three steps:

- Definition of a standardized metric for evaluation that permits comparison between NUCs and standard QAM schemes.
- Definition of the evaluation cases that represent real terrestrial broadcast scenarios.
- Creation of an evaluation tool that provides accurate results for the metric and scenarios defined.

2.2.1 Metric

The evaluation results of NUCs are given in terms of SNR value for a determined BER at LDPC decoding step. This metric is widely used for the evaluation of physical layer techniques [115], [118], [166] and validation of the system performance of any communication system [7], [167], [168]. Error free transmission is assumed and the simulation step is 0.1 dB.

2.2.2 Evaluation Cases

Physical layer technologies developed for DTT broadcast systems are commonly evaluated under two main channel conditions, i.e., AWGN and Rayleigh iid channel models [115]. AWGN provides a first system performance insight of the technique developed, when no fading is considered. Ricean channel is used to describe the fixed, outdoor rooftop-antenna reception conditions when there is line of sight ray. Rayleigh iid channel model is commonly used to describe the portable indoor or outdoor reception conditions with no line of sight.

In this work, Rayleigh iid channel model is considered instead of Rice model as it represents a more challenging fading scenario. DVB-T and DVB-T2 standards define a particular Rayleigh channel model for fading conditions. The channel does not include any Doppler and should therefore be considered as a snapshot of the real time-variant Rayleigh channel with 20 taps. Finally, the 0 dB Echo at 90% of the Guard Interval (GI) profile defined in DVB-T2 is also considered as the worst case in Single Frequency Networks (SFN).

2.2.3 Evaluation Tools

In order to carry out the different evaluation cases, two different evaluation tools have been developed in this thesis. For AWGN and Rayleigh iid evaluation cases, a very low time consuming BICM communication chain was designed. This tool (implemented in Matlab) is shown in Figure 3.3 and includes the necessary basis blocks to test the physical layer of any BICM communication system. The first block is a data generator based on a Pseudo-Random Binary Sequence (PRBS) that provides a fixed sequence of data bits. Next, the FEC encoder codifies the data bits using BCH as outer coder in order to elimite the error floor of the LDPC codes. The next block is the LDPC inner coder which includes the new LDPC code rates and PCM structures explained in Section 1. The bit interleaver block is based on the one proposed in [173]. The transmitter block ends with the mapper block where the bits are mapped into symbols of the NUCs.

The evaluation tool uses the rotation and component interleaver defined in DVB-T2 is performed. RC technique from DVB-T2 is a well established technique for both the transmitter [169] – [172] and the receiver blocks [120] – [124]. However, RC technique from DVB-NGH is a recently developed technology and further research must be performed to prove its viability in DTT systems.

The BICM system model includes two different types of channel models: AWGN and Rayleigh iid.

The receiver part contains all the necessary blocks to recover the information sent by the transmitter. The receivers' blocks provide BER measurements in order to evaluate the system performance.

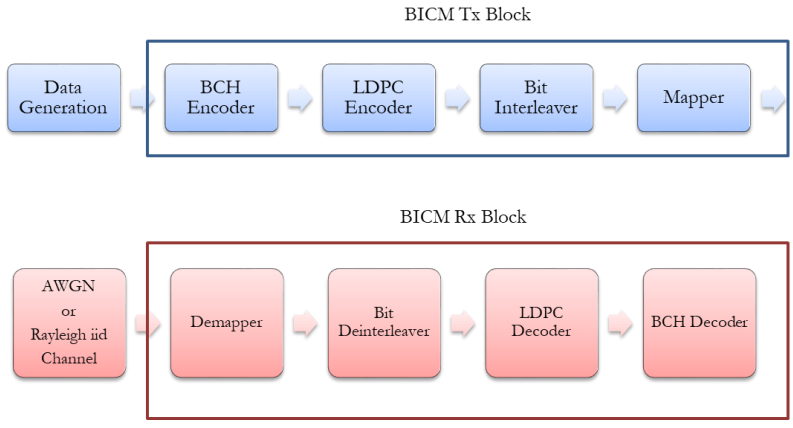

Figure 3.3. BICM system model simulation tool.

The system performance evaluation of NUCs is carried out using the BICM tool described above. If RC technique is applied, superior performance under demanding fading scenarios is achieved [170].

In order to evaluate RC under Rayleigh P1 and 0 dB Echo at 90% of GI channels, BICM tool is no longer valid. Therefore, the OFDM transceiver shown in Figure 3.4 is designed. This system model includes the OFDM blocks defined in DVB-T2 standard for single Physical Layer Pipe (PLP). The BICM part remains the same as defined before. The configuration of the simulation parameters is as follows:

- 300 FEC blocks with 64,800 bit length.
- All the interleavers for single PLP are used.
- Ideal Channel State Information (CSI) and perfect synchronization is considered.
- Simulation step 0.1 dB.

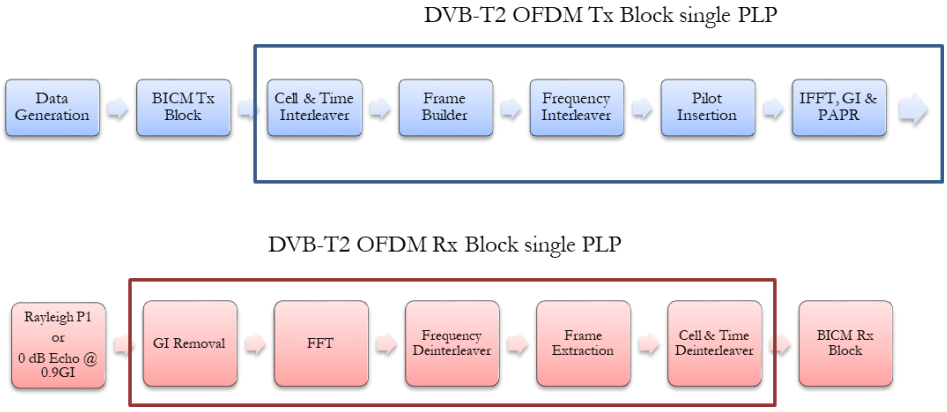

Figure 3.4. OFDM system model simulation tool.

3. RESULTS

This section presents the results obtained from the evaluation of NUCs and RCs using the evaluation methodology detailed in Section 2.2.

3.1 Non-Uniform Constellations

NUCs are evaluated for constellation points from 16 to 256 and code rates 3/15, 6/15, 9/15 and 12/15. These results were obtained using the BICM system model simulation tool described in the previous section. The system performance is tested under AWGN and Rayleigh iid channels and QAM results are also obtained for comparison. Figure 3.5 shows the results obtained for the above mentioned system configurations.

The main conclusion extracted from the results is that NUCs outperform QAMs for the same constellation order. The only case when their performance is similar occurs with 16 constellation points on a Rayleigh iid channel. In this case, the designed NUCs provide gain over QAM for the AWGN channel but not on the Rayleigh. For higher order constellations, NUCs outperform QAM for both channel models. Higher gains are achieved for the AWGN channel than for the Rayleigh iid due to the optimization procedure (the objective SNR is set for AWGN channel). In general, the four schemes show that NUCs greatly outperform QAM for low and mid code rates (in the range from 3/15 to 6/15) and the gain is lowered for code rates from 9/15 to 12/15. As stated in Section 2.1, NUCs are designed via GS and, in the range of high SNR values, their shape is similar to the standard QAM.

The observation of the four subfigures shows that the highest gain for 16 constellation point schemes is found on the lowest code rate. If the results of higher constellation orders are evaluated, the highest gain is found for 6/15 code rate, i.e., the higher the constellation order the higher the code rate is for achieving the highest gain. The reason of this trend is that the number of DoFs for higher order constellatios is higher for mid code rates as there are no geometrical restrictions such as condensation or QAM shaping.

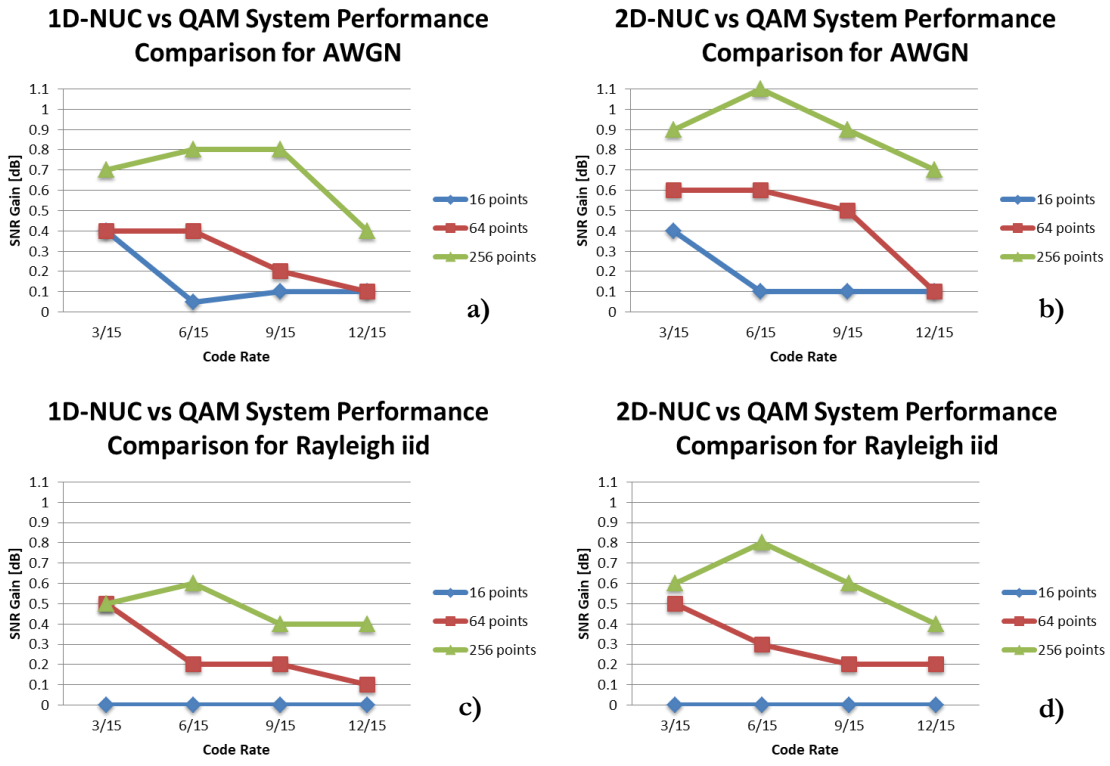

Figure 3.5. M-ary NUC versus M-ary QAM system performance comparison for M = 16, 64 and 256. a) 1D-NUC vs QAM for AWGN channel. b) 2D-NUC vs QAM for AWGN channel. c) 1D-NUC vs QAM for Rayleigh iid channel. d) 2D-NUC vs QAM for Rayleigh iid channel

The results from Figure 3.5 also show that 2D-NUCs do not only outperform QAM schemes but also 1D-NUCs. The cases where a slight difference exists between 1D-NUCs and 2D-NUCs are 16 constellation point schemes and some constellations of 64 points (in the range of mid code rates).

3.2 Combination of Non-Uniform and Rotated Constellations

This sub-section tests the combination of NUCs and RCs with the new designed code rates. Only fading scenarios are considered, i.e., Rayleigh iid using BICM system model and Rayleigh P1 and 0 dB Echo at 90% of the GI. In the case of the RC technique the I and the Q components of a constellation point are separated, interleaved individually and afterwards combined with Q and I components, respectively, of other rotated symbols. The individual transmitted samples experience fading that affects both components identically in the form of a (time- or frequency-) variant channel. At the receiver, the I and Q components of the received samples are split again, de-interleaved individually and recombined to their original rotated symbols. If there is no fading, i.e., AWGN channel, the receiver will see the rotated constellation plus the additive noise. In case of fading, the I and/or Q components will be squashed. The evaluation of NUCs and RC for different constellation orders is shown in Section 3.2.1. The results are obtained for code rates from 5/15 because RC technique only provides system gains for high code rates [169], [170]. NUCs and RC for P1 and 0 dB Echo channels are tested in Section 3.2.2 using the OFDM simulation platform.

3.2.1 Different constellation orders

This sub-section evaluates the RC system performance gain considering NUCs of different number of constellation points. Constellation orders from 4 to 64 points and code rates from 5/15 to 13/15 using the BICM evaluation tool described in Section 2.2.3 for the Rayleigh iid cannel model.

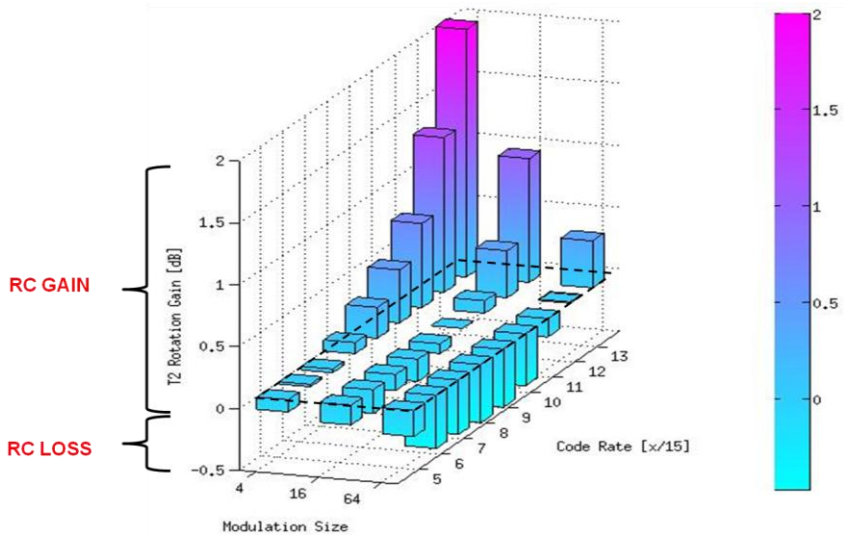

Figure 3.6. System performance gain of RC technique for ModCods defined in ATSC 3.0.

As shown in Figure 3.6, system performance gains of up to 2dB are achieved for QPSK and *R*=13/15. On the other hand, there are some Modulation and Coding (ModCod) combinations that provide losses of up to 0.5 dB (for 64 constellation points and 8/15). The curve tendency suggests that for constellations higher than 64 constellation points there is no gain if RC is used. If RC is applied to 256-NUCs there is only gain of 0.1 dB for 13/15 code rate. Figure 3.6 suggests that rotated constellations provide gains for low order constellations and high code rates. For high order constellations, the range of code rates at which RC provides gain is lower than for low order constellations. What is more, for low code rates and high order constellations RC implies system performance losses. The gains shown with RC are in regions with minimum importance for broadcast applications.

3.2.2 Different channel models

This section describes the performance tests of RC under different fading scenarios. The system performance is studied on two very demanding stationary channels used in broadcast communication systems, i.e., Rayleigh P1 and 0 dB Echo at 90% of the GI. As a result of the study carried out in the previous section, only code rates ranging from 8/15 to 13/15 are evaluated.

Figure 3.7 shows the gain of RC with respect to non-rotated constellations using QPSK. Results show that if the RC technique is applied under 0 dB Echo

channels, the system performance gain is higher than the one in Rayleigh P1 channels. The highest gain is obtained for QPSK and R=13/15 with an SNR gain of 4 dB under the 0 dB Echo channel. This ModCod is 2 dB more efficient for the 0 dB Echo channel than for the Rayleigh P1 channel. If the analysis is extended to 16NUC and 64NUC, the tendency (gain difference among the 0 dB Echo and the Rayleigh P1) remains unaltered between both channel models with gains of 1.2 dB and 0.4 dB for the 13/15 code rate, respectively.

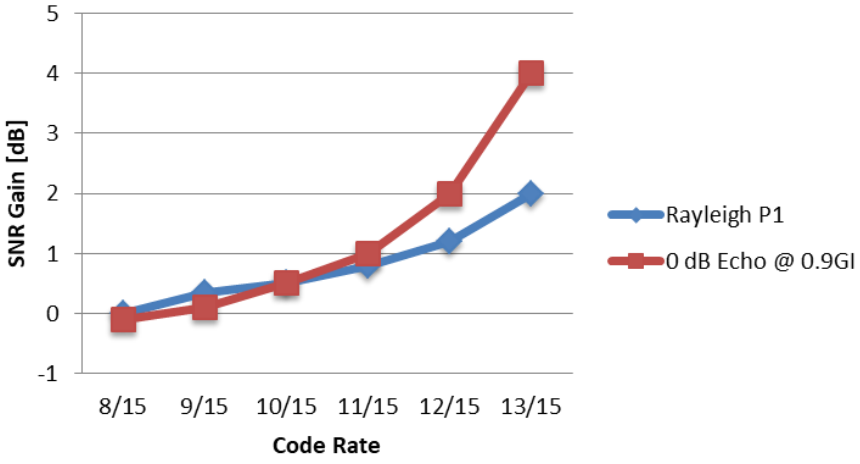

Figure 3.7. RC versus non-rotated QPSK performance gain for Rayleigh P1 and 0 dB Echo channels.

In conclusion, RC technique performs better for the most demanding scenario tested, i.e., 0 dB Echo at 90% of the GI.

3.3 Equivalent ModCod Combinations

The results in Section 3.2 show that RC provides gains for ModCods of high code rate with low order constellation. These ModCod combinations are not commonly used in broadcast applications because the system performance is degraded with respect to their counterparts, i.e., high order constellation with low code rate. However, the RC technique improves the system performance of those not very used ModCods under fading conditions. As a consequence, this section discusses the use of RC with low order constellations and high code rates.

The possible ModCod combinations consider constellation orders from 4 to 256 and code rates from 2/15 to 13/15. A total number of 48 ModCod

combinations are obtained, as shown in Table 3.1. There are several combinations with the same throughput value (boxes with same color) but with different SNR threshold value for the same BER value, as depicted in Section 3.1. Table 3.1 shows the throughput in terms of information bit/symbol for all the ModCod combinations.

Table 3.1. Classification of ModCod combinations with similar throughput value [Information bit/symbol]

Const. order	Code Rate [x/15]											
	2	3	4	5	6	7	8	9	10	11	12	13
4	0.26	0.40	0.53	0.66	0.80	0.93	1.06	1.20	1.33	1.46	1.60	1.73
16	0.53	0.80	1.06	1.33	1.60	1.86	2.13	2.40	2.66	2.93	3.20	3.46
64	0.80	1.20	1.60	2.00	2.40	2.80	3.20	3.60	4.00	4.40	4.80	5.20
256	1.06	1.60	2.13	2.66	3.20	3.73	4.26	4.80	5.33	5.86	6.40	6.93

Table 3.1 shows that there are different ModCod combinations which provide similar throughput. Table 3.2 compares the system performance of a high order constellation with low code rate (referred as ModCod A) with the ModCods of similar throughput with lower order constellation and higher code rate with the RC technique (referred as ModCod B). Rayleigh P1 and 0 dB Echo at 90% of the GI channels are considered. Results represent the gains in dB of ModCod A over ModCod B.

Results in Table 3.2 demonstrate that ModCods A outperforms ModCods B. The reason behind these results is the robustness of the new LDPC codes designed for the low SNR range. Any ModCod with such a low code rate outperforms the ModCods with similar throughput and higher code rate value.

In conclusion, RC technique only provides system performance gains for ModCods with high code rates and low order constellations. In the case of ModCods with similar throughput, the ones with low code rates and high order constellations outperform rotated ModCods with high code rates and low order constellations.

Table 3.2. System performance comparison between ModCod A and ModCod B for the Rayleigh P1 and the 0 dB Echo channels.

ModCod A vs. ModCod B	Rayleigh P1	0 dB Echo @ 90% GI
R=4/15+64NUC vs. R=12/15+QPSK	+1.4	+1.77
R=8/15+64NUC vs. R=12/15+16NUC	+1.3	+1.77
R=9/15+256NUC vs. R=12/15+64NUC	+0.9	+1.98
R=5/15+16NUC vs. R=10/15+QPSK	+0.6	+0.88
R=5/15+256NUC vs. R=10/15+16NUC	+0.7	+0.96
R=3/15+64NUC vs. R=9/15+QPSK	+0.3	+0.12
R=4/15+16NUC vs. R=8/15+QPSK	+0.3	+0.06

4. Conclusions

This chapter has evaluated new modulation techniques with new LDPC code rates and PCM structures. A methodology has been proposed for testing their performance

First, the basis of geometrically shaped NUCs has been detailed showing the geometrical changes experienced by the constellation designed depending on the SNR target value at decoding threshold value. The higher the target SNR, the constellation is more similar to the standard QAM scheme. In the range of low SNR values, adjacent constellation points tend to merge into a single position. This effect is known as condensation. For low and mid SNR values, the shape of the NUC depends of the number of DOF considered in the design process. 1D-NUCs present square shaping meanwhile 2D-NUCs resembles an APSK constellation. The number of DoFs in the design defines not only the design complexity but also the receiver complexity. 1D-NUCs present lower demapping complexity than 2D-NUCs, $O\left(2\sqrt{M}\right)$ and $O(2M)$, respectively.

BICM and OFDM transceivers resembling DTT broadcast communication system including NUCs, RC and the new LDPC codes have been designed for the evaluation of the modulation techniques. Commonly used broadcast scenarios such as Rayleigh iid, Rayleigh P1, 0 dB Echo at 90% of the GI and AWGN are considered for the evaluation. The results are given in terms of SNR threshold value at LDPC decoding step for a BER = 10^{-6}.

The results demonstrate that NUCs outperform QAM schemes. 2D-NUCs do not only outperform QAM schemes but also 1D-NUCs with a maximum gain of 1.1 dB over QAM scheme for 2D-256NUC with 6/15 code rate for AWGN channel. The results obtained for RC show that the rotation and component interleaving provides gain for high code rates. Besides, the lower the constellation order, the higher the gain with RC is with a maximum gain of 2 dB for QPSK and 13/15 code rate. If different fading scenarios are considered, i.e., Rayleigh P1 and 0 dB Echo at 90% of the GI the results show that RC provides higher robustness for the most demanding scenario, i.e., 0 dB Echo.

Finally, for the same throughput, ModCods with low code rates and high order constellations outperform rotated ModCods with high code rates and low order constellations

CHAPTER 4: **DESIGN OF ADVANCED CONSTELLATION SCHEMES TO IMPROVE BICM SYSTEM CHANNEL CAPACITY**

This chapter presents a generic methodology to optimize constellations based on their geometrical shape for BICM systems. While the method can be applicable to any wireless standard design it has been tailored to two delivery scenarios typical of broadcast systems: 1) robust multimedia delivery and 2) UHDTV quality bitrate services. The design process is based on maximizing the BICM channel capacity for a given power constraint. The major contribution is a low complexity optimization algorithm for the design of optimal constellation schemes for AWGN and Rayleigh channels. The proposal consists of a set of initial conditions for a particle swarm optimization algorithm, and afterwards, a customized processing procedure for further improving the constellation alphabet. The method has been optimized according to the broadcast application cases and the sizes of the constellations proposed range from 16 to 4096 symbols. The BICM channel capacities and performance of the designed constellations are compared to conventional quadrature amplitude modulation constellations for different application scenarios. The results show a significant improvement in terms of system performance and BICM channel capacities under additive white Gaussian noise and Rayleigh independently and identically distributed channel conditions.

1. Introduction

The optimization of constellation sets has been one of the most appealing research fields in the last years for the information theory community. As it has been shown in Chapter 2, GS constellations are the modulation scheme that best fits in broadcast applications. The analysis carried out in Chapter 3 demonstrates that NUCs show a relevant system performance improvement in comparison with the commonly used quadrature amplitude modulation (QAM) schemes.

The design of advanced constellation schemes (both GS or PS) must be analyzed taking into account three main Key Performance Indicators (KPI): system performance evaluation (Chapter 3), design complexity (Chapter 4) and receiver complexity (Chapter 5). In the case of the design of NUCs via GS for BICM systems, the optimization problem is very complex as the objective function (BICM channel capacity) is a non-linear expression. Several works deal with the design of NUCs with the objective of maximizing the BICM channel capacity equation. In [113] and [63] 1D-NUCs are designed lowering the gap to the ultimate Shannon limit. In [65], those results are extended to 2D-NUCs for configurations up to 32 constellation points. The work presented in [115] deals with the design of 1D-NUCs and 2D-NUCs. The design procedure used is the interior point optimization algorithm [116]. In [28] the standard Nelder-Mead method is selected to design NUCs. These techniques are both too complex and computationally expensive and, what is more, the importance of initial conditions is not highlighted. Another weak aspect in those publications is the lack of description of some of the post-processing steps. In terms of time consumption, the computational complexity of the above mentioned methods may result into hours or even days to design even in the case of the simplest constellation, i.e., 16 constellation points.

This chapter presents an efficient design process to optimize NUCs applicable to BICM systems. The proposed solution must provide significant lower design and computational complexity when compared to proposals described in Chapter 2 for both AWGN and Rayleigh channels. The work is focused on broadcast use cases, but it is also valid for generic wireless standards designs.

In order to validate the proposed procedure, the efficiency of the designed constellations is evaluated and compared with QAM schemes looking at two corner use cases in the broadcasting field: from robust service delivery targeting mobile and portable indoor (from around 0 dB of SNR) to high bitrate applications such as UHDTV (around 25 dB of SNR). The demapping complexity of each of the designed NUCs is also presented.

2. ANALYSIS OF THE OPTIMIZATION PROBLEM

2.1 BICM Channel Capacity

A BICM system consists of a consecutive coding, interleaving and mapping process. Zehavi firstly recognized that the combination of binary encoding, bit-wise interleaving and *M*-ary modulation provides better performance over fading channels than Trellis Coded Modulation (TCM) or Coded-Modulation (CM) [41]. The channel capacity for a BICM system was firstly shown in [46].

Nowadays, many communication systems make use of the BICM architecture in order to improve their performance (ATSC 3.0 [173], DVB-T2 [177], DVB-S2 [167], DVB-C2 [168]). The BICM structure is also on the core of the most successful broadband communication systems (LTE [178]) and very well implemented wireless systems such as IEEE 802.11n [179].

The total BICM channel capacity can be calculated as the sum of the capacity of each bit mapped to the constellation. The capacity of a bit is the amount of information known by the receiver given that the source transmits the bit b_i. Equation 4.1 shows the capacity of each of the bits associated to a constellation symbol.

$$C_{b_i} = \int_{r_y} \int_{i_y} \frac{p(y|b_i \; is \; 0) \log_2 p(y|b_i \; is \; 0) + p(y|b_i \; is \; 1) \log_2 p(y|b_i \; is \; 1)}{2} - p(y) \log_2 p(y) \, dr_y di_y \tag{4.1}$$

Where b_i is one of the bits mapped to the symbol constellation and r_y and i_y are the real and imaginary parts of the received symbol y, respectively. Furthermore $p(y|b_i \; is \; 0)$ is the conditional probability of receiving y given that the b_i transmitted is 0 and $p(y|b_i \; is \; 1)$ is the conditional probability of receiving y given that b_i transmitted is 1. We consider that $p(b_i \; is \; 0) = p(b_i \; is \; 1) = 0.5$.

Given the computational complexity associated to the double integral expression, the BICM channel capacity calculation is approximated by replacing the integrals in Equation 4.1 by a sum of the possible received symbols. The received symbols are uniformly distributed along the constellation diagram and the separation between them depends on the expected noise power value, i.e., the higher the noise value the higher the distance among adjacent points is. Following this proposal, the computational calculation of the channel capacity is highly reduced and the capacity results remain unaltered up to the fourth decimal in the capacity value.

Consequently, assuming that *M* stands for the number of symbols associated to the transmission alphabet and $n = \log_2(M)$ is the number of bits per symbol, the simplified BICM channel capacity can be expressed as:

$$C = \sum_{i=1}^{n} C_{b_i} \tag{4.2}$$

Eventually, it is important to note that the transmitted constellation symbols $\boldsymbol{x}$ must fulfill the power constraint below:

$$P_x = \frac{1}{M} \sum_{m=1}^{M-1} |x_m|^2 \overset{!}{=} 1 \tag{4.3}$$

Analyzing the BICM channel capacity calculation in Equation 4.1 it is clear that for a given channel and signal to noise ratio (SNR) value, the factors which affect the BICM channel capacity are the placement of the constellation points and the bit labeling. As most of the communication systems experiment some sort of channel impairment, the distortion suffered by the constellation is taken into account during the optimization process. This can be easily done modifying the conditional probabilities. For example, in the case of a Rayleigh iid channel, the average BICM channel capacity is shown in [115] where a third integral is added to Equation 4.1 to take into account the fading coefficients. In the proposed approach, this third integral is also suppressed, reducing highly the calculation complexity with similar capacity results.

2.2 **Selection of the Optimization Procedure**

Figure 4.1 shows a diagram that illustrates the different approaches that can be followed to solve the optimization problem. The green path shows the options selected based on the criteria explained below.

The BICM channel capacity equation is a non-linear expression. Therefore, its optimization is carried out via non-linear programming techniques. The presence of many local maximums in this function results into searching for the global one. A global optimization method is used to solve the problem.

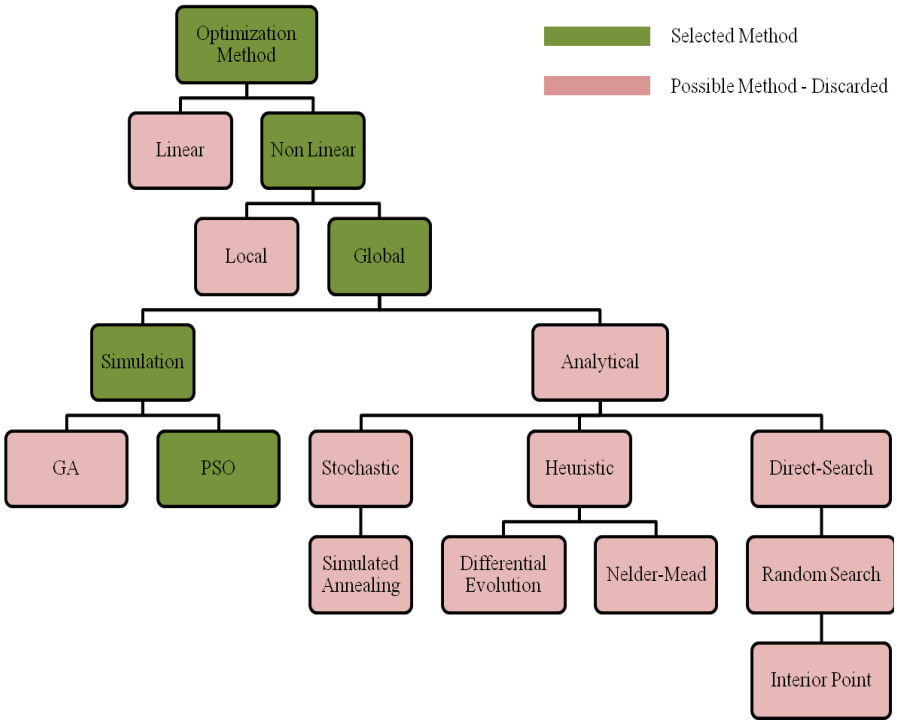

Figure 4.1. Diagram tree of the optimization methodology choices

In a first attempt, the analytical derivation of the optimization problem was considered using software tools such as Matlab and Mathematica. First, Mathematica tool was tried using the optimization methods provided in the software (stochastic, heuristic and direct-search). After having carried out several trials with all of the methods above proposed, the least time consuming one is the direct search method with similar performance to the other ones in most of the cases. In addition, new optimization functions were developed and obtained from other partners with similar results to the direct-search method. However, using these techniques the only case where the optimization process provided relevant results was 16NUC. Optimization methods based on analytical derivation did not converge for higher order constellations and the optimization time was very high.

Simulation based optimization was then chosen in order to reduce the complexity associated to the analytical derivation model. The key solution was to convert the equation based channel capacity calculation into a simulation based calculation. A set of constraints were imposed to the method:

- Equation independent algorithm.

- Low simulation time (simple algorithm).
- Accurate results.

At this point, there are several candidate optimization techniques to solve the optimization problem via simulation derivation. In the field of constellation optimization, simulated annealing and genetic algorithm have been proposed in [66] and [136], respectively. Taking the previous three mandatory conditions into account, the use of the Particle Swarm Optimization (PSO) algorithm [180] is proposed. As shown in [181] and [182], the key characteristic of the PSO is that the algorithm itself is highly robust yet remarkably simple. In addition, while possessing similar capabilities as the genetic algorithm and simulated annealing, the much simpler implementation and reduced bookkeeping of the particle swarm make the PSO an adequate choice for constellation capacity optimization. Briefly outlined, PSO is an algorithm that finds the optimal solution to a given problem by iteratively moving a set of candidate solutions at a certain velocity. The details of the theory behind the PSO can be found in [183] and [184].

A customized PSO is proposed, where the movement is driven by two metrics: inertia and correction factor. On the one hand, the inertia factor determines the influence of a particle's previous velocity to its velocity at the current iteration. On the other hand, the correction factor determines the contribution rate of the best particles from previous and current iterations to the velocity value of the next iteration.

2.3 **Evaluation Metrics**

Three different metrics are considered to quantify the viability of the constellation design procedure. The first metric refers to the computational complexity of the optimization process. This metric is expressed in time units (minutes) and takes into account all the process involved in the design of a single *M*-ary NUC. The remaining two metrics aim at analyzing the capacity and system performance of the designed constellation. The metric used for the theoretical validation of the constellation designed is the BICM channel capacity (Equation 4.2) in terms of bit/s/Hz. To evaluate the system performance of the designed constellation in a real communication system, the metric described in Chapter 3 Section 2.2.1 is used, i.e., the SNR threshold of the designed NUC for BER = 10^{-6}.

The evaluation cases (AWGN and Rayleigh iid) and tools correspond to those shown in Chapter 3 Section 2.2.1.

3. Proposed Optimization Methodology

3.1 Key Factors

Four main factors have been identified as key players for performance and computation simplicity in the design of the proposed NUCs:

- Number of degrees of freedom of the constellation to be designed.
- SNR range where optimization is performed.
- The constellation shape for a specific SNR region.
- The bit labeling of the initial constellation.

The impact of each factor is further developed in the following subsections.

3.1.1 Degrees of Freedom

The number of Degrees of Freedom (DoFs) of the constellation points determines the complexity in the design and demapping steps and, also, the system performance. NUCs can be arranged into two families as a function of their DoFs: One-Dimensional (1D-NUC) and Two-Dimensional (2D-NUC). Every 1D-NUC *M*-ary constellation presents $\frac{\sqrt{M}}{2}$ DoFs, provided that quadrant symmetry condition is fulfilled. 1D-NUC schemes present a characteristic square shape given that the I and Q components are two independent PAM components. As a consequence, in this first case only the constellation points corresponding to each *M*-ary PAM require optimization, and thus, the complexity at the design and demapping steps is significantly reduced. Indeed, the demapping complexity remains the same as in the case of uniform *M*-ary QAM constellations:

$$Q = 2\sqrt{M} \tag{4.4}$$

Where Q represents the number of computed distances at the demapping stage.

Assuming quadrant symmetry, any 2D-NUC *M*-ary constellation presents $\frac{M}{2}$ DoFs. 2D-NUC schemes are characterized by their circular shape. This shape is originated by absence of any movement restriction of all the constellation points along the optimization process. It is important to note that one more degree of symmetry is possible at low noise values for 2D-NUCs. In this case, sub-quadrant

symmetry can be carried out without any performance loss. In sub-quadrant symmetry, only constellation points from one half of the quadrant are optimized while the other half are symmetrically mirrored. This type of symmetry provides a complexity reduction, being the number of DoFs $\frac{M}{4}$. The demapping complexity of 2D-NUC is therefore given by:

$$Q = 2M \tag{4.5}$$

If Equations 4.4 and 4.5 are compared, it is clear that the demapping complexity of 2D-NUCs is higher than 1D-NUCs.

3.1.2 SNR Value Range

The SNR range at which the NUC is designed is an important factor in the optimization process.

Table 4.1 gathers the different SNR regions which will determine the specific way to perform the optimization. These ranges are relevant for 2D-NUCs only. The SNR range is not important for 1D-NUCs because the initial constellation is independent of the SNR value. These values have been determined after several optimization trials checking out the geometric shaping of each of the designed 2D-NUCs for different SNR values. For example, at low SNR values, several constellation points tend to merge. The capacity of their LSBs is sacrificed and passed to the MSBs because of the high noise values. This sort of NUCs is called condensed NUCs.

Table 4.1. SNR range [dB] values for different constellation orders.

SNR Group	16 NUC	64 NUC	256 NUC
Low	(-∞, 1)	(-∞, 7)	(-∞, 10)
Intermediate	[1 , 10)	[7, 15)	[10, 20)
High	[10 , ∞)	[15, ∞)	[20, ∞)

The high SNR values cover the region where the channel capacity is saturated. In this region, distances between adjacent constellation points are almost uniformly distributed. The region of intermediate SNR values gathers all the values from low to high SNR regions.

3.1.3 Initial Constellation

The potential convergence of the optimization algorithm depends on the selection of the initial constellation. The initial constellation is determined by three factors: the dimension (1D-NUC or 2D-NUC), the SNR value and the bit labeling (covered below). The simplest case is the 1D-NUC where the initial constellation is the *M*-ary QAM, regardless of the SNR value. In the case of 2D-NUC, there are three cases: low, intermediate and high SNR values. The low and high SNR cases are simpler than the intermediate SNR case because their shape has distinctive characteristics. Studying the final shape of several designed 2D-NUCs, this chapter proposes the most appropriate initial constellations for each SNR range. In the range of low SNR values, the initial constellation corresponds to the optimized lower order constellation designed for the same SNR value. In the case of high SNR values, the initial constellation points are the ones from the uniform *M*-ary QAM constellation. The initial constellation selection for intermediate values is not as simple as for the previous cases because it requires an iterative process. The next section focuses on the selection of the initial constellation as the starting boundary condition of the optimization process.

3.1.4 Bit Labeling of the Initial Constellation

The bit labeling of the initial constellation is a primary element in order to design NUCs. When the initial constellation is *M*-ary QAM or 1D-NUC, two-dimensional gray code is used where the horizontal and vertical adjacent constellation points differ in the LSB, and diagonal adjacent points differ in the 2 LSB as shown in Figure 4.2 (right).

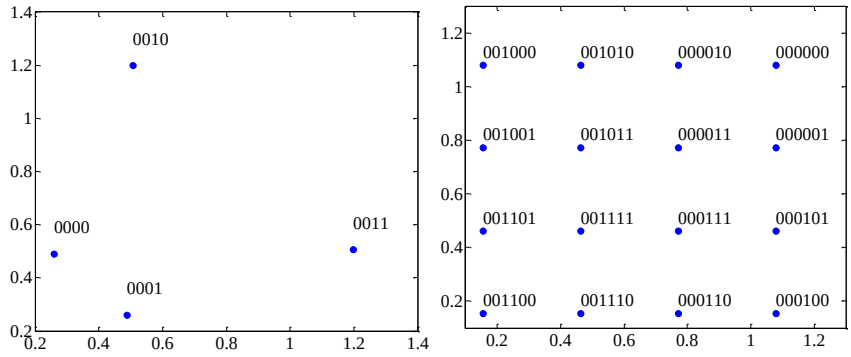

Figure 4.2. Bit labeling for 2D-16NUC (left) and 64QAM (right).

The mapping for 2D-NUCs is obtained via heuristics after analyzing the geometrical shape of optimized NUCs from 16 to 256 constellation points and SNR range values of 2 dB. The mapping proposed here is a gray coding with some restrictions. The different bits of the constellation points do not carry the same amount of capacity (the LSB carries less information than the MSB). Therefore, the closest points, which are more affected by noise and channel impairments, differ only in the LSB. In this case, selecting one point, the two closest points to that point differ in the LSB and the third closest point in the two LSB as shown in Figure 4.2 (left). With this bit labeling, the error probability of the MSB is lowered. Figure 4.2 shows one quadrant and the other ones are obtained by symmetry.

3.2 **Optimization System Model**

The optimization procedure explained in Algorithm 1 is proposed. It is composed of three main steps. First of all, find the SNR value at which the NUC is designed; second, select the initial constellation (Algorithm 2), and finally, perform the optimization algorithm (Algorithm 3).

Algorithm 1 describes the generic procedure in order to design an efficient NUC for a BICM system. The SNR_{obj} is the SNR value at which the system performs after waterfall of FEC for a determined constellation. The value is obtained by simulating the system performance for a determined *M*-ary QAM constellation and BER [176]. Secondly, depending on the SNR_{obj} obtained in the first step, the initial constellation (*Init_Const*) is obtained following Algorithm 2. With the SNR value and the initial constellation as initial conditions, the PSO algorithm (Algorithm 3) outputs the *OptNUC* associated to the SNR_{obj} value. Then, the Algorithm 1 is repeated iteratively but with the optimized NUC (*OptNUC*) until the SNR_{obj} converges (The convergence situation is reached when the integer and first decimal value are the same).

Algorithm 1 Generic System for the Non-Uniform Constellation Design

INITIALIZATION: Define iteration $i = 1$, sort of NUC *sort_NUC*:

1. Define the optimized NUC *OptNUC* for iteration *i:*
   I. **If** $i = 1$, **then** *OptNUC* is the M-ary uniform constellation, **continue**.
   II. **Else**, *OptNUC* is the NUC designed in the PSO optimization process block (phase 5), **continue**.
2. Calculate the SNR threshold ($SNR_{obj(i)}$) for a determined BER value for the *OptNUC*.
3. Decide if the current *OptNUC* is the last one:
   I. **If** $SNR_{obj(i)} = SNR_{obj(i-1)}$, **end**. The *OptNUC* is the final optimized NUC.
   II. **Else**, **continue**.
4. Initial Constellation (algorithm 2) block. Calculate the initial constellation $Init\_Const_{(i)}$ and the optimization SNR $SNR_{optim(i)}$ to be introduced in the PSO algorithm.
5. Perform the PSO optimization process (algorithm 3). This algorithm outputs the optimized NUC *OptNUC* for the $SNR_{optim(i)}$:
   I. **If** $SNR_{optim(i)} = SNR_{obj(i)}$, **then** $i = i+1$ and **return** to phase 1.
   II. **Else**, **return** to phase 4.

The selection of the initial constellation is a key aspect in the design of NUCs. In order to determine the *Init_Const*, the process described in Algorithm 2 is followed. SNR_{optim} is the SNR input to the PSO algorithm. SNR_{obj} is the objective SNR at which the constellation is designed. Therefore, an iterative process must be carried out until SNR_{optim} is equal to SNR_{obj}. The value of $SNR_{optim(i)}$ is calculated as the value of $SNR_{optim(i-1)}$ plus 2 dB. After designing a whole set of NUCs for every SNR range with step of 1dB, we conclude that the shape of a NUC varies significantly, if the target SNR varies 2 dB.

Algorithm 2 Initial Constellation Determination for the PSO Algorithm

1. Select the sort of NUC:
   I. **If** *sort_NUC* = 1D-NUC, then $Init\_Const_{(i)}$ = *M*-ary QAM and $SNR_{optim(i)} = SNR_{obj(i)}$, **end**.
   II. **Else**, **continue.**
2. Determine the initial constellation for the PSO algorithm:
   I. **If** i = 1, **continue**.
   II. **Else**, $SNR_{optim(i)} = SNR_{optim(i-1)}$ + 2dB, **end**.
3. Select the SNR group:
   I. **If** $SNR_{obj(i)} \in$ High, **then** $Init\_Const_{(i)}$= Uniform Constellation and $SNR_{optim(i)} = SNR_{obj(i)}$, **end**.
   II. **Else**, $Init\_Const_{(i)}$= QPSK and $SNR_{optim(i)}$ = -2 dB, **end**

Algorithm 3 PSO Optimization Process for Maximizing the BICM Channel Capacity

INIZIALIZATION: Define the maximum number of iterations k_{max} and a set of constellations $Const\_set_{(k)}$ based on $Init\_Const_{(i)}$:

For k = 1: k_{max}

1. **If** k>1, define a new $Const\_set_{(k)}$ based on *velocity* , **continue**
2. Calculate the BICM Channel Capacity of each constellation $Capacity(Const\_set_{(k)})$
3. $OptNUC = max(Capacity(Const\_set_{(k)}))$

end

The optimization of SNR_{optim} is an intermediate step in order to calculate the most appropriate initial constellation for the PSO optimization process and design the optimized NUC for SNR_{obj}. The value of SNR_{optim} and its *Init_Const* associated are calculated and are input to the PSO algorithm. In the PSO optimization process (Algorithm 3), the NUC is designed based on SNR_{optim} and *Init_Const*. The *velocity* parameter of PSO depends on the best constellation (between current and previous iteration *k*) values and on two parameters of the PSO algorithm (inertia and correction factor). After several trials, the most adequate values for inertia and correction factor are 1 and 2 respectively.

The procedure of the PSO algorithm is as follows: first, a set of constellations is provided by dispersing the constellation points of *Init_Const*. Then, the capacity

of each set of constellations is calculated and the one with the highest capacity is chosen. In the next iteration, all the constellation sets are moved taking into account the inertia and correction factors, the best constellation from k_{th} iteration and the best constellation from k_{th-1} iteration.

3.3 **One-Dimensional Optimization**

This sub-section details the procedure to follow in the Algorithm 3 to perform effectively the customized PSO algorithm. Based on heuristics obtained from the changes in the shape of the different constellations designed for different SNR regions, the movement of the constellation points is explained.

Taking the real parts of the constellation diagram, only one point of each row is moved and the rest of the points are displaced exactly the same distance. For the imaginary parts, the movement is column wise. This procedure to design 1D-NUCs is valid for any number of constellation points. The only difference is that 1D-NUCs with a large number of constellation points imply an increase in the optimization time. Furthermore, the initial constellation is always the *M*-ary conventional QAM.

3.4 **Two-Dimensional Optimization**

This sub-section details the procedure to follow in the Algorithm 3 to perform effectively the customized PSO algorithm, i.e., the inertia and correction factor parameters. Based on heuristics obtained from the changes in the shape of the different constellations designed for different SNR regions, a procedure to move the different constellation points in an effective way is proposed.

When 2D-NUC schemes are designed, the complexity of the optimization procedure increases notably. Once the initial constellation has been determined using the proposed Algorithm 2, the optimization process is carried out. This process is crucial to find the global maximum of the objective function and depends on the constellation order. The higher the number of constellation points, the more difficult the optimization is.

In the case of QPSK constellation, the optimized points are the same as the uniform constellations. The Euclidean distances of this constellation are optimal as long as the power of the constellation is set to 1 for all the SNR values.

The initial constellation for designing 2D-16NUCs is the QPSK. The number of constellation points to be optimized is very low, four in this case and the influence of the initial constellation is negligible.

In the cases of 2D-64NUCs and 2D-256NUCs, 16 and 64 constellation points per 2D-NUC have to be optimized assuming quadrant symmetry, respectively. These numbers are remarkable from an optimization perspective and in consequence the design complexity increases.

For 2D-64NUCs two different levels of constellation points are processed separately as shown in Figure 4.3. The external points (level 1) tend to change more than the ones which are closer to the origin of the constellation diagram (level 2). Therefore, in order to optimize correctly this sort of constellations, two optimization steps must be followed:

- External optimization: the external points (level 1) have an extended movement and internal points (level 2) have a reduced movement.
- Refinement optimization: all the points are slightly moved in order to achieve the optimum capacity.

For low and intermediate values, the regions are circular because of the shape of the initial constellation. However, for high SNR values these regions are square because the initial constellation is the uniform *M*-ary one.

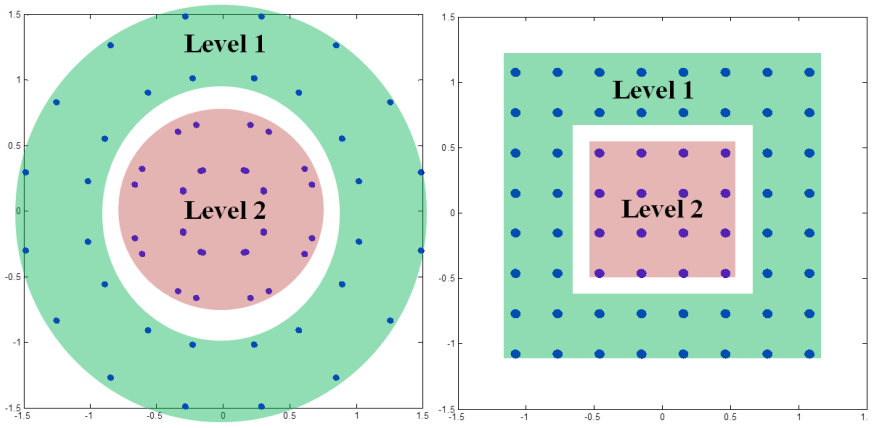

Figure 4.3. Levels of 64NUC for both low and intermediate SNR values (left) and high SNR values (right).

In the case of 256NUCs, the number of levels increases up to 8. The first level corresponds to the points with the highest mobility (outermost points) and the eighth level corresponds to the points with the lowest mobility (innermost points). In addition, each level has 8 points included. Two steps of optimization are considered:

- First step; only the first four level points are moved (external points).
- Second step; all the points are slightly moved. In this second step, each level must be slightly moved and several trials may be needed, i.e., in one trial intermediate levels are moved and in the next trial lower levels are moved.

When the optimization is carried out for high SNR values, there are eight different levels of optimization as shown in Figure 4.4 for one quadrant. The points of the first level are the ones with the highest movement while the points of the level eight are slightly moved, i.e., the lower the level the higher the movement of the constellation points in the optimization process.

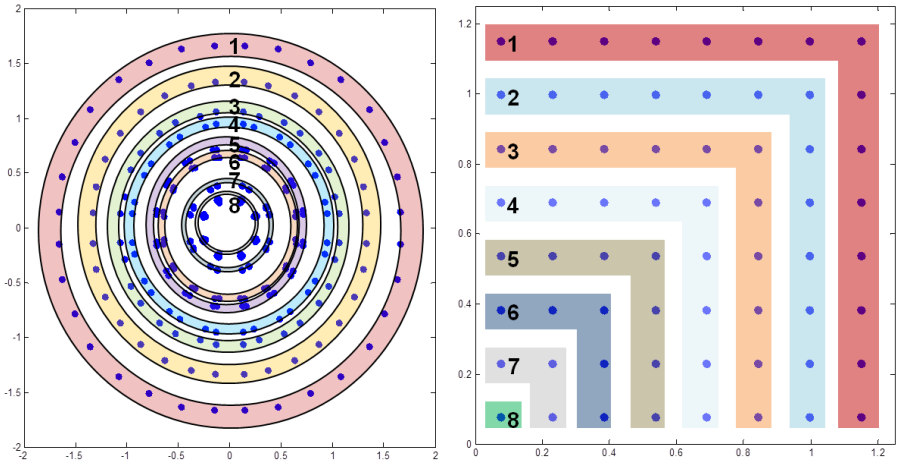

Figure 4.4. Levels of 256NUC for both low and intermediate SNR values (left) and high SNR values (right, one quadrant).

3.5 **Optimization for the Rayleigh iid Channel**

In the design of NUCs for the Rayleigh iid channel, the pdf of this channel is taken into account. Unfortunately, the designing time is very high due to the variability of the fading coefficients.

After analyzing several NUCs designed for both channels (AWGN and Rayleigh iid) the constellations appear with a similar shape for the same constellation order and SNR value. Having similar shape, there were only differences on the positions of the constellation points. In the case of the Rayleigh iid channel, the main impact on the NUC design comes from the specific noise value. The heuristic analysis carried out reveals that the Rayleigh iid channel model plays a secondary role in the design of NUCs.

Based on this finding, a simplified approach to design NUCs for the Rayleigh iid channel with low computational cost is proposed. The target SNR value is set to the performance threshold of a Rayleigh iid channel (at the SNR waterfall region) but the channel specified for the optimization process is the AWGN. The results obtained are similar to the ones obtained by setting the SNR and channel model to Rayleigh iid (losses below 0.1 dB) reducing significantly the optimization time (from days to minutes).

4. NUC Optimization Results

This section investigates the results of optimizing constellations for a BICM system considering the AWGN channel for a wide range of SNR values. For comparison purposes, the BICM channel capacities of the designed constellations are compared with the Shannon limit and with *M*-ary QAM constellations.

4.1 Overall Results

The NUCs designed with the proposed algorithm show capacity gains from 0.0050 to 0.2983 bit/s/Hz with respect to the *M*-ary QAMs. The highest gains are achieved for the intermediate SNR group, except for 16NUCs where the highest gains are obtained for low SNR values. The next sub-sections show in detail the results of the optimized NUCs.

The ultimate goal of the optimization process is the design of efficient constellations at a reasonable time. In consequence, the overall KPI is the time duration of the optimization process.

In addition to this KPI, several optimization parameters are considered: the number of constellation points, the number of the iterations, the number of DoFs and the number of constellations inside the constellation set. Table 4.2 shows the simulation time results. All the optimization processes have been carried out on an Intel(R) Xeon(R) CPU E5-2609 v2 @ 2.50GHz (2 cores) with RAM 64.0 GB.

Table 4.2. Optimization time for the proposed NUCs.

Constellation order	2D-16NUC	2D-64NUC	2D-256NUC	1D-1024NUC	1D-4096NUC
Time	5 min	20 min	120 min	10 min	20 min

Results in Table 4.2 show that when designing NUCs, the higher the constellation order, the higher the optimization time is. The difference in time between 2D and 1D optimization is remarkable. For 1D, only one PAM is optimized while for 2D the whole set of constellation points is taken into account. Looking at the results, the algorithm proposed in this work designs NUC constellations in a very short period of time.

4.2 **16NUC**

This section provides BICM capacity values for the AWGN channel corresponding to 1D-16NUCs and 2D-16NUCs. The curves represent the gap to the Shannon limit. This gap is usually referred as "shortcoming" and is a measurement metric commonly used to study the efficiency of NUCs [113], [115]. These values are given as a function of the SNR and have been obtained carrying out the optimization procedure shown in the previous section. For comparison purposes conventional 16QAM values are also included.

Figure 4.5 shows the BICM channel capacity shortcoming for different SNR values ranging from -2 to 12 dB. In the case of 1D-16NUCs, the region of low SNR values (up to 1 dB) is where the highest gains can be achieved (in this region, the optimal constellation resembles a conventional QPSK, Figure 4.6 (left image)). The shortcoming for intermediate and high SNR values (above 1 dB) is slightly lower than for 16QAM. Indeed, in this range of SNR the shape of optimized 1D-16NUCs is slightly similar to the 16QAM. The demapping complexity of these constellations is just $Q = 8$, the same as for 16QAM. 1D and 2D-16NUC schemes achieve the highest gains in the low SNR zone. Bigger gains than for 1D-16NUCs are achieved for intermediate SNR values. In fact, the intermediate SNR zone (1 - 10 dB) is where the freedom of movement of the constellation points is wider, as shown in Figure 4.6 (right image). The shortcoming of 2D-16NUCs for high SNR values (above 10 dB) increases because they present a similar shape to the conventional 16QAM. In consequence, for high SNR values higher order constellations are recommended. The demapping complexity of 2D-16NUC is $Q = 32$.

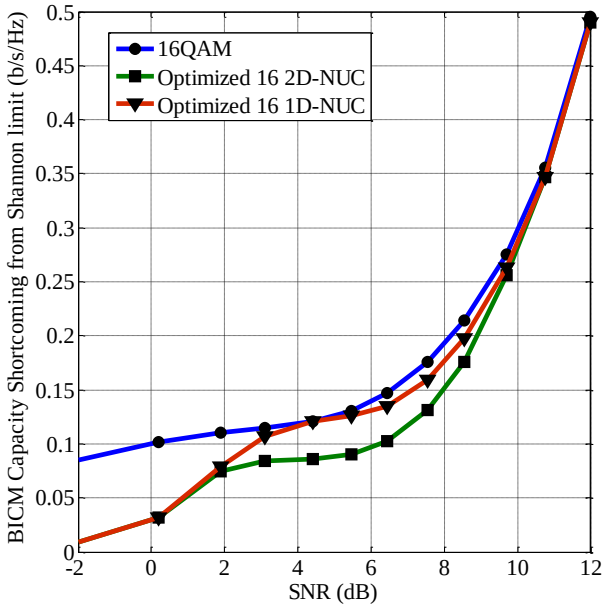

Figure 4.5. 16 point 2D-NUC, 1D-NUC and 16QAM BICM channel capacity shortcoming from Shannon limit.

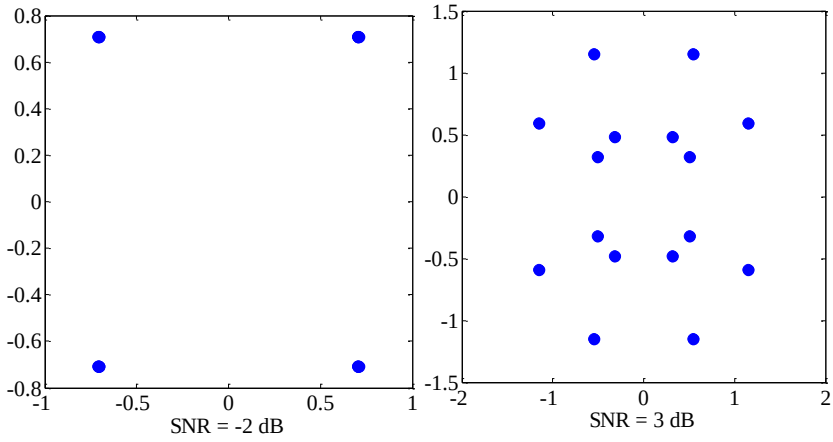

Figure 4.6. Optimized 2D-16NUC for two different SNR values.

4.3 **64NUC**

Figure 4.7 shows the shortcoming from the Shannon limit of 64 constellation points. The SNR value ranges from 0 to 16 dB containing the three SNR groups

described in Table 4.1. The shortcoming for the optimized 1D-NUCs and 2D-NUCs at intermediate SNR values is lower than in the 16 points case. The main reason is that the number of points to be optimized (DoFs) is higher. The shortcoming of 64NUCs is very similar to 16NUCs at low SNR values because the constellation points of the 64NUCs are condensed into 16NUCs. The optimized 2D-64NUCs present the highest gains for intermediate SNR values (from 7 to 15).

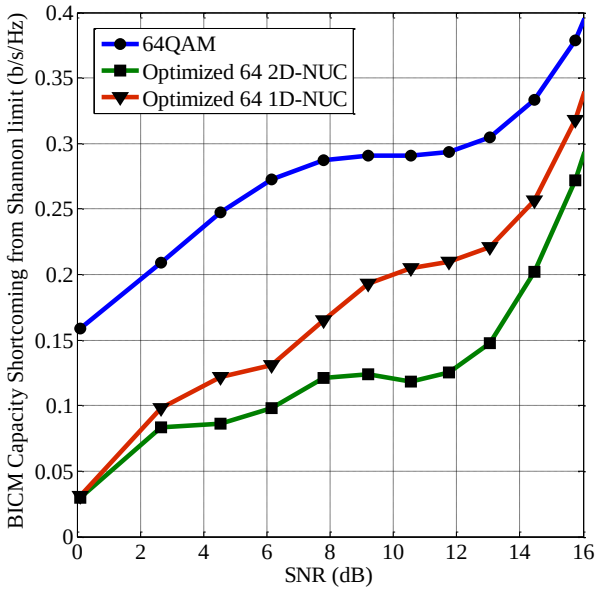

Figure 4.7. 64 point 2D-NUC, 1D-NUC and 64QAM BICM channel capacity shortcoming from Shannon limit.

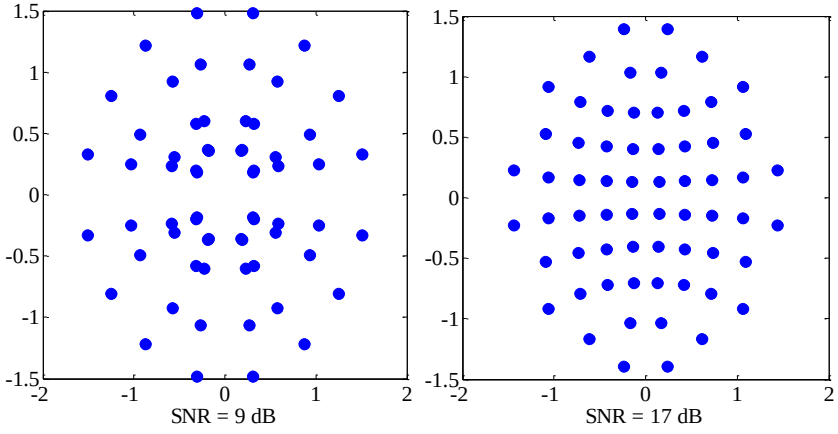

Figure 4.8. Optimized 2D-64NUC for two different SNR values.

The intermediate SNR region is where the highest capacity difference can be found among 1D-NUCs and 2D-NUCs. The freedom of movement of the 2D-NUCs constellation points with respect to 1D-NUCs provides higher gains. In the region of high SNR values (above 15 dB), the shortcoming of the optimized 64NUCs increases. Figure 4.8 shows that in this region the distances between the constellation points are more uniformly distributed. The channel capacity values for 2D-64NUCs are higher than for 1D-64NUCs as well as the demapping complexity.

4.4 **256NUC**

Figure 4.9 shows the reduction presented by 256NUC schemes in the shortcoming at the intermediate SNR zone with respect to 64NUCs. 256NUCs show the highest gains for intermediate SNR values (from 10 to 20 dB). In the low SNR values region, similar capacity values to the ones obtained with 16NUCs and 64NUCs are achieved with similar constellation shapes. In addition, the shortcoming from the Shannon limit increases for high SNR values.

Figure 4.10 displays two different 2D-256NUCs optimized for intermediate and high SNR values. All the constellation points can be differentiated for intermediate values as there are no condensed points because of the low noise. The shape of the optimized 2D-256NUCs tends to be close to the conventional 256QAM for high SNR values while for low SNR values it is similar to16NUCs and 64NUCs.

4.5 **1024NUC**

NUCs for 1024 and 4096 will be only proposed as one dimensional constellations. In such high order constellations (1024, 4096 and above), the number of DoFs is very high, and the design and demapping complexity is greatly increased. Therefore, the use of 2D-NUCs is not adequate for current communication systems in which the latency is an important factor. Figure 4.11 shows that the highest gains are achieved for low and intermediate SNR values. However, there is a region (local maximum) where the shortcoming curve reaches a maximum value (around 11dB) as shown in [113]. This is the zone where all the constellation points are moved for 2D-NUCs but the limited DoFs of the 1D-NUCs cause an increase in the shortcoming. The rest of the curve follows the same tendency as for lower order constellations. Figure 4.12 displays the shape of the optimized 1D-1024NUCs for two different SNR values. In the peak zone (left

image), several constellation points are condensed as the noise power value is high. The right image shows that the shape is similar to the 1024QAM for 21 dB as the noise is low.

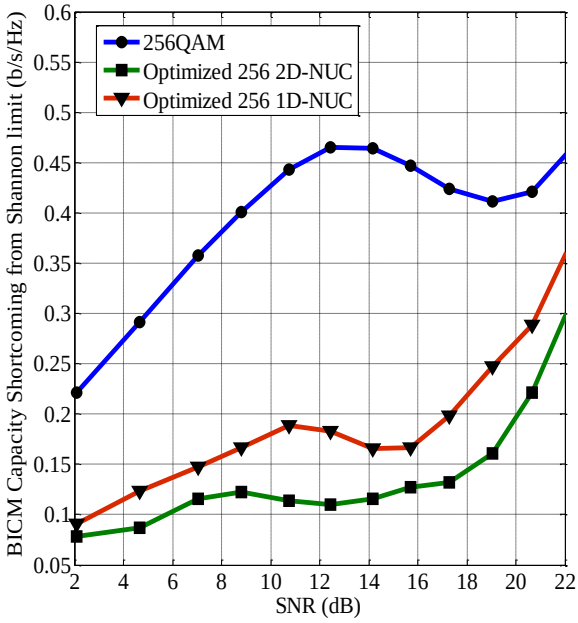

Figure 4.9. 256 point 2D-NUC, 1D-NUC and 256QAM BICM channel capacity shortcoming from Shannon limit.

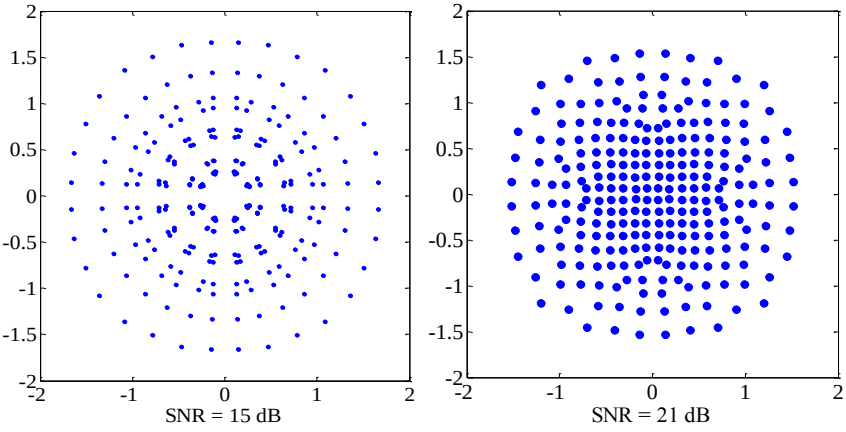

Figure 4.10. Optimized 2D-256NUC for two different SNR values.

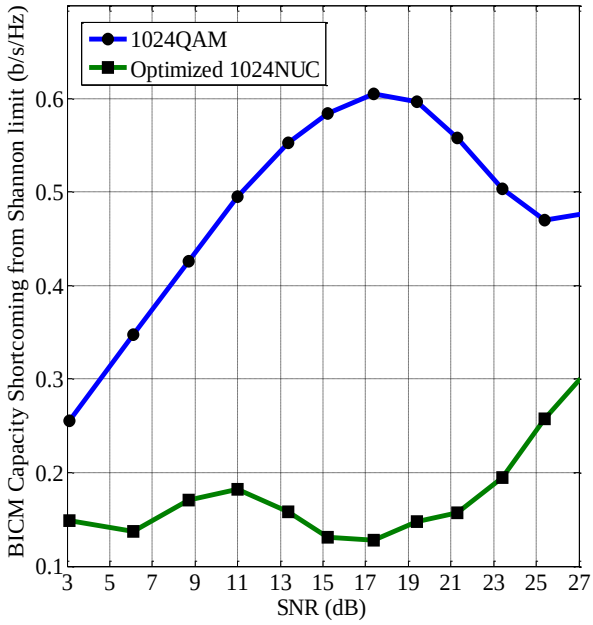

Figure 4.11. 1024 point 1D-NUC and 1024QAM BICM channel capacity shortcoming from Shannon limit.

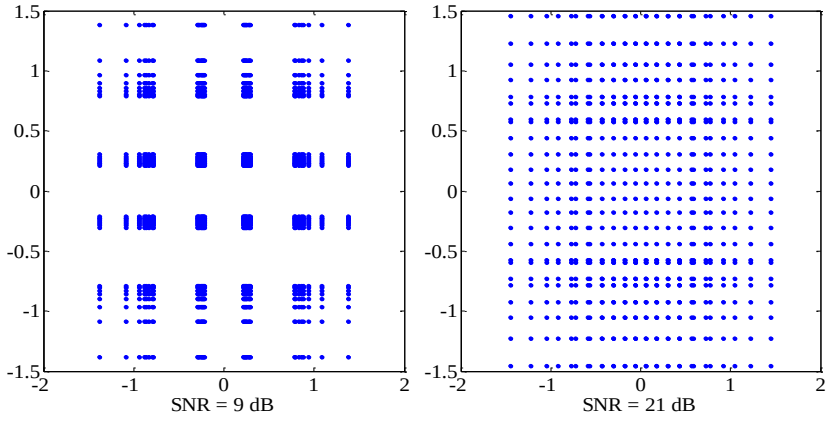

Figure 4.12. Optimized 1D-1024NUC for two different SNR values.

4.6 **4096NUC**

The case of 4096NUCs is similar to the 1024NUCs. The zone where the shortcoming increases, remains the same. However, the shortcoming values are

lower as the number of DoFs increases. In addition, the zone with higher gains is the intermediate SNR zone (from 18 to 25 dB).

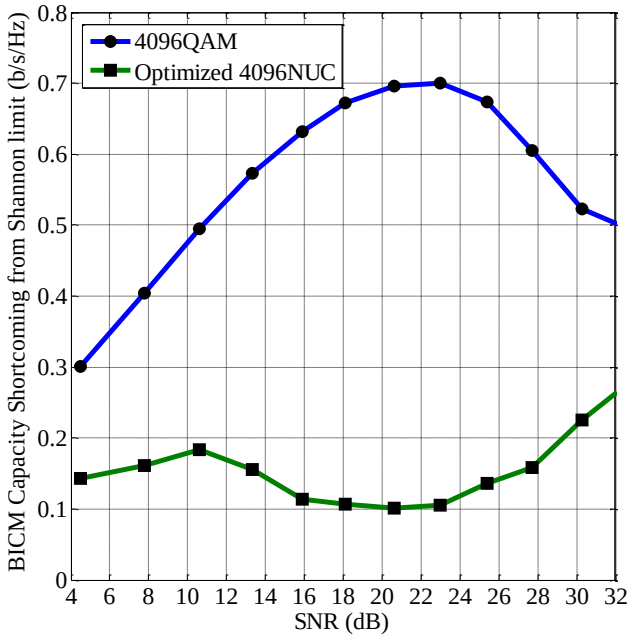

Figure 4.13. 4096 point 1D-NUC and 4096QAM BICM channel capacity shortcoming from Shannon limit.

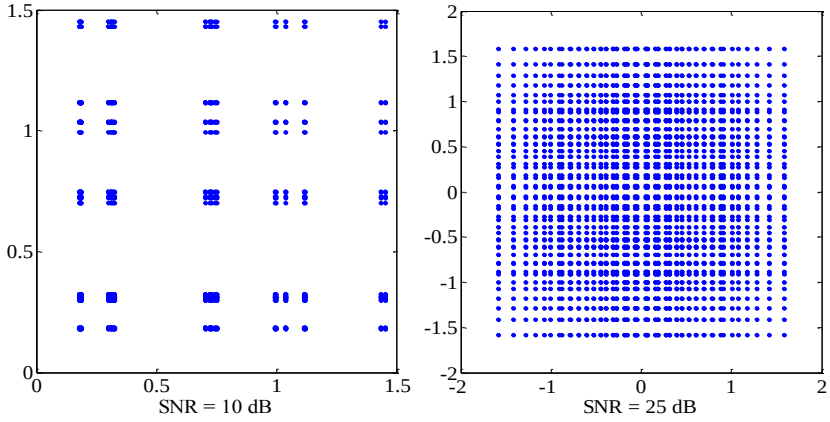

Figure 4.14. Optimized 1D-4096NUC for two different SNR values.

4.7 **System Performance**

In this section, the system performance of optimized 1D-NUCs and 2D-NUCs for AWGN and Rayleigh iid channels is studied testing their performance in a real communication system based on ATSC 3.0. The BICM based transceiver shown in Chapter 3 Section 2.2.3 is used. This tool has been completed with a bit interleaver block and a low density parity check (LPDC) coder [162]. The LDPC code rates used in this study are 3/15, 6/15, 9/15 and 12/15 with a block length of 64800 bits representing a wide variety of SNR values. The results are obtained for a given SNR threshold value when the BER is 10^{-6} and the simulation step is 0.1 dB. Results for 16NUCs and 64NUCs for the Rayleigh iid channel have been obtained taking into account the pdf of this channel. In the case of 256NUCs, 1024NUCs and 4096NUCs, however, the approach described in part 3.5 is applied.

Table 4.3. Optimized 1D-NUC versus *M*-ary QAM system performance gain.

Channel	Code rate	16 points	64 points	256 points	1024 points	4096 points
AWGN	3/15	0.4	0.4	0.7	1	1
	6/15	0.05	0.4	0.8	1.3	1.7
	9/15	0.1	0.2	0.8	1.3	1.8
	12/15	0.1	0.1	0.4	0.7	0.9
Rayleigh iid	3/15	0	0.5	0.5	0.8	0.8
	6/15	0	0.2	0.6	1	1
	9/15	0	0.2	0.4	0.7	0.9
	12/15	0	0.1	0.4	0.5	0.5

Table 4.3 gathers the system SNR performance gains of the optimized 1D-NUC versus the conventional M-ary QAM for AWGN and Rayleigh iid channels. 16NUC present gains from 0.05 to 0.4 dB under AWGN channel conditions. Nevertheless, there is no gain for the Rayleigh iid channel. In the case of 64NUC, higher or similar gains are achieved ranging from 0.1 to 0.4 dB for the AWGN channel and from 0.1 to 0.5 dB for the Rayleigh iid channel. The gain achieved in 256NUC increases up to 0.8 dB for AWGN and up to 0.6 dB for Rayleigh iid. Following the same behavior, 1024NUC present gains ranging from 0.7 to 1.3 dB (AWGN) and from 0.5 to 1 dB (Rayleigh iid).

Finally, 4096 constellations provide the highest gains ranging from 0.9 to 1.8 dB for AWGN and from 0.5 to 1 dB for Rayleigh iid. As expected, the higher the constellation order the higher the gain is. In fact, for the AWGN channel, the

maximum gain achieved is 1.8 dB for the 9/15 code rate and the optimized 1D-4096NUC. Besides, for the Rayleigh iid channel the maximum gain is 1 dB for the 6/15 code rate and 1D-4096NUC.

It must be taken into account that the demapping complexity of these optimized 1D-NUCs is the same as the conventional *M*-ary QAM considering the number of distances to be computed by the ML demapper. Table 4.4 shows the system performance of the optimized 2D-NUCs versus the conventional *M*-ary QAM.

In this case, the designed 2D-NUCs present higher gains than 1D-NUCs as the number of DoFs increases. Constellations with 16 symbols show gains from 0.1 to 0.4 dB for AWGN. However, there is no gain for Rayleigh iid. In the case of constellations with 64 points higher gains are achieved. In the case of the AWGN channel the gain ranges from 0.1 to 0.6 dB whereas the gain in a Rayleigh channel varies from 0.2 to 0.5 dB. 256 constellation points present gains from 0.7 to 1.1 for AWGN and from 0.4 to 0.8 for Rayleigh iid. The highest gain is achieved for the optimized 2D-256NUC and 6/15 code rate with value 1.1 dB. In the case of 1D-256NUC this value is 0.8 dB. However, the demapping complexity of 2D-NUC is higher and increases with the constellation order.

Table 4.4. Optimized 2D-NUC versus *M*-ary QAM system performance gain

Channel	Code Rate	16 points	64 points	256 points
AWGN	3/15	0.4	0.6	0.9
	6/15	0.1	0.6	1.1
	9/15	0.1	0.5	0.9
	12/15	0.1	0.1	0.7
Rayleigh iid	3/15	0	0.5	0.6
	6/15	0	0.3	0.8
	9/15	0	0.2	0.6
	12/15	0	0.2	0.4

Figure 4.15 displays the system performance curves for 9/15 code rate, both for the AWGN and Rayleigh iid channels. Curves with circular markers represent the optimized 2D-NUCs, the square markers the optimized 1D-NUCs and the star markers the *M*-ary QAM. These curves are important in order to show that the waterfall characteristics of the LDPC codes persist and that there is no error floor penalty at the demapping and decoding steps of the optimized NUCs.

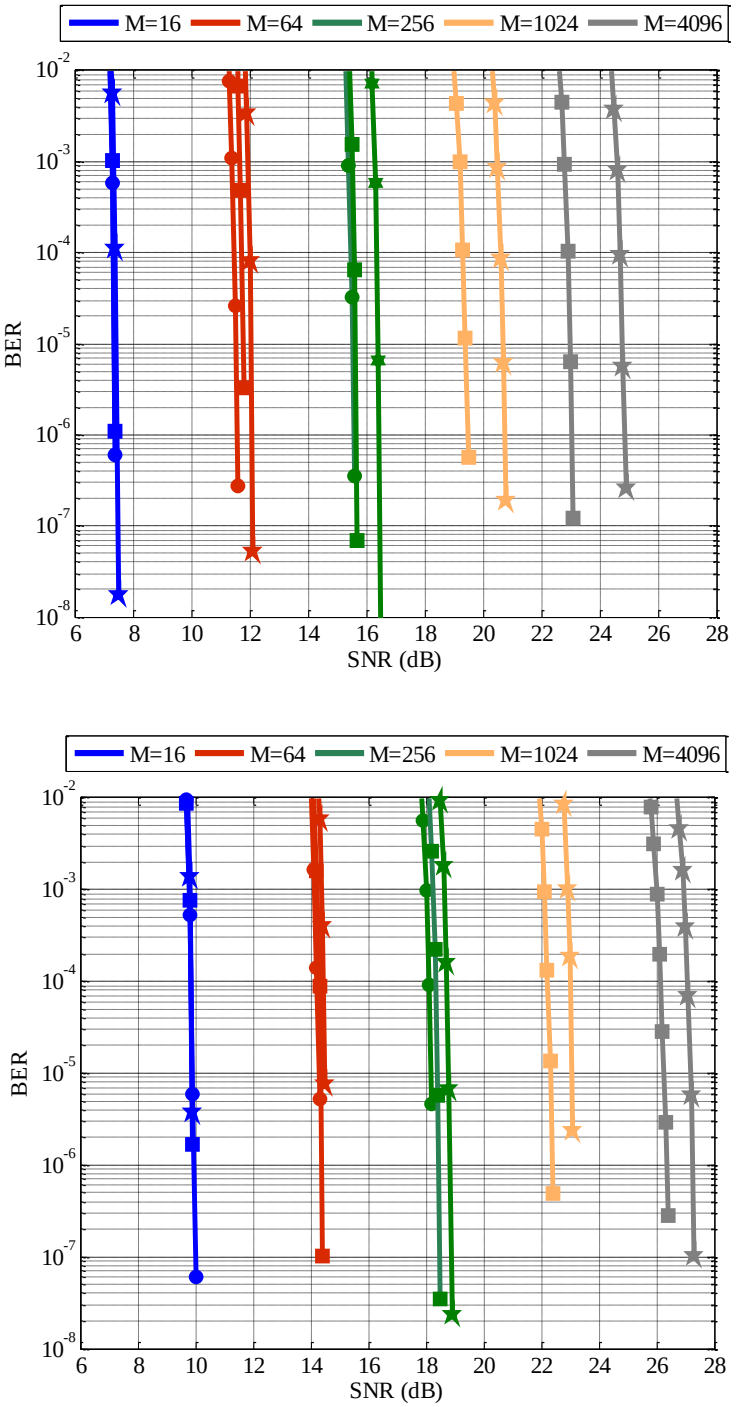

Figure 4.15. System performance of the optimized 2D-NUC, 1D-NUC and *M*-ary QAM for the AWGN (upper) and Rayleigh iid (lower) channels.

5. Advanced NUC Schemes Based on Condensation

Taking one step further in the design of NUCs, where all the points are positioned individually in the constellation diagram, a condensed version of each NUC can be designed. Indeed, one characteristic of NUCs is that for low SNR values, the shaping of the constellation tends to be a version of the NUC with at least one less bit of efficiency, i.e., as shown in Figure 4.16 the shaping of a 64NUC for code rate 2/15 resembles a 16NUC. Therefore, in the design process adjacent constellation points can be situated at the same position, resulting in a condensed NUC with optimal performance. In addition, at the receiver part, where the demapper holds an important role, the demapping complexity can be greatly reduced [128]. Indeed, the higher the constellation order the higher the complexity reduction.

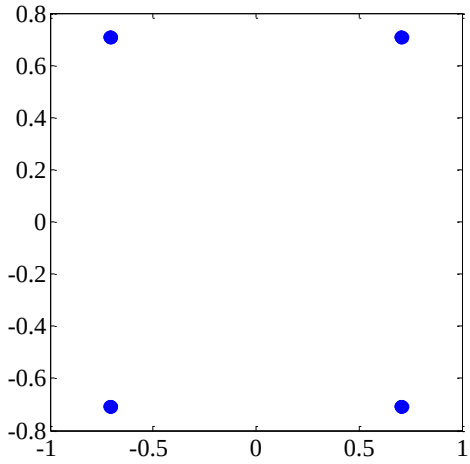

Figure 4.16. Condensed 64NUC for 2/15 code rate.

5.1 Proposed Condensation Methodologies

The design of NUCs takes advantage of condensation for low and intermediate SNR regions. If condensation is applied to the design of NUCs, it involves a lower number of constellation points to optimize and demap. If condensation is applied after the design process, the demapping complexity is lowered but the design complexity remains unaltered.

Two possible ways to make the condensation are proposed. The first one, called condensation with optimization (CWO), consists of restricting the number

of DoFs of several constellation points at the design process, imposing them to be positioned at the same location in the constellation diagram. The advantage of this sort of condensation is that the design procedure is less complex because the number of constellation points to be optimized is lower. However, the issue in this solution is that the most suitable points to be gathered at the same position must be known before the optimization is carried out, i.e., if the points gathered are not the suitable ones, the optimization will never reach the best solution. Therefore, in a first moment without knowing the final shape of a constellation for a determined SNR value, the best degree of condensation is unknown.

The second one, called condensation after optimization (CAO), is based on post processing the optimized constellation via condensation, i.e., first of all, the optimization of the constellation is performed without taking into account any condensation. Next, a condensation algorithm is applied to the optimized constellation which merges the closest points in the constellation diagram. The advantage of this solution is that it will always find the optimum solution as long as the initial optimization has been correctly developed. However, the design procedure is more complex than the first one proposed (CWO) because the number of points to be optimized is higher.

In this work, the design of the condensed 2D-NUCs has been made applying the same degree of condensation to both of the techniques, i.e., both techniques present the same complexity reduction at the demapping stage. The condensed 2D-NUCs designed with the two methods are similar as the degree of condensation is the same.

5.2 **Condensed NUC Optimization Results**

5.2.1 Design Complexity

When evaluating the complexity in the design process of one constellation, the number of variables included in the optimization procedure (I and Q components of the constellation symbols) is one of the main KPIs.

Table 4.5. Comparison of the number of constellation points to optimize for different ModCods

Code Rate	2D-64NUC		2D-256NUC		2D-1024NUC		2D-4096NUC	
	CWO	CAO	CWO	CAO	CWO	CAO	CWO	CAO
2/15	8	32	8	128	8	512	8	2048
3/15	8	32	8	128	32	512	32	2048
4/15	8	32	32	128	32	512	128	2048
5/15	24	32	36	128	128	512	-	-
6/15	24	32	52	128	-	-	-	-
7/15	28	32	60	128	-	-	-	-
8/15	28	32	80	128	-	-	-	-
9/15	28	32	96	128	-	-	-	-
10/15	-	-	102	128	-	-	-	-
11/15	-	-	110	128	-	-	-	-

Table 4.5 presents the number of variables included in the optimization process of 2D-64NUCs, 2D-256NUCs, 2D-1024NUCs and 2D-4096NUCs. The study includes code rates ranging from 2/15 to 9/15 for 2D-64NUCs, 2/15 to 11/15 for 2D-256NUCs, 2/15 to 5/15 for 2D-1024NUCs and from 2/15 to 4/15 for 2D-4096NUCs. The ModCods with no value correspond to the combinations where condensation makes no sense, i.e., the degradation of the system performance is high. Evaluating the results from Table 4.5, the number of variables for CWO algorithm is lower than for the CAO. In CWO, the lower the code rate the lower the design complexity as the condensation degree is higher. Moreover, the higher the constellation order, the higher the reduction in the design complexity is. However, if the condensation degree is not adequately selected the system performance is degraded. CWO is appealing for massive order 2D-NUCs (beyond 2D-256NUCs) where the design of 2D-NUCs is highly difficult.

5.2.2 Receiver Complexity

One of the most important advantages of using condensed 2D-NUCs instead of non-condensed 2D-NUCs is the simplification of the demapping algorithm. The number of operations to compute the Log-likelihood Ratio (LLR) values is greatly reduced on condensed 2D-NUCs. What is more, there is a significant number of bits (the quantity depends on the degree of condensation) which carry no information at all, i.e., their capacity is zero. Therefore, it is not necessary to calculate the LLR values for these bits as shown in [128], [129]. Table 4.6 shows the number of EDs to be computed by the demapper for the proposed

constellations. The ModCods with no value correspond to the combinations where condensation makes no sense, i.e., the degradation of the system performance is high. Results for condensed 2D-NUCs are the same for CWO and CAO because the condensation degree is the same.

Table 4.6. Demapping complexity analysis of the proposed condensed 2D-NUCs.

CR	2D-64NUC	2D-256NUC	2D-1024NUC	2D-4096NUC
2/15	32	32	32	32
3/15	32	32	128	128
4/15	32	128	128	512
5/15	96	144	512	-
6/15	96	176	-	-
7/15	112	240	-	-
8/15	112	320	-	-
9/15	112	384	-	-
10/15	-	408	-	-
11/15	-	456	-	-

Results in Table 4.6 show that for condensed 2D-NUCs, the higher the code rate the higher the number of operations to be computed. This is due to the fact that 2D-NUCs with high code rates perform similar to *M*-ary QAMs and, thus, condensation is not suitable for such constellations. Another interesting point is that for low code rates, the complexity when using condensed 2D-NUCs is reduced by a factor of 4 for 2D-64NUCs and by a factor of 16 for 2D-256NUCs if compared with non-condensed NUCs. However, for 2D-256NUCs with high code rates, condensed constellations are less attractive because of the complexity and performance losses. In case of high order 2D-NUCs, the demapping complexity is highly reduced if a condensed 2D-NUC is used. High order NUCs included in ATSC 3.0 present lower demapping complexity because they are 1D-NUC at the cost of worse system performance.

5.3 **System Performance**

This section provides an insight into the performance degradation when condensation is applied to 2D-NUCs in a communication system. Table 4.7 shows the SNR losses if the condensation technique is applied to the ATSC 3.0 2D-NUCs. Results are obtained by calculating the SNR threshold of the condensed

NUCs and subtracting this value from the SNR of the ATSC 3.0 constellation. The results are obtained for the SNR value at which the BER is 10^{-5}.

Table 4.7. Newly designed condensed 2D-NUCs versus ATSC 3.0 NUCs SNR loss in the ATSC 3.0 system for AWGN and Rayleigh iid channels.

CR	2D-64NUC		2D-256NUC		2D-1024NUC		2D-4096NUC	
	AWGN	Ray iid	AWGN	Ray iid	AWGN	Ray iid	AWGN	Ray iid
2/15	0	0	0	0	0.1	0.1	0.2	0.1
3/15	0	0	0	0	0.1	0	0.1	0.1
4/15	0	0	0	0	0.1	0.1	0	0
5/15	0	0	0	0	0.3	0	-	-
6/15	< 0.1	0.1	< 0.1	< 0.1	-	-	-	-
7/15	< 0.1	< 0.1	< 0.1	< 0.2	-	-	-	-
8/15	< 0.1	< 0.1	< 0.2	< 0.3	-	-	-	-
9/15	< 0.1	< 0.1	< 0.1	< 0.2	-	-	-	-
10/15	-	-	< 0.1	< 0.2	-	-	-	-
11/15	-	-	< 0.2	< 0.3	-	-	-	-

Table 4.7 shows that the performance of the designed condensed 2D-NUCs is similar to the set of 2D-NUCs adopted in ATSC 3.0. Condensed 2D-64NUCs present losses from 0 to 0.1 dB for both AWGN and Rayleigh iid channel models. In the region of low code rates (from 2/15 to 5/15) there are no losses. For mid code rates, the losses are lower than 0.1 dB.

High code rates are not analyzed because condensation makes no sense as the 2D-NUCs shaping is similar to the *M*-ary QAM. As it is explained Section 4, the optimum constellation for the high SNR region is the standard *M*-ary QAM where all the constellation points are uniformly spaced in the constellation diagram. Lossless condensed 2D-256NUCs are obtained for low code rates. For mid and high code rates, the highest performance losses are less than 0.2 dB for the AWGN channel and less than 0.3 dB for the Rayleigh iid channel. Results from Table 4.7 show that all of the newly designed condensed high order 2D-NUCs provide higher gain than the ones from ATSC 3.0 for the AWGN channel (except for 2D-4096NUC and 4/15). However, for the Rayleigh iid channel, there are some configurations that present no gain. In addition, the gain range is from 0.1 dB to 0.3 dB (for 1D-1024NUC with code rate 5/15 and AWGN channel).

6. **Conclusions**

In this chapter a methodology for an efficient NUC design for BICM systems has been presented. The first contribution is an approximation for the BICM channel capacity that can be used both for the AWGN and Rayleigh iid channels. The key factors to maximize the capacity have also been studied. Next, another important outcome of this work is the study of the possible approaches to face the optimization problem and the proposal of the most suitable algorithm. The algorithms designed to optimize NUCs have been described. All the key factors and optimization parameters based on a heuristic study of the optimization problem have been described and the key steps to design efficient NUCs for a given SNR value have been studied for constellations from 16 to 4096 points. The noise has been shown to be the main influence source in the design of NUCs. An approach to design efficient NUCs for the Rayleigh iid channel with low computational cost has been presented. The target SNR is set to the performance threshold of the Rayleigh iid channel and the channel specified for the optimization process is the AWGN. This method provides losses below 0.1 dB with respect to the pure Rayleigh optimization and reduces significantly the optimization time (from days to minutes).

In order to validate the process proposal, several NUC schemes for different SNR target values have been designed and their channel capacities have been calculated. The results obtained have shown that the designed NUCs present channel capacity gains from 0.0050 to 0.2983 bit/s/Hz with respect to the conventional *M*-ary QAM. Moreover, in order to validate the designed NUCs, their system performance has been analyzed in the ATSC 3.0 BICM system. The results show gains of up to 1.8 dB with respect to their equivalent conventional *M*-ary QAM. In addition, the study shows that the demapping complexity of 1D-NUCs is the same as the uniform QAM constellations. However, for 2D-NUCs the demapping complexity is higher and there should be a trade-off between performance and complexity depending of the communication system.

Condensed 2D-NUCs have also been presented, proposing two different condensation methodologies. The system performance remains unaltered for low code rates and the demapping complexity is reduced.

To sum up, the methodology proposed in this work facilitates the design of efficient NUCs for a BICM system both for the AWGN and Rayleigh iid channels.

CHAPTER 5: **LOW COMPLEXITY DEMAPPING SOLUTIONS FOR NUCs**

With the advent of new constellation schemes, the receiver must provide enough tools to deliver real-time content independent of the constellation type. The inclusion of 1D-NUCs and 2D-NUCs in the new ATSC 3.0 standard makes necessary the research on new demappers which adapt to the constellation characteristics and provide low delay with a system performance similar to the Maximum Likelihood (ML) approach. This chapter proposes two solutions for low complexity demapping of 1D-NUCs and 2D-NUCs.

For 1D uniform constellations, a novel technique is proposed based on dividing the 1D-NUC into lattices of identical dimensions and compare its demapping complexity and system performance with the ML. The value of the received symbol is modified in order to provide an entry to a Look-Up Table (LUT) where the closest point is stored. This solution provides low complexity for demodulation of the I and Q PAM components of the non-uniform constellation. The complexity is $O(2+\log_2 \sqrt{M})$ while the exhaustive search, i.e., ML is $O(\sqrt{M})$. The complexity implications in terms of memory and computations and the system performance are analyzed.

For 2D-NUCs a novel demapper is proposed, exploiting the characteristics of these constellations. It represents the combination of two underlying demapping techniques targeting the ATSC 3.0 compliant OFDM transceiver. On the one hand, for low code rates, we define a metric to perform condensed demapping. On the other hand, for high code rates, adaptive sub-region demapping is proposed. In this work, a combination of both demapping methods is designed showing comparable performance to the classical ML demapper with lower complexity.

1. Introduction

The analysis of new constellation schemes is commonly associated to the transmitter side, i.e., design complexity, memory requirements and channel capacity. The constellation scheme designed may be very efficient from the transmitter point of view, however, the impact of the constellation in the receiver must be also taken into account. A very efficient scheme in terms of channel capacity and system performance could be prohibitive in a real implementation if the demapping complexity is very high. When a new constellation scheme is proposed, the demapping complexity must be taken into account and decoding solutions that reduce the complexity associated to the exhaustive search method (ML) must be provided.

In the case of NUCs, two different topologies are distinguised: 1D-NUCs and 2D-NUCs. For 1D-NUCs and constellation orders from 4 to 256, the demapping complexity is very low as it is shown in Chapter 4 Section 3.1. For massive order 1D-NUCs (from 1024 constellation points) the major restriction is the number of computations required at the demapping stage. Several methods based on decomposing the gray-labeled QAM into two independent I and Q gray-labeled PAMs are shown in [107], [110]. These proposals perform one-dimensional soft demapping on the separated components of a received symbol. 1D-NUCs can be also decomposed into two independent non-uniform QAMs, reducing the number of Euclidean distances (EDs) computed.

In hardware applications, the Max-Log approximation of the ML demapper is commonly used [185]. The number of mathematical computations is reduced with respect to the ML but the number of EDs remains the same. The value of the Log-Likelihood Ratio (LLR) metric given by the Max-Log approximation is mainly influenced by the closest point to the received observation. In [94] a low-complexity demapper based on a simplified detection of the closest point to the received observation is proposed. Nevertheless, this solution is not valid for 1D-NUCs as the constellation points are not uniformly spaced. Another approach is considered in [186] for demapping non-uniform *M*-PAM constellations efficiently based on finding the intervals where the LLRs are linear functions. The overall complexity is reduced from $O(\sqrt{M})$ to $O(2+\log_2\sqrt{M})$ but at the cost of high memory requirements.

2D-NUCs cannot be created using two non-uniform PAM signals. This implies that the I and Q components of the constellation symbols are no longer independent. As a consequence, a two-dimensional demapper must be applied to

each received symbol. Several works have dealt with the design of 2D-demappers, each one applicable to a specific constellation topology. Several algorithms have been specifically designed for systems using APSK modulation. A simplified soft demapper was created for satellite communications [138].This demapper decomposes the APSK into two different PAM signals, which is not directly applicable to 2D-NUCs. In [147] a simplified demapper was proposed for the DOCSIS 3.1 system where non-square quadrature amplitude modulation schemes are used. In this case, the independence between several bits of the symbol is exploited to simplify the demapping process. This approach is not applicable to 2D-NUCs where all the bits are dependent.

On a different research thread, the inclusion of the RC technique, has also led to several studies of low complexity demappers. In [124], the authors reformulate the received rotated QAM as two PAM signals applying MMSE decorrelation. This technique is not applicable to 2D-NUCs because it is not possible to decorrelate I/Q components without high performance losses. Another family of demapping approaches reduces the area where Euclidean distances are evaluated. The latest proposal in this direction is a fixed sub-region demapper proposed in [121], [122]. The result is a reduction in complexity ranging from 25% to 50% with variable performance losses. Another interesting result can be found in [129] where a sub-region demapper applicable to 2D-NUCs was proposed, following the foundations set by the previous results in [122]. This demapper provides low demapping complexity and low system performance losses when compared to the ML demapper for high code rates. Although this demapper is focused on 2D-NUCs, there is still room for improvement.

A first set of solutions of the optimization techniques implements non-fixed sub-region demappers targeting the variable nature of the region size. The parameter defining the size of the region of interest is key in the performance. In previous works this parameter is kept constant for all the transmission/reception scenarios, no matter the SNR and the propagation channel scenario. Indeed, the dimension of the region is defined empirically and it will be a fixed feature of the ModCod choice at the design stage. The size of the area is calculated statistically from the system performance results around the vicinity of the LDPC code waterfall region. In terms of network planning, this corresponds to tweaking the broadcast system depending on LDPC code threshold for the worst supported transmission channel scenario. In particular, the available SNR for most users will be significantly higher than the threshold SNR. Therefore due to high SNR users, the sub-region will be often too wide in terms of possible computation volume

reduction. While this has been the use in traditional broadcast system design, an improved approach is feasible using our demapping proposal.

An additional limitation is associated to the propagation channel variations: the sub-region size optimization is carried out for a static situation and does not adapt to the channel. This fact will result into system performance losses for several channel scenarios. Therefore, we propose a novel solution called adaptive sub-region demapper for 2D-NUCs with lower complexity and better system performance than constant sub-region demappers. The dimension of the region varies for each received symbol through adaptation to the characteristics of the ModCod, perceived SNR and channel conditions. Finally, sub-region demappers do not provide complexity reduction for low code rates.

The objective of this chapter is to design low complexity demappers for 1D-NUCs and 2D-NUCs. The goal is to overcome the limitations shown above for the state-of-the-art demappers providing lower demapping complexity. Furthermore, low system performance losses and memory usage are also required.

2. EVALUATION METHODOLOGY

Prior to the design, evaluation and comparison of demappers for NUCs, this section details the procedure to be followed for the analysis of the proposed demappers and existing solutions. The procedure is as follows:

- Definition of standardized metrics that permit the evaluation and comparison of the complexity and performance of demapping strategies.
- Definition of the evaluation cases that represent real terrestrial broadcast scenarios.
- Creation of an evaluation tool that provides accurate results for the metrics and scenarios defined.

2.1.1 Metric

There are two metrics that mainly define the performance of a demapper. First, the demapping complexity associated to the solution. The most commonly used metric for demapping complexity is the reduction of the number of Euclidean distances (EDs) computed at the demapping stage [122], [128], [129]. This metric is given in terms of percentage of the number of EDs that are not computed if compared with the ML solution.

The second metric is the system performance of the designed demapper. The results are obtained for a given SNR threshold value when the BER is 10^{-6} and the simulation step is 0.1 dB. These results are compared with the exhaustive search method, i.e., ML decoder or with the Max-Log decoder.

2.1.2 Evaluation Cases

Two different evaluation cases are distinguished for the analysis of demappers. First, if the Channel State Information (CSI) is considered ideal and the channel itself does not play a main role in the calculation of the EDs, the evaluation cases are reduced to AWGN and Rayleigh iid channels. If the channel is used in any calculation during the reduction of the number of EDs to be computed or non-ideal CSI is supposed, then the evaluation cases are extended to fading channels with multipath. For this case, Ricean F1 and Rayleigh P1 channels are used as they are the most common fading scenarios in DTT broadcast systems.

2.1.3 Evaluation Tools

For the first evaluation case, the system performance of the demapper is carried out using the BICM tool described in Chapter 3 Section 2.2.3. For the second case, a transceiver based on the ATSC 3.0 physical layer is designed.

The configuration of the parameters is as follows:

- The transmitted signal is composed of 300 FEC blocks with 64,800 bit length.
- In the OFDM system, all the interleavers defined in ATSC 3.0 for single PLP are used.
- The Scattered Pilot Pattern is SP12_2, 16K FFT is used and the guard interval is 1024 samples. The pilot boosting is 4.7 dB.
- Two-dimensional channel estimation based on the Discrete Fourier Transform (DFT) interpolation method [189] is performed jointly with frequency and time filtering.
- Perfect synchronization is considered.

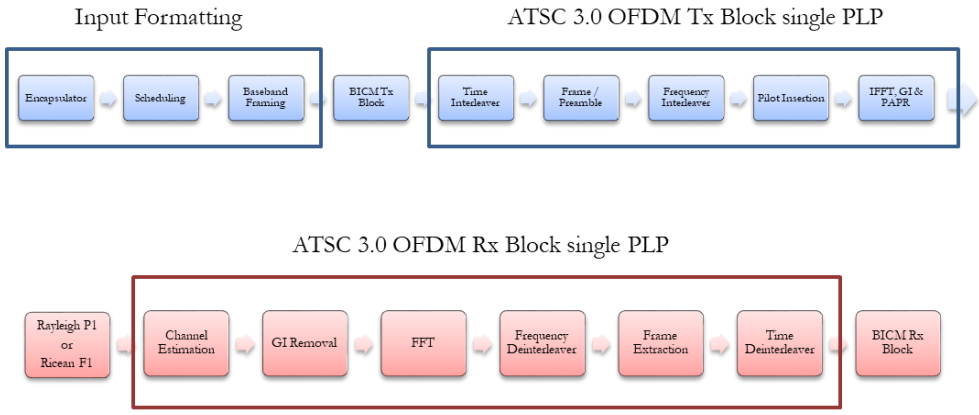

Figure 5.1. ATSC 3.0 OFDM system model simulation tool.

3. LOW-COMPLEXITY LATTICE REDUCTION DEMAPPER FOR MASSIVE ORDER ONE-DIMENSIONAL NON-UNIFORM CONSTELLATIONS

This section proposes a low-complexity demapper based on lattice reduction for massive order 1D-NUCs.

3.1 Proposed 1D-NUC Demapper

3.1.1 Method

In BICM systems, the LLRs are calculated for each transmitted bit using the conditional probability of receiving y given that the b_i transmitted is 0 $p(y|b_i \text{ is } 0)$ and that b_i transmitted is 1 $p(y|b_i \text{ is } 1)$. For the Max-Log, the LLR value for bit b_i is given by the two closest symbols to the received observation with bit $b_i = 0$ and $b_i = 1$, respectively. We propose a simplified detection of these two symbols based on dividing the 1D-NUC into lattices of the same dimension.

The minimum length of the lattices d_{min} is the minimum distance between adjacent constellation points of the designed 1D-NUC. The 1D-NUC is designed with the restriction that the distances between adjacent constellation symbols are multiples of d_{min}. Thus, these distances might produce a small degradation if compared with ideal constellations. Then, the constellation diagram is divided into lattices of length d_{min}. The length of the lattices is normalized to unity and the lattices are numbered from 1 to n, where n is the number of lattices. Next, the received symbol is discretized taking values from 1 to n+1 corresponding to the boundaries of the lattices. The two closest symbols to the discrete received observation with bit $b_i = 0$ and 1 are stored in a Look-Up-Table (LUT). The closest symbols used for LLR calculation are found in the column specified by the value of the discrete received symbol.

3.1.2 1D-NUC Design

Chapter 4 described the design procedure of optimal NUCs in BICM systems. The distances between adjacent constellation points in these designed 1D-NUCs do not fulfill the requirements expressed above. All the distances between adjacent points must be multiples of d_{min}, and consequently, the designed 1D-NUCs are post-processed in order to fulfill the design condition.

After the post-optimization, negligible losses are obtained for low and mid code rates due to the granularity given by the value of the d_{min}. For this range of code rates (from R=2/15 to R=10/15), this is translated into negligible system performance losses. For high code rates, the BICM system capacity losses increase due to the low granularity of the value d_{min}. Nevertheless, the system performance losses are below 0.2 dB.

3.1.3 Simplified Detection of the Closest Point to the Received Observation

The objective is to create a LUT which stores the two closest symbols with b_i = 0 and 1 respectively to a particular value of the received symbol. The value of the received symbol is modified representing the entry to the LUT and the LLR value using the max-log approximation is obtained. Three main steps are considered: divide the non-uniform PAM into uniform lattices, create the LUT and modify the value of the received observation. For simplicity, the gray labeled 1D-16NUC shown in Figure 5.2 is considered.

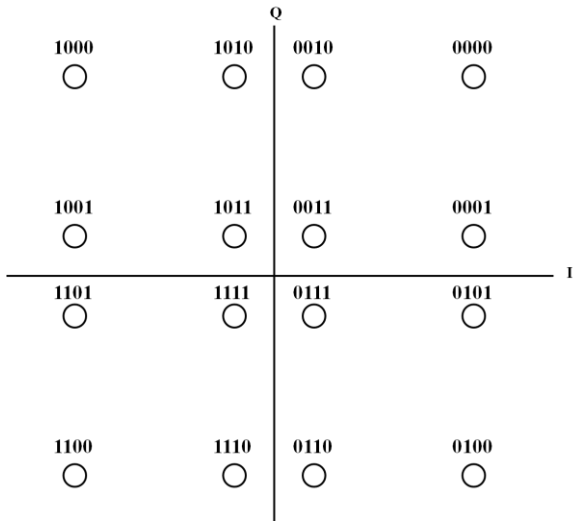

Figure 5.2. Gray labeled 1D-16NUC

1-) First step: Divide the non-uniform PAM into uniform lattices

The key aspect of the first step is to create lattices of dimension unity whose limits in the constellation diagram are integers starting from 1. Each limit corresponds to one entry of the LUT. The processed value of the received

observation is equal to one value of the boundaries. Figure 5.3 a) shows one non-uniform PAM with four components (S_1, S_2, S_3 and S_4) with multiple distances of d_{min} between adjacent components. The value of d_{min} is 0.3922. This non-uniform PAM has been designed following the procedure explained in Chapter 4. Next, the positions of the PAM components are normalized dividing their positions by d_{min} (S_{1b}, S_{2b}, S_{3b} and S_{4b}). This step is shown in Figure 5.3 b). Finally, the constellation points are shifted to the right of the constellation diagram, giving S_{1c} value 1. In this way, there are five different lattices (from L_1 to L_5) with a total of six boundaries, as Figure 5.3 c) shows.

After processing the received observation (third step), the modified received

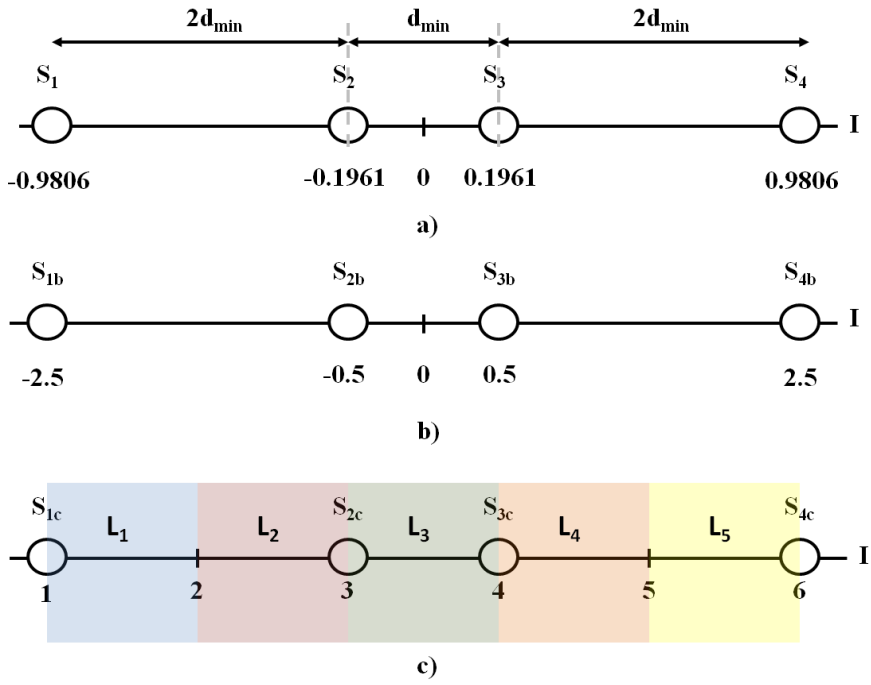

Figure 5.3. Procedure of division of the non-uniform PAM into uniform lattices

constellation symbol can only take integer values, i.e., in this case from 1 to 6.

2-) Second step: Create the Look-Up Table

The LUT is composed by *n* rows and *m* columns, where *n* is the number of bits of the PAM multiplied by two (as each bit can take value 0 or 1) and *m* is the number of boundaries of the lattices.

$$n = \log_2 M$$

$$m = L + 1 \tag{5.1}$$

Equation 5.1 represents the number of rows and columns of the LUT, where M is the constellation order of the QAM constellation and L is the number of unity lattices of the PAM.

Following the example, $M = 16$ and $L = 5$. Therefore the number of rows is $n = 4$ and columns $m = 6$. Each row represents each bit of the PAM constellation with value 0 or 1. Each column includes the possible integer values of the boundaries. The I and Q PAMs of the designed 1D-16NUC contain $\frac{\log_2 M}{2}$ bits each one, i.e., 2 bits. The in-phase PAM carries bit 2 and 4 of the 1D-16NUC and

Table 5.1. Look up table example for 1D-16NUC

Bit	Scaled received observation					
	1	2	3	4	5	6
b2=0	S1c	S1c	S1c	S4c	S4c	S4c
b2=1	S2c	S2c	S2c	S3c	S3c	S3c
b4=0	S1c	S1c	S2c	S2c	S2c	S2c
b4=1	S3c	S3c	S3c	S3c	S4c	S4c

the quadrature PAM bit 1 and 3. Table 5.1 shows the LUT for the in-phase PAM. The content of the quadrature PAM is the same but for bits 1 and 3.

3-) Third step: Modify the value of the received observation

The value of the received symbol is normalized by d_{min} and increased by the value of the highest constellation point, i.e., in the example S_{4b}. This value is increased by 1, the same as in the first step, Figure 5.3c for the PAM. Next, in order to obtain the closest boundary to the value of the received point, a value of 0.5 is added to the value of the received point (because the dimension of the lattice is one) and the resulting value is rounded to the lowest integer value. Equation 5.2 shows the calculation of the scaled value of the received symbol.

$$r_I\_scaled = \left\lfloor \frac{r_I + S_{max}}{d_{max}} + 1.5 \right\rfloor \tag{5.2}$$

Where r_I is the in-phase component of the received observation. S_{max} is the value of the highest constellation point and r_I_scaled is the value of the modified

received point. It must be taken into account that r_{I_scaled} could be positioned in the middle of two points which carry the same bit value. In this case, there exists a small deviation of the ED. However, as results in next section show, the impact in the system performance is negligible. The ED is easily calculated as shown in Equation 5.3.

$$ED = \left| \frac{r_I + S_{max}}{d_{max}} + 1.5 - S_{xc} \right| \tag{5.3}$$

Where S_{xc} is the value obtained from the LUT.

3.2 Complexity Analysis and Simulation Results

3.2.1 Complexity Analysis

In this section massive order 1D-NUC constellations (1024 and 4096) are considered. The main complexity of the proposed demapper comes from the Euclidean distances computations and the modification of the received observation. For each PAM, $1 + \log_2 \sqrt{M}$ distances are required and one step for the scaling of the received observation (with one division and three additions). The overall complexity is O($2 + \log_2 \sqrt{M}$) . The Max-Log method requires the computation of $\sqrt{M}$ distances between the received symbol and the constellation points. The overall complexity is O($\sqrt{M}$). If the proposed demapper is compared with the conventional methods, i.e., ML and Max-Log and 1D-1024NUC, 1D-4096NUC are considered, the complexity reduction is 78.1% and 87.5%, respectively.

In terms of memory requirements, the dimensions of the LUT are m x n and the number of bits assigned to each cell is $\log_2 \sqrt{M}$. Table 5.2 summarizes the memory requirements for the designed 1D-1024NUCs and 1D-4096NUCs in bytes. The memory is reduced by two as the LUT is the same for both I and Q components.

Table 5.2. Look up table memory requirements

Code rate	LUT memory requirements [Kilobytes]	
	1D-1024NUC	1D-4096NUC
2/15	0.01	0.25
3/15	0.44	0.94
4/15	0.55	1.93
5/15	0.30	1.67
6/15	0.67	0.75
7/15	0.51	1.47
8/15	1.44	2.76
9/15	1.13	2.52
10/15	1.00	0.87
11/15	0.14	0.63
12/15	0.12	0.33
13/15	0.1	0.29

3.2.2 System Performance Simulation Results

All the results shown in this section have been obtained using an ATSC 3.0 BICM transceiver with 300 FEC blocks of length 64,800 bits. LDPC code options (R=2/15 to R=13/15) included in ATSC 3.0, with 1D-1024NUC and 1D-4096NUCs under Rayleigh iid channel are considered. Results for the ML and Max-Log are obtained using the 1D-NUCs defined in ATSC 3.0. For the proposed demapper, newly designed 1D-NUCs explained in Section 3.1 are used.

Table 5.3 shows the system performance losses of the proposed solution (newly designed 1D-NUCs and low complexity demapper) compared with ML and Max-Log detection with ATSC 3.0 1D-NUCs. The system performance losses of the designed demapper against the ML range from 0.1 to 0.4 dB for 1D-1024NUCs and from 0.1 to 0.5 dB for 1D-4096NUCs. As it is shown in [112] and [186] the Max-Log approximation has a perceptible deviation from the value given by the ML for non-uniform constellations. When the constellation points are not equidistant, the ML cannot be purely approximated by the Max-Log.

Results in Table 5.3 show that the system performance losses of the proposed solution compared with the Max-Log are negligible for 1D-4096NUCs (maximum of 0.1 dB for high code rates). In the case of 1D-1024NUCs, losses of up to 0.3 dB are present for high code rates. For mid and low code rates, the performance losses

are negligible. The system performance losses with respect to the Max-Log come from the restriction imposed in the design of 1D-NUCs.

Table 5.3. System performance losses of the proposed demapper compared with the ML and Max-Log demappers

CR	1D-1024NUC		1D-4096NUC	
	ML	Max-Log	ML	Max-Log
2/15	0.1	0	0.5	0
3/15	0.3	0	0.4	0
4/15	0.3	0	0.4	0
5/15	0.4	0	0.2	0
6/15	0.2	0	0.2	0
7/15	0.2	0	0.1	0
8/15	0.1	0	0.2	0
9/15	0.1	0	0.2	0
10/15	0.1	0	0.1	0
11/15	0.3	0.2	0.2	0
12/15	0.2	0.2	0.2	0.1
13/15	0.3	0.3	0.3	0.1

4. LOW-COMPLEXITY ADAPTIVE DEMAPPER FOR TWO-DIMENSIONAL NON-UNIFORM CONSTELLATIONS

This section proposes a low-complexity demapper based on adaptive sub-region for 2D-NUCs.

4.1 Proposed 2D-NUC Demapper

4.1.1 Method

In this section we define a condensation metric for the receiver and we present a study of the most appropriate value to provide low demapping complexity with negligible impact on performance for low code rates. For mid and high code rates, we propose an adaptive sub-region demapper. The combination of the two demapping techniques (condensation and sub-region) called Switched Condensed and Adaptive Sub-Region (SCASR) is proposed providing lower demapping complexity than state-of-the-art 2D-NUC demappers with negligible impact on performance for all the studied code rates. All the results shown in this section have been obtained using a fully compliant ATSC 3.0 BICM transceiver with 300 FEC blocks of length 64,800 bits. LDPC code options (R=2/15 to R=13/15) included in ATSC 3.0 are used.

4.1.2 Condensed Demapper Optimization

The condensed demapper takes advantage of the condensation applied to the 2D-NUCs designed for low and mid code rates [187], [188]. When designing a condensed demapper, the most important parameter is the condensation degree (or number of merged points) to be applied to the 2D-NUCs. Most of the 2D-NUCs included in ATSC 3.0 do not present complete condensation. Indeed, points are not merged, but close to each other.

The ED between adjacent points is used as metric for condensation. Figure 5.4 shows the bit error probability difference between the ML and the condensed demapper for different metric values (0.05, 0.1, 0.15 and 0.2). The bit error probability is calculated for the SNR threshold at the LDPC waterfall region. ATSC 3.0 2D-256NUCs are analyzed for all code rates over AWGN and Rayleigh iid channels using the ATSC 3.0 BICM chain.

The condensed demapper presents similar bit error probability to the ML demapper for the four metric values and low code rates up to R=7/15. In this region, 2D-256NUCs present the highest condensation degree. In the code range from R=8/15 to R=13/15 the bit error probability for 0.15 and 0.2 metrics increases significantly. Condensation applied to 2D-256NUCs within this code rate range behaves poorly. The bit error probability penalty is even higher in the case of the Rayleigh iid channel. For both channels, the metrics 0.05 and 0.1 present similar error probability to the ML demapper (except for 0.1 at R=11/15 code rate for Rayleigh iid channel).

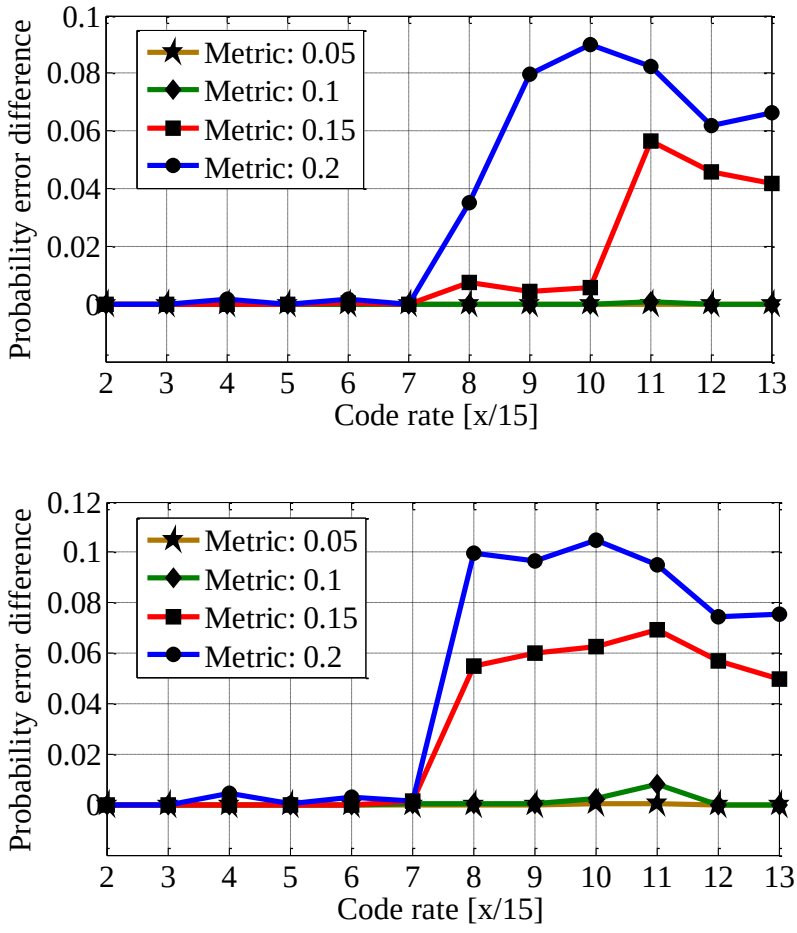

Figure 5.4. Probability error difference between the ML and condensed demapper for the AWGN channel (above) and Rayleigh iid channel (below)

Figure 5.5 shows the reduction in terms of percentage of the number of Euclidean distances to be computed in the condensed demapper with respect to the ML demapper for all code rates. The complexity reduction increases with the value of the condensation metric. However, as shown in Figure 5.4, the system performance gets worse as the metric increases. We propose to use a metric value of 0.05 as the best tradeoff between demapping complexity and system performance.

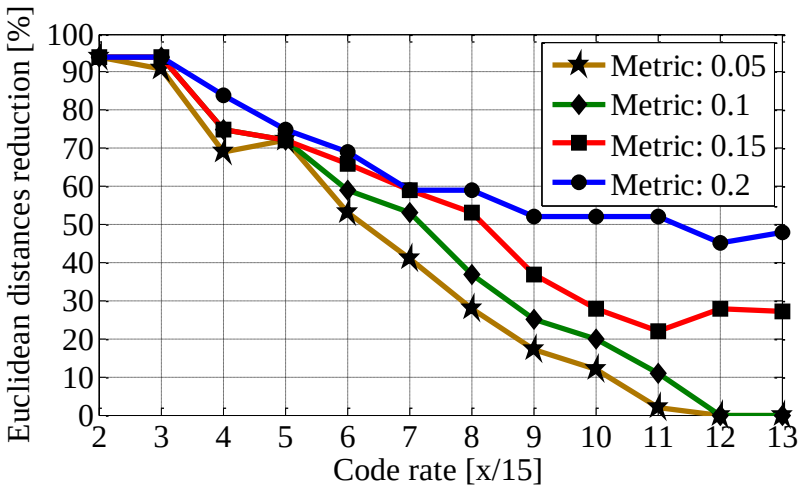

Figure 5.5. Percentage of the Euclidean distances reduction between the ML and condensed demapper.

4.1.3 Adaptive Sub-Region Demapper

The second demapper sub-module makes use of the design methodology of 2D-NUCs described in chapter 4. 2D-NUCs are obtained as a function of the operating SNR and the considered channel model. An adaptive sub-region demapper with a variable region size depending on these two parameters is proposed. The size varies for each received constellation symbol.

4.1.3.1 Concept and functional diagram of adaptive sub-region demapper

The adaptive sub-region demapper is based on computing the EDs between the received symbol and the symbols inside a square sub-region of the constellation diagram with a determined length.

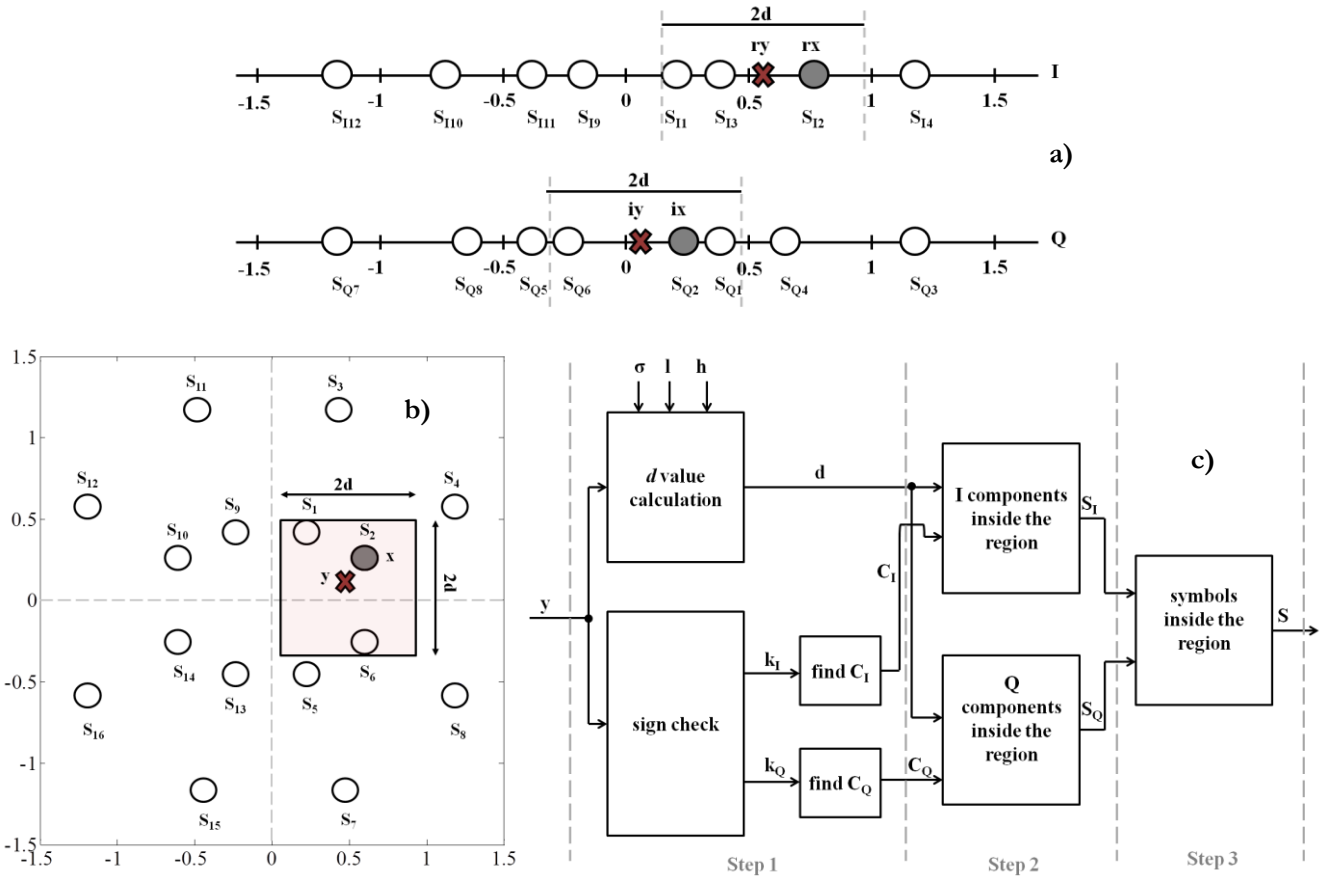

Figure 5.6. a) In-phase and quadrature representation of the adaptive sub-region demapper for 2D-16NUC at 8 dB. b) Constellation diagram representation of the adaptive sub-region demapper for 2D-16NUC at 8 dB. c) Functional diagram of the adaptive sub-region demapper

In the case of 2D-NUCs, we propose a square sub-region varying with the operating SNR and considered channel model. In this way, the length of the sub-region closely fits the design conditions of each 2D-NUC, providing an efficient demapping process. Figure 5.6 c) depicts the functional diagram of the adaptive sub-region demapper. The first demapping step consists of calculating the length d of the sub-region for each received symbol. In parallel, in order to calculate the closest constellation symbol to the received symbol, two processes are considered. First, a sign check of each component of the received symbol will determine the quadrant choice. The sign check is stored in K_I (in-phase) and K_Q (quadrature). Then, the I and Q components of the closest constellation symbol to the received symbol are obtained (C_I and C_Q) following the procedure described in Section 4.1.3.4.

In the second step, using the I and Q components of the closest symbols (C_I and C_Q), the I and Q components of the symbols inside the sub-region are obtained and stored in arrays $\mathbf{S_I}$ and $\mathbf{S_Q}$, respectively.

The final step consists of merging the I and Q components of the symbols inside the sub-region, obtaining the constellation symbol set to calculate LLR values. These symbols are stored in the array **S**.

A graphical description behind the idea of the adaptive sub-region demapper is shown in Figure 5.6 a) and Figure 5.6 b). For simplicity, the optimal 2D-16NUC for 8 dB of SNR is considered. This constellation is composed of 16 symbols S_i where i = 1…16. Each symbol has one I and Q component associated S_{Ii} and S_{Qi}. Figure 5.6a shows a graphical representation of the sub-region demapper for components I and Q. For the I component, the sub-region is limited by the I components of the constellation symbols inside the sub-region of length $2d$ centered at r_y, where r_y is the real part of the received symbol. In this case, these components are S_{I1}, S_{I2} and S_{I3}. The real part of the transmitted symbol is represented as r_x. The same applies for the Q components, being S_{Q1}, S_{Q2} and S_{Q6} the Q components of the symbols inside the sub-region. Figure 5.6b shows the sub-region in the constellation diagram and the symbols inside it. The transmitted symbol is represented as x and the received symbol as y. Symbols S_1, S_2 and S_6 are inside the sub-region for the particular x and y symbols.

4.1.3.2 Length of the square adaptive sub-region demapper

The value of the length of the sub-region is based on having, at least, the transmitted symbol inside the sub-region. Constellation symbols situated at the

limit of the sub-region are also included. Equation 5.4 shows the received symbol in a communication system with Gaussian noise for a determined channel.

$$y = hx + n \tag{5.4}$$

Where *y* is the received symbol, *x* the transmitted symbol, *n* the noise value (in this case Gaussian noise is assumed) and *h* the fading coefficients of the channel. All the parameters are complex values. Manipulating Equation 5.4, the position of the transmitted symbol *x* is obtained as:

$$x = \frac{y}{h} - \frac{n}{h} \tag{5.5}$$

The first term $\frac{y}{h}$ refers to a zero forcing equalization. Manipulating the second term in Equation 5.5, we derive the length of the sub-region *d* in Equation 5.6. This length is calculated for each received symbol, i.e., it adapts to the channel and noise variations.

$$d = \left|\frac{(l+jl)\sigma}{h}\right| \tag{5.6}$$

Where σ is the standard deviation of the Gaussian distribution and *l* is the maximum random value which determines the percentage of values that lie within a band around the mean in a normal distribution. As shown in Equation 5.6, the value of the length is directly proportional to the noise value. The higher the noise value the higher the length value and vice versa.

4.1.3.3 Design of adaptive sub-region demapper

The adaptive sub-region demapper presents a series of special cases. The first case is considered when there is no symbol inside the sub-region. In this case, the length of the sub-region is increased until at least, two symbols are inside. Second, in the calculation of the LLR values for each transmitted bit, the conditional probability of receiving *y* given that the b_i transmitted is 0 $p(y|b_i \text{ is } 0)$ and the conditional probability of receiving *y* given that b_i transmitted is 1 $p(y|b_i \text{ is } 1)$ are needed. However, it can occur that for a determined b_i all the symbol values inside the sub-region are 0 or 1 for that particular bit. In this case, taking into account that a FEC soft decoder performs better under pessimistic assumptions (consider one symbol as if it was closer than its real position) the conditional probability of the missing bit value is calculated for the furthest symbol inside the sub-region. This can derive into both conditional probabilities with the same value if the EDs

are the same for both bit values. This is solved by increasing the length value and forcing that there are, at least, two symbols with different EDs.

This solution performs efficiently for low and mid code rates (up to R=9/15). However, for higher code rates, system performance gets worse. For low code rates, the sub-region covers mainly the totality of constellation points and this demapper does not reduce complexity. For high code rates the sub-region only covers part of the constellation diagram and the case explained above in which one bit value is not inside the sub-region commonly happens for the two MSBs. In this case, another approach is proposed: compute the ED from the received point y to the origin of the constellation diagram (0+0j) since it represents the intersection of the four quadrants. This option requires only one Euclidean distance to be computed. As shown in Section 4.2, this solution has negligible impact on the demapping complexity and system performance.

Figure 5.7 shows the percentage reduction in the number of EDs to be computed with respect to the ML demapper. For low code rates, limited reduction is observed. In this zone, where the noise components are high, the length of the sub-region is highly increased gathering almost all the constellation points. In the region of mid code rates, as the noise value is lower, the number of points inside the sub-region is lower and the number of EDs to be computed is reduced. High code rates present the highest complexity reduction as the length of the sub-region is highly reduced.

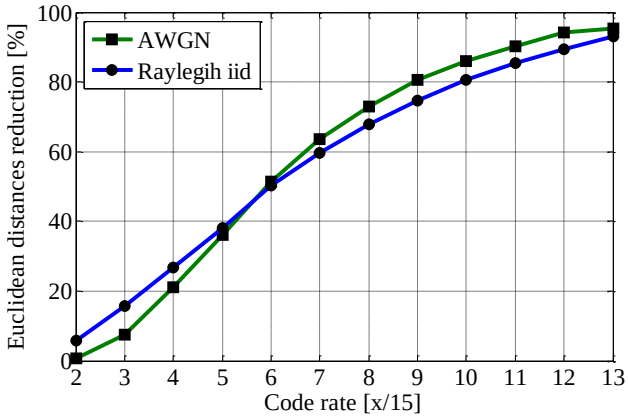

Figure 5.7. Percentage of the Euclidean distances reduction between the ML and adaptive sub-region demapper for the AWGN and Rayleigh iid channels.

The adaptive sub-region demapper proposed in this section provides high demapping complexity reduction in the region of mid and high code rates with negligible performance loss. A complexity reduction from 60% for R=7/15 to 95% for R=13/15 is achieved. In order to decrease the complexity for low and mid code rates, a combination of the adaptive sub-region and condensed demapper is proposed (Section 4.1.4).

4.1.3.4 Determination of points inside the adaptive sub-region

The efficient determination of the points inside the sub-region is critical. We propose a methodology based on finding the closest constellation symbol to the received symbol. Then, a comparison process starting from this symbol is performed in order to determine the first point outside the sub-region.

The procedure is explained for one axis (I) and the methodology is then repeated for the other axis (Q). First, a sign check of the I component of the received symbol is performed in order to determine the quadrant. Next, dichotomy process is applied to the real part of the constellation points in order to determine the closest constellation point to the received point. The dichotomy process consists of dividing the set of I components into two subsets with equal number of components. The I component of the received symbol is compared with the limit value of the two subsets. A subset is chosen based on this comparison. An iterative procedure is performed until there is only one I component in the subset. This I component belongs to the closest symbol. Next, starting from the I component of the closest constellation point, comparisons are performed between the real part of the constellation symbols and the value of the length of the sub-region. In this way, the number of comparisons performed is reduced, i.e., the number of the points inside the sub-region plus the first one outside the region having a larger value than the considered length.

4.1.3.5 Determination of the size of the sub-region

The next step consists of determining the most suitable value of l. We approximate Equation 5.6 to a normal distribution to set l = 3 as initial value. In this way, we assume that the transmitted symbol will be inside the sub-region during a high percentage of time. Then, an iterative procedure is performed to obtain the optimal value of l. Table 5.4 shows the study carried out to determine the optimal value of l with the lowest demapping complexity jointly with system performance losses below 0.1 dB. Steps of 0.1 are considered for the determination

of the l value. Results from Table 5.4 show that for l = 3.6, the performance penalty of the adaptive sub-region demapper with respect to the ML demapper is below 0.1 dB for all code rates. For R=2/15 and R=6/15 a value of l = 3 also provides a negligible performance penalty and the same applies for R=10/15 code rate with l = 3.3. These values imply lower demapping complexity than for l = 3.6 (in the range of 2 - 5% lower demapping complexity). For simplicity and targeting a hardware implementation, we take l = 3.6.

It is important to note that the value l = 3.6 is also valid for the ATSC 3.0 OFDM platform under ideal CSI. However, for non-ideal CSI the same study has been done obtaining a new value of l = 5. Therefore, the value of l will depend on the implemented channel estimation algorithm

Table 5.4. Search of the optimal L value

Channel	Code rate [R/15]	l value						
		3	3.1	3.2	3.3	3.4	3.5	3.6
		System performance losses [dB] of the adaptive sub-region w.r.t. the ML demapper						
AWGN	R=2	<0.1	<0.1	<0.1	<0.1	<0.1	<0.1	<0.1
	R=6	<0.1	<0.1	<0.1	<0.1	<0.1	<0.1	<0.1
	R=10	<0.1	<0.1	<0.1	<0.1	<0.1	<0.1	<0.1
	R=13	3.3	3.3	1.9	1.7	0.5	0.3	<0.1
Rayleigh iid	R=2	<0.1	<0.1	<0.1	<0.1	<0.1	<0.1	<0.1
	R=6	<0.1	<0.1	<0.1	<0.1	<0.1	<0.1	<0.1
	R=10	1.1	1.1	1.1	<0.1	<0.1	<0.1	<0.1
	R=13	1.5	0.8	0.5	0.3	0.3	0.3	<0.1

4.1.4 Switched Condensed and Adaptive Sub-Region Demapper

Being a combination of the two proposed demapping techniques, the combined SCASR demapper applies the metric value of 0.05 for the underlying condensed demapper and $l = 3.6$ for the adaptive sub-region demapper with ideal CSI. For these parameters, observed performance remains within 0.1 dB from the ML demapper.

Figure 5.8 shows the functional diagram of the SCASR demapper. The first block corresponds to the decision block where, depending on the code rate, either one or both demappers are switched on. The criteria depend on the code rate range: for the code rates of R=2/15 and R=3/15 only the condensed demapper is applied. From code rates R=4/15 to R=10/15, both demappers (condensed and adaptive sub-region) are used. From code rates of R=11/15 to R=13/15, only the adaptive sub-region demapper is used.

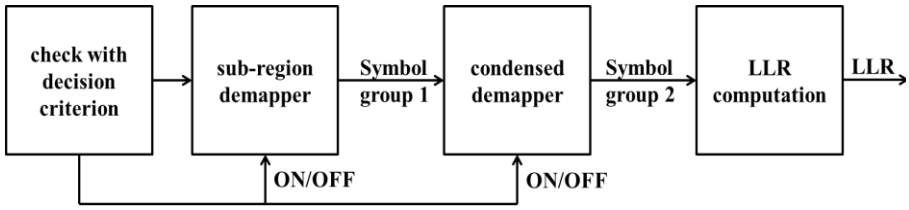

Figure 5.8. Functional diagram of the SCASR demapper

Figure 5.9 shows the reduction in terms of percentage of the number of EDs to be computed with respect to the ML demapper. The SCASR demapper presents a demapping complexity reduction ranging from 77% to 95% for the AWGN channel. This reduction ranges between 79% and 93% in the case of the Rayleigh iid channel. For this latter channel type, the fading coefficients and the SNR value (higher than in the AWGN channel for error-free decoding) increase the size of the sub-region.

The influence of the condensed demapper is remarkable for low code rates as it provides low demapping complexity. The adaptive sub-region demapper performs at its best for high code rates. In the range of mid code rates, both demappers have similar influence in the complexity reduction.

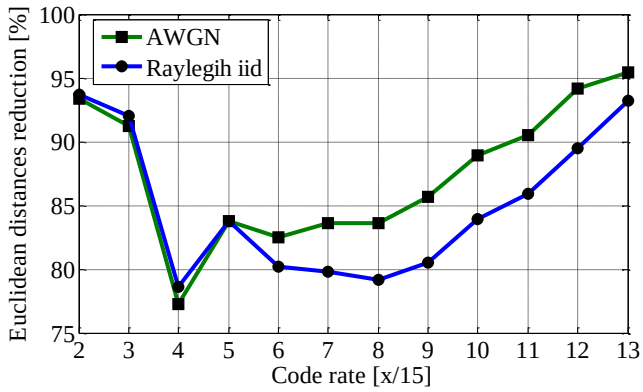

Figure 5.9. Percentage of the Euclidean distances reduction between the ML and condensphere demapper for the AWGN and Rayleigh iid channels.

4.1.5 Hardware Implications

The additional hardware complexity of the SCASR demapper with respect to the ML or Max-Log demappers is the calculation of the length of the sub-region and the constellation points inside the sub-region. Regarding the calculation of the parameter *d*, the remarkable operations in terms of hardware requirements are one multiplication and one division. The multiplication can be easily implemented via an addition since the SNR is constant for all the received symbols. The division can be considered equivalent to an ED computation and it is taken into account in the complexity analysis in Section 4.2. The rest of operations are comparisons or additions which are negligible where compared with ED computation. The maximum possible number of simple operations is *M*, where *M* is the number of constellation points, which is still negligible if compared with the computation of the EDs needed to calculate the LLR of each bit of the received symbol.

4.2 Complexity Analysis and Simulation Results

4.2.1 Demapping Complexity and System Performance

In this section, the system performance of the proposed SCASR demapper is analyzed. As a contribution, the results of a low complexity demapper for 2D-256NUCs are presented using, for the first time, the fully compliant ATSC 3.0 OFDM transmitter – receiver chain described in Figure 5.1. The transmitted signal

is composed of 300 FEC blocks with 64,800 bit length. Four different channel models are simulated: AWGN, Rayleigh iid for the BICM system and DVB-T P1 (Rayleigh) and DVB-T F1 (Rice) for the OFDM system. Four different code rates are used (R=2/15, R=6/15, R=10/15 and R=13/15). In the OFDM system, all the interleavers defined in ATSC 3.0 for single PLP are used. Table 5.5 shows the results for ideal CSI. No pilots are used and perfect synchronization is considered. Complexity results consider the maximum number of EDs used to compute an LLR among all the LLRs calculated during the simulations.

Table 5.5. System performance and demapping complexity reduction of the SCASR demapper for ideal CSI

Channel	Parameter	Code rate [R/15]			
		R=2	R=6	R=10	R=13
AWGN	ML: SNR [dB]	1.7	10.6	17.2	22.3
	SCASR Losses [dB]	<0.1	<0.1	<0.1	<0.1
	Complexity Reduction [%]	93.4	82.5	88.9	95.4
Rayleigh iid	ML: SNR	2.9	12.9	20.1	26.7
	SCASR Losses [dB]	<0.1	<0.1	<0.1	<0.1
	Complexity Reduction [%]	93.7	80.2	83.9	93.2
P1	ML: SNR	2.3	12.5	19.7	26.6
	SCASR Losses [dB]	<0.1	<0.1	<0.1	<0.1
	Complexity Reduction [%]	93.7	79.2	81.5	92.2
F1	ML: SNR	1.3	10.5	17.1	22.3
	SCASR Losses [dB]	<0.1	<0.1	<0.1	<0.1
	Complexity Reduction [%]	93.7	80.1	86.7	94.6

In all channel conditions, results from Table 5.5 show that the SCASR performance is comparable to the ML demapper with a negligible gap (under 0.1 dB). Meanwhile, complexity reduction from 6% to 27% with respect to the state-of-the-art demappers for 2D-NUCs [129] and from 79.2% to 95.4% with respect to the ML demapper is obtained.

Table 5.6 extends the results for non-ideal CSI. The value of l is 5 as explained in Section 4.1.3.5. All the interleavers defined in ATSC 3.0 for single PLP are used, the pilot pattern is SP12_2, 16K FFT and the guard interval is 1024 samples. The

pilot boosting is 4.7 dB. Two-dimensional channel estimation based on the Discrete Fourier Transform (DFT) interpolation method [189] is performed jointly with frequency and time filtering.

Results in Table 5.6 validate the proposed SCASR demapper under non-ideal CSI. The percentages of the demapping complexity reduction are quite similar to the ideal CSI case (from 8.7% to 23% w.r.t. [129] and from 71.8% to 93.7% with respect to the ML demapper). The corresponding performance penalties on DVB-T P1 channel are 0.1 and 0.2 dB for *R*=10/15 and *R*=13/15 code rates respectively.

Table 5.6. System performance and demapping complexity reduction of the SCASR demapper for non-ideal CSI

Channel	Parameter	Code rate [R/15]			
		R=2	R=6	R=10	R=13
P1	ML: SNR [dB]	3.4	13.3	20.3	27.7
	SCASR Losses [dB]	<0.1	<0.1	0.1	0.2
	Complexity Reduction [%]	93.7	74.2	75.2	90
F1	ML: SNR	2.2	11.1	17.5	22.8
	SCASR Losses [dB]	<0.1	<0.1	<0.1	<0.1
	Complexity Reduction [%]	93.7	71.8	78.7	91.1

4.2.2 Extension to 2D-1kNUC and 2D-4kNUC

The main problem for high order 2D-NUCs (1k and 4k), is their design and demapping complexity. Indeed, proposed NUCs in ATSC 3.0 for these constellation orders are 1D-NUCs. As a contribution, the system performance and complexity reduction of the SCASR demapper for such high order constellations is presented. In Chapter 4 Section 5, 2D-1kNUCs and 2D-4kNUCs are designed. 2D-1kNUC for *R*=5/15 code rate and 2D-4kNUC for *R*=3/15 code rate are used in this study. Ideal CSI is considered.

Results in Table 5.7 validate the use of the SCASR demapper for high order 2D-NUCs. Demapping complexity reduction ranges from 96.5% to 99.7% (AWGN) and from 96% to 99.1% (Rayleigh iid). In all cases, performance penalty remains within 0.1 dB when compared with the ML demapper. High order 2D-

NUCs could be taken into account in future communication systems with the use of low complexity demappers such as the SCASR demapper.

Table 5.7. System performance and demapping complexity reduction of SCASR demapper for high order 2D-NUC

Channel	Parameter	Constellation order & code rate	
		2D-1kNUC & R=5/15	2D-4kNUC & R=3/15
AWGN	SCASR Losses [dB]	<0.1	<0.1
	Complexity Reduction [%]	96.5	99.7
Rayleigh iid	SCASR Losses [dB]	<0.1	<0.1
	Complexity Reduction [%]	96	99.1

5. **Conclusions**

In this chapter, two different demapper solutions have been presented in order to reduce the complexity associated to the demapping phaseof NUCs.

Regarding 1D-NUCs, a low complexity demapper has been proposed. It is based on finding the closest constellation points to the received observation in an efficient way. The 1D-NUC is divided into two PAMs. The constellation points of the PAMs are transformed in order to create equidistant lattices. The boundaries of the lattices are used to create a LUT with the closest symbols depending of the value of the scaled received observation.

The complexity of this solution for each PAM is O($2 + \log_2 \sqrt{M}$) as opposed to O($\sqrt{M}$) for the ML and Max-Log demappers where *M* is the constellation order of the M-ary 1D-NUC. Negligible system performance losses are obtained for low and mid code rates. For high code rates, the performance losses are below 0.3 and 0.1 dB for 1D-1024NUC and 1D-4096NUC, respectively. Very low memory requirements are observed.

For 2D-NUCs, a novel low complexity demapper switching between two different demapping techniques based on condensation and on adaptive sub-region (SCASR) is proposed. First, the main characteristics of the 2D-NUCs are identified in order to design a demapper which adapts to these characteristics. Clear criteria are proposed for the switching between the two underlying demappers providing the best performance. The functional diagram of the SCASR demapper is shown and the configuration of the sub-modules is detailed.

The second main contribution of this work is the design of an adaptive sub-region demapper closely suited to the shape of 2D-NUCs. The dimension of the sub-region with best compromise between performance and complexity is proposed. The design and functional diagram of the demapper are also defined. This demapper presents high demapping complexity reduction for high and mid code rates.

For low code rates, the use of a condensed demapper is proposed. A metric to appropriately condense 2D-NUCs aiming at low demapping complexity with negligible impact on performance is designed.

In order to validate the proposed SCASR demapper, simulation results are presented using a fully compliant ATSC 3.0 OFDM transceiver. Results show that performance remains within 0.1 dB from the ML demapper. Meanwhile, a

significant reduction in the number of computed EDs ranging from 79.2% to 95.4% is obtained when compared to the ML demapper. When other 2D-NUC demapping proposals are considered, the SCASR demapper still shows lower complexity (from 6% to 27%) and performs better (degradation always below 0.1 dB).

For non-ideal CSI, similar performance results and complexity reductions as for ideal CSI are still obtained. An extension of this demapper is proposed for high order 2D-NUCs showing a complexity reduction of up to 99.7% with respect to the ML demapper.

CHAPTER 6: **CONTRIBUTIONS AND FUTURE WORK**

This dissertation presents contributions in two key areas of the physical layer of BICM based communication systems: constellation and low complexity demapping design. First, a technical background and comprehensive survey on constellation and demapping techniques is presented. The different approaches to construct efficient constellation schemes and demappers are shown based on the analysis of different evaluation criteria.

With the development of the latest digital terrestrial broadcast systems, two new constellation techniques are available today: NUCs and RCs. In this thesis, both techniques are analyzed in order to study their applicability to DTT broadcast systems. In the field of NUC design, this dissertation presents an efficient design of optimal constellation schemes for BICM systems for a wide range of SNR values. Constellation orders from 16 to 4096 points are considered and 1D-NUCs and 2D-NUCs are proposed. Two different condensation techniques are developed. All the schemes are evaluated using a fully ATSC 3.0 compliant transceiver.

Finally, taking into account the computational complexity at the demapping stage, new demappers for 1D-NUCs and 2D-NUCs are designed. Higher complexity reduction than state-of-the-art demappers is achieved with negligible system performance losses.

1. Contributions

The work presented in this thesis contributes to the development of advanced DTT broadcasting systems focusing on high spectral efficiency and robustness with low computational complexity.

The first contribution of this thesis is the evaluation of new modulation techniques for inclusion in DTT broadcast systems. The second contribution is the efficient design of advanced constellation schemes providing high spectral efficiency with low computational cost. Finally, the receiver part of the communication system is considered in order to lower the computational complexity associated to the new constellation schemes by means of low complexity demapping techniques.

1.1 System Performance Analysis of Advanced Modulation Techniques in DTT Broadcast Systems

Two different modulation techniques have been taken into account in this work: NUCs and RC. NUCs target the spectral efficiency of the communication system whereas RC technique provides signal space diversity in fading scenarios. Table 6.1 describes the evaluation methodology followed in this work.

Table 6.1. Methodology to evaluate the performance of NUCs and RC technique.

Technique	Metric	Evaluation cases	Evaluation tools
NUC	System performance (SNR value at BER 10^{-6})	AWGN Rayleigh iid	BICM communication tool
RC	System performance (SNR value at BER 10^{-6})	Rayleigh P1 0 dB Echo at 90% of GI	OFDM communication tool

Three contributions are derived from this chapter:

1) System performance evaluation of NUCs and comparison with standard QAM schemes.

The results obtained for the BICM channel capacity calculation shows that NUCs outperform QAM schemes for each ModCod combination. What is more,

the higher the constellation order the higher the channel capacity gain is. The main reason is the increment in the number of constellation points considered in the design process of NUCs. The highest gains are presented for mid code rates (from 6/15 to 10/15) because for this code rates the constellation points present the highest freedom of movement. Channel capacity gains from 0.0280 to 0.6351 bit/s/Hz are obtained and the most spectral efficient ModCods is 4kNUC and 9/15 code rate.

2) System performance evaluation of NUCs with RC technique.

Table 6.2 gathers the performance evaluation of the RC technique jointly with NUCs. Code rates from 5/15 to 13/15 and NUC constellations from 4 to 64 points are evaluated under Rayleigh iid channel.

The results show that up to 1.85 dB of BICM system performance gain can be achieved for QPSK and R=13/15 if RC technique is applied. For 16 and 64 NUCs, gains of up to 0.98 and 0.43 dB are obtained, respectively. If the RC technique is applied to NUCs, system performance gains can be obtained for low order constellations and high code rates. For high order constellations, the range of code rates at which RC provides gain is lower than for low order constellations, e.g., if RC is applied to 256NUCs there is only gain of 0.1 dB for 13/15 code rate. For low code rates and high order constellations RC implies system performance losses. If this analysis is extended to Rayleigh and 0 dB Echo channels, the trend shown in Table 6.2 is maintained. Besides, for 0 dB Echo channel the rotation gains are higher than for Rayleigh P1 because the influence of the fading coefficients in 0 dB Echo at 90% of the GI channels is more harmful.

Table 6.2. RC technique gain [dB] from DVB-T2 for NUCs and LDPC codes.

Code rate	Constellation		
	QPSK	16NUC	64NUC
5/15	-0.1	-	-
6/15	0	-	-
7/15	0.1	-	-
8/15	0.16	-0.09	-
9/15	0.36	0.01	-
10/15	0.54	0.03	-
11/15	0.82	0.23	0
12/15	1.19	0.49	0.16
13/15	1.85	0.98	0.43

3) System performance evaluation and comparison of ModCod combinations with similar throughput.

The last analysis consists of comparing the system performance of ModCods with similar throughput applying RC technique with those of higher code rate and lower order constellations (where RC technique provides gain). Rayleigh P1 and 0 dB Echo (at 90% of the GI) channels are considered. The results shown in Chapter 3 Section 3.3 show that if ModCods with similar throughput are considered, those with lower code rate and higher order constellation outperforms those with RC technique and higher code rate and lower constellation order. The influence of the code rate is the key parameter in the system performance of ModCods with similar throughputs.

1.2 Design of Advanced Constellation Schemes for BICM System Models with Low Computational Complexity

The fourth chapter of this work presents the whole procedure to efficiently design geometrically shaped constellation schemes for BICM systems applicable to any communication system.

Three different metrics are used to quantify the viability of the developed NUC design algorithm. The first metric is the BICM channel capacity in terms of bit/s/Hz. The second metric is the time consumption of the algorithm proposed to design a constellation. The last metric is the system performance of the NUCs designed with the proposed algorithm in terms of BER versus SNR using the Matlab based BICM system simulation tool developed in this thesis.

Four contributions are derived from this chapter:

1) Optimization problem study with a detailed analysis of the different methods to solve it and the selection of the most appropriate optimization procedure to design NUCs.

The BICM channel capacity is taken as the objective function conditioned to the transmitted signal power is one. The optimization algorithm must fulfill a set of constraints which are: 1) equation independent algorithm. 2) Low simulation time. 3) Accuracy. After a detailed study of the existing alternatives, PSO is the algorithm that fulfills the three conditions in a more effective way than other solutions such as genetic algorithm and simulated annealing.

2) A new methodology to design NUCs.

The main factors that have the highest impact in the constellation design process are:

a. Number of DoFs of the constellation.
b. Range of SNR values to perform the optimization for each constellation order.
c. The constellation shape depending of the SNR value.
d. The bit labeling of the initial constellation

The optimization procedure consists of 4 steps:

a. Calculate the SNR at which the NUC is designed.
b. Obtain the initial constellation.
c. Compute the PSO algorithm.
d. Return to step one if the constellation is not the optimal one.

The procedure to design 1D-NUCs and 2D-NUCs is detailed. For 1D-NUCs, the design procedure is the same independently of the constellation order. In the real part, only one point of each row is optimized and the remaining ones in the same row are displaced exactly at the same distance. In the imaginary part, this movement is column-wise. For 2D-NUCs, the design procedure is different for each constellation order. For 16NUCs, all the constellation points from one quadrant are optimized together and the rest of the quadrants are obtained via symmetry. For 64 and 256NUCs, the quadrant is divided into regions of points inside a defined circumference. The points inside the external circumferences have an extended movement meanwhile the internal ones (close to the origin of the constellation diagram) have a reduced movement. For high SNR values, the points are gathered in rectangular zones, as the final constellation is rectangularly shaped.

If the optimization problem considering Rayleigh iid channel is carried out with no simplification, the designing time is very high due to the variability of the fading coefficients. This thesis proposes a method to solve this problem. The target SNR value is set to the performance threshold of a Rayleigh iid channel, but the channel specified in the optimization process is the AWGN. In this way, the results obtained are similar to the ones obtained by setting the SNR and channel model to Rayleigh iid (losses below 0.1 dB).

3) Performance analysis of the proposed algorithm and results obtained.

Results in Table 6.3 show the simulation time needed to design a constellation. Two important conclusions can be extracted. First, the higher the constellation order is, the higher the optimization time is. Second, 2D optimization (16, 64 and 256 constellation orders) is more time consuming than 1D optimization (1024 and 4096 constellation points) due to the higher number of constellation points involved in the optimization process. Regarding the system performance gains of NUCs, the highest gains are achieved for mid code rates (where the freedom of movement of the constellation points is the highest one) and high order constellations (where more degrees of freedom are available). Gains of up to 1.7 dB and 1 dB are achieved for 1D-4096NUC and R=6/15 for the AWGN and Rayleigh iid channel, respectively.

Table 6.3. Optimization time and system performance of the proposed NUCs.

Average of the optimization time for the proposed NUC					
Constellation order	16NUC	64NUC	256NUC	1024NUC	4096NUC
Time	5 min	20 min	2 hr	10 min	20 min
Highest system performance gains of the designed NUCs versus M-ary QAM (dB)					
Channel/Code Rate	2D-16NUC	2D-64NUC	2D-256NUC	1D-1024NUC	1D-4096NUC
AWGN R=6/15	0.1	0.6	1.1	1.3	1.7
Rayleigh iid R=6/15	0	0.3	0.8	1	1

4) Low complexity condensation techniques

Two different condensation techniques are proposed to reduce the complexity at the design step of NUCs and the demapping complexity for low SNR values. The first condensation method is called condensation with optimization (CWO) and restricts the number of constellation points at the design process. This solution provides low design complexity, but the final shape of the constellation to be designed must be known before the optimization. Otherwise, the constellation designed is sub-optimal. The second proposal is called condensation after optimization (CAO) where first, the constellation is fully optimized and then, it is processed in order to condense the closest points. This solution provides the optimal constellation, but the design procedure is more complex than CWO.

Results from Table 6.4 show that the number of variables involved in the optimization process for CWO is lower than for CAO as the condensation is applied in the optimization procedure. Besides, the higher the constellation order, the lower the design complexity. If the demapping complexity is taken into account, both techniques (CAO and CWO) present the same complexity reduction. The highest reductions are found for low code rates, where condensation technique has the best performance. For high order NUCs and low code rates, condensation techniques present the highest reduction of demapping complexity as most of the constellation points closed to the origin of the constellation diagram are condensed. Finally, it is important to remark that all the condensed NUCs present negligible system performance losses (below 0.1 dB).

Table 6.4. Design and demapping complexity of the condensed methods proposed

Design complexity in terms of number of constellation points involved in the optimization process								
Code rate	64NUC		256NUC		1024NUC		4096NUC	
	CWO	CAO	CWO	CAO	CWO	CAO	CWO	CAO
2/15	8	32	8	128	8	512	8	2048
5/15	24	32	36	128	128	512	-	-
9/15	28	32	96	128	-	-	-	-
Demapping complexity in terms of number of Euclidean distances to be computed								
Code rate	64NUC		256NUC		1024NUC		4096NUC	
2/15	32		32		32		32	
5/15	96		144		512		-	
9/15	112		384		-		-	

1.3 **Proposal of Low Complexity Detection Methodologies for NUCs**

The design of new constellation schemes implies an increment of the computational requirements of the demapping stage. The fifth chapter contributes to the design of low complexity demapping solutions to reduce the demapping complexity associated to 1D-NUCs and 2D-NUCs. Table 6.5 describes the evaluation methodology followed in this work.

Table 6.5. Methodology to evaluate the performance of NUCs and RC technique.

Demapper	Metric	Evaluation cases	Evaluation tools
1D	Number of Euclidean distances System performance (SNR value at BER 10-6)	AWGN Rayleigh iid	BICM communication tool
2D		AWGN Rayleigh iid Rayleigh P1 Ricean F1 Ideal and non ideal CSI	BICM and OFDM communication tool

Two contributions are derived from this chapter:

1) Low complexity lattice reduction demapper for massive order 1D-NUCs.

This demapper is focused on 1D-NUCs, particularly for massive order constellations (from 1024 constellation points). We consider the Max-Log demapper approximation in order to provide lower number of mathematical operations than the ML. The proposed demapper is divided into two parts. First, the design of 1D-NUCs is slightly modified to fulfill the condition that the distances between adjacent constellation points must be multiples of the minimum existing distance among all the constellation points. 1D-NUCs designed for low and mid code rates fulfilling such condition have negligible losses due to the granularity provided by the minimum distance. The constellations designed for high code rates present lower granularity than in the previous case and, as a consequence, system performance losses below 0.2 dB are achieved. Once the 1D-NUC is designed, the next step consists of creating a LUT where each row

represents a specific bit of the PAM constellation. The columns of the LUT represent the grid of the closest point to the received observation.

The complexity analysis of the 1D-demapper shows that the proposed solution presents an overall complexity of O($2 + \log_2 \sqrt{M}$) meanwhile the complexity of the Max-Log is O($\sqrt{M}$). The additional memory requirements of the 1D-demapper are, as maximum, 2.76 Kilobytes of additional memory for the LUT. This is negligible if compared with the reduction achieved in the computational complexity.

In terms of system performance, the results obtained show negligible system performance losses of the proposed 1D demapper compared with the Max-Log for 1D-4096NUCs. For 1D-1024NUCs, results for low and mid code rates present negligible system performance losses. For 11/15, 12/15 and 13/15 code rates, 0.2, 0.2 and 0.3 dB of losses are achieved, respectively.

2) Low complexity adaptive sub-region demapper for 2D-NUCs.

This demapper exploits the geometrical characteristics of the 2D-NUCs in order to reduce the demapping complexity. Two different demapping techniques are developed and the selection of the technique depends on the code rate used. A condensation technique is proposed for low and mid code rates. A condensation metric (Euclidean distance between adjacent constellation points in a 2D diagram) is defined in order to set the region of constellation points that are condensed. The condensation metric that provides the best tradeoff between system performance and complexity reduction has been analyzed. The results obtained for both AWGN and Rayleigh iid channel show that the metric value that provides the best tradeoff is 0.05.

A second technique applied to this 2D demapper is the variable sub-region. This technique is based on the fact that the region of points that are considered in the demapping stage varies for each received symbol. With this technique, the geometrical characteristics of the 2D-NUCs and fading coefficients of the channel are considered in the calculation of the region providing an efficient demapping process. The length of the square sub-region d is given by Equation 6.1 where σ is the standard deviation of the Gaussian distribution and l is the maximum random value which determines the percentage of values that lie within a band around the mean in a normal distribution.

$$d = \left| \frac{(l + jl)\sigma}{h} \right| \tag{6.1}$$

As shown in Chapter 5, $l = 3.6$ provides negligible system performance losses for the whole range of code rates evaluated (2/15 – 13/15). This value is valid for BICM and OFDM system models, where ideal CSI is considered. In the case of non-ideal CSI, the value of $l = 5$ in order to cope with the deviation in the fading coefficients. Table 6.6 shows the system performance losses and complexity reduction of the proposed demapper (SCASR) compared with the ML demapper under non-ideal CSI using the ATSC 3.0 simulation platform developed in this dissertation. The results show that demapping complexity reductions of up to 23% with respect to state-of-the-art demappers and 93.7% with respect to the ML demapper in terms of the number of Euclidean distances computed are achieved. Furthermore, negligible system performance losses are obtained for the evaluated cases except for R = 10/15 and R = 13/15 with 0.1 and 0.2 dB of losses,

Table 6.6. System performance and demapping complexity reduction of the SCASR demapper for non-ideal CSI

Channel	Parameter	Code rate [R/15]			
		R=2	R=6	R=10	R=13
P1	SCASR Losses [dB]	<0.1	<0.1	0.1	0.2
	Complexity Reduction [%]	93.7	74.2	75.2	90
F1	SCASR Losses [dB]	<0.1	<0.1	<0.1	<0.1
	Complexity Reduction [%]	93.7	71.8	78.7	91.1

respectively. The extension of this study to massive order constellations demonstrates that demapping complexity reduction of up to 99.7% compared with the ML demapper are achieved for 4096 constellation points.

2. Dissemination

2.1 International Journals

Title: "Low Complexity Adaptive Demapper for 2-D Non-Uniform Constellations"

Authors: Barrueco, J.; Montalban, J.; Angueira, P.; Abdel Nour, C.; Douillard, C.

Publication: IEEE Transactions on Broadcasting. DOI: 10.1109/TBC.2018.2811619.

Date of Publication: 12 March 2018

Contributions: This paper presents a novel low complexity 2D demapper for 2D-NUCs. The basis behind this demapper is to exploit the geometrical characteristics of the 2D-NUCs and provide an adaptive sub-region demapper with rate adaption each constellation symbol period. The first contribution presents a metric definition in order to efficiently condense NUCs for low and mid code rates. The metric is the existing Euclidean distance between constellation points and the maximum metric value that enables condensation with negligible system performance losses is 0.05 for AWGN and Rayleigh iid channels. The second contribution consists of an adaptive sub-region demapper where the area of points considered in the demapping stage varies for each received constellation symbol. In this way, not only the geometrical shape of the constellation is taken into account but also the channel model. Finally, both demapping techniques are put together creating the so called switched condensed and adaptive sub-region (SCASR) demapper. Depending on the code rate, either one or both demappers are switched on, i.e., for 2/15 and 3/15 code rates only the condensed demapper is enabled, from 4/15 to 10/15 both demappers are used and from 11/15 to 13/15 only the adaptive sub-region demapper is switched on. The system performance of the SCASR demapper is carried out using a fully compliant ATSC 3.0 OFDM transmitter-receiver chain. AWGN, Rayleigh iid, DVB-T P1 and DVB-T F1 channels are evaluated considering the code rates 2/15, 6/15, 10/15 and 13/15 with ideal CSI. For all the channel conditions, the system performance of the SCASR demapper is similar to the exhaustive search ML method. The advantage is that the SCASR presents complexity reduction from 6% to 27% with respect state of the art demappers for 2D-NUCs and from 79.2% to 95.4% compared with ML demapper. This analysis is extended to non-ideal CSI providing similar computational complexity reduction to the ideal CSI case. In this case, the system performance under DVB-T P1 is 0.1 and 0.2 dB worse than the ML case for 10/15 and 13/15 code rates, respectively. However, the system performance and complexity reduction is better than the state of the art demappers. Finally, massive order constellations (1024 and 4096 constellation points) are considered to check out the complexity reduction of the SCASR demapper obtaining demapping complexity reductions ranging from 96% to 99.7%.

Title: "Constellation Design for Bit-interleaved Coded Modulation (BICM) Systems in Advanced Broadcast Standards"

Authors: Barrueco, J.; Montalban, J.; Regueiro, C.; Velez, M.; Ordiales, J.L.; Kim, H-M.; Park, S-I.; Kwon, S.

Publication: IEEE Transactions on Broadcasting. Volume: 63, Issue 4, Dec. 2017.

Date of Publication: 21 March 2017

Contributions: This paper contributes to the design of geometrical shape constellations for BICM system models providing a comprehensive study of the optimization problem jointly with the best optimization algorithm to solve it and the design algorithm to obtain optimal constellation schemes for a wide range of SNR values. Besides, a solution to design constellations for the Rayleigh iid channel model is also derived as this channel model is very demanding in terms of computational cost. Regarding the detailed analysis of the optimization problem and the most appropriate optimization algorithm to solve the problem, PSO algorithm is the most efficient algorithm that enables equation independent optimization with low simulation time and accurate results. Next, three different metrics are used to evaluate the feasibility of the constellation design process taking into account design time consumption, the BICM channel capacity and BER versus SNR system performance. As one of the main contributions, this paper presents the key factors with the highest impact in the design of BICM capacity approaching constellation schemes: number of degrees of freedom (1D-NUC or 2D-NUC), range of SNRs adequate for each constellation order, constellation shape (circular for low and mid SNR and rectangular for high SNR), and bit labeling (special case of binary Gray labeling code). The next main contribution is the optimization system model to design efficiently (low time and optimal BICM channel capacity results) constellation schemes. This system model is derived in 4 general steps: SNR calculation, obtain the initial constellation, perform the PSO algorithm and repite iteratively the process until the capacity result remains unaltered. The next contribution is the way to move the constellation points in order to obtain in a quick way the optimal constellation. It is shown that constellations from 64 points must be divided into circunferences, each one with a defined freedom of movement. The fourth contribution is an optimized process to design constellations for Rayleigh iid channel. The solution is based on setting the target SNR value to the performance threshold of a Rayleigh iid channel specifying the channel as AWGN. The results obtained are similar to the exhaustive calculation (losses below 0.1 dB). Finally, the results of the metrics defined are obtained to check out the viability of this solution. In terms of design time consumption, 2D constellations (16, 64 and 256) require 5, 20 and 120 minutes, respectively. For 1D constellations (1024 and 4096) 10 and 20 min are needed, respectively. BICM channel capacity and system performance results show that all the designed constellations outperform the standard QAM schemes (widely used in DTT broadcasting systems) with gains of up to 0.6351 bit/s/Hz and 1.8 dB for 4096NUC and 9/15 code rate. The results also show that the higher the constellation order, the higher the gain that can be achieved as the number of variables involved in the design process is incremented. Besides,

the SNR region where higher gains are achieved is the mid region as in the high region the shape of the designed constellations is similar to the QAM and in the low SNR region their shape is condensed. In terms of receiver complexity, 1D-NUCs present the same complexity as standard QAM schemes whereas the complexity associated to 2D-NUCs is higher and there should be a trade-off between complexity and system performance.

2.2 International Conferences

Title: "Low-Complexity Lattice Reduction Demapper for Massive Order One-Dimensional Non-Uniform Constellations"

Authors: Barrueco, J.; Montalban, J.; Angueira, P.; Abdel Nour, C.; Douillard, C.

Conference: IEEE International Symposium on Broadband Multimedia Systems and Broadcasting (BMSB)

Date: June 2018

Place: Valencia

Contributions: The contribution of this paper is a low-complexity demapping technique for *M*-ary 1D-NUCs. The solution is based on the lattice reduction technique used in MIMO systems in order to reduce the number of constellation points involved in the demapping process. This paper proposes a methodology to find efficiently the closest point to the received observation and reduce the number of lattices in the search of the closest point when the constellation presents a non-uniform geometrical shape. The first step consists of designing a 1D-NUC that fulfills the condition that the distances between adjacent constellation points must be multiples of the minimum existing distance among all the constellation points. Next, a LUT is defined where a specific bit of the PAM constellation is represented in each row. The grid of the closest point to the received observation is represented in the columns of the LUT. The overall computational complexity of this solution is $O(2 + \log_2 \sqrt{M})$ meanwhile the exhaustive search is $O(\sqrt{M})$. In terms of percentages, if the proposed demapper is compared with conventional methods such as ML and Max-Log computational complexity reductions of 78.1% and 87.5% are achieved for 1D-1024NUCs and 1D-4096NUCs, respectively. If the system performance of the designed demapper is analyzed, negligible system performance losses of the proposed demapper are obtained compared with the Max-Log for 1D-4096NUCs. The same occurs for 1D-NUCs for low and mid code rates. For 11/15, 12/15 and 13/15 code rates, 0.2, 0.2 and 0.3 dB of losses are achieved, respectively.

Title: "Condensation Methodologies for Two-Dimensional Non-Uniform Constellations"

Authors: Barrueco, J.; Regueiro, C; Montalban, J.; Velez, M.; Angueira, P.; Kim, H-M.; Park, S-I.; Kwon S.

Conference: IEEE International Symposium on Broadband Multimedia Systems and Broadcasting (BMSB)

Date: June 2017

Place: Italy

Contributions: This paper presents two efficient condensation methodologies for massive order 2D-NUCs. The first proposal, called condensation with optimization (CWO), is performed at the design process of the constellation. Constellation points close to each other with an Euclidean distance among them lower than a predefined value are positioned at the same location in the constellation diagram. The maximum Euclidean distance between constellation points that provides negligible system performance losses is 0.1. This solution has the advantage that the design process is less complex as the number of constellation points is lowered. However, if the Euclidean distance metric is not suitably chosen the designed constellation might not be the optimal one and, thus, the system performance would worsen. The second solution, condensation after optimization (CAO), consists of condensing the designed constellation after the constellation is designed. This solution always obtains the optimal condensed constellation as long as the optimization process is correctly carried out. However, CAO is more complex than CWO as two processing steps are followed (optimization and condensation). If the system performance of both techniques is evaluated for AWGN and Rayleigh iid channels, the results show that 2D-64NUCs and 2D-256NUCs present negligible system performance losses for code rates from 2/15 to 9/15 where condensation makes sense. In terms of design complexity, CWO involves lower design complexity than CAO where the maximum difference in complexity is found for 2D-256NUC and code rate 2/15 (8 variables in the optimization process for CWO and 128 for CAO). In terms of demapping complexity, both techniques present the same complexity as the condensation degree applied in both cases is the same. If the demapping complexity of the proposed condensed NUCs is compared with the exhaustive method ML, complexity reductions up to 93.75% are found for 2D-256NUC and 2/15 code rate.

Title: "Low Complexity and High Order Two-Dimensional Non-Uniform Constellation for High Capacity Broadcasting Systems"

Authors: Barrueco, J.; Regueiro, C.; Montalban, J.; Velez, M..; Angueira, P.; Kim, H-M.; Park, S-I.; Kwon, S.

Conference: IEEE International Symposium on Broadband Multimedia Systems and Broadcasting (BMSB)

Date: June 2016

Place: Japan

Contributions: This paper presents massive order NUCs (from 1024 constellation points) with better system performance than existing massive order NUCs and low demapping complexity. The basis behind the design of such efficient massive order constellations is to take advantage of the two dimensional design of NUCs and the condensation technique that can be applied for low SNR values. The designed NUCs are compared with massive order 1D-NUCs from ATSC 3.0 for code rates from 2/15 to 6/15. First, the channel capacity of both constellation schemes is compared where the 2D-NUCs designed outperform all the 1D-NUCs schemes under AWGN channel. The highest channel capacity gain (0.0818 bit/s/Hz) is achieved for 2D-1kNUC and 5/15 code rate. Next, both constellation schemes are analyzed via BICM system performance for AWGN and Rayleigh iid channels for a BER threshold of 10^{-5}. System performance results show that the designed condensed 2D-NUCs provide higher gain than 1D-NUCs for both channels with gains from 0.01 dB to 0.28 dB. Regarding design complexity of the condensed 2D-NUCs, for 2D-1kNUCs the optimization time takes 10 minutes and, in the case of 2D-4kNUCs, 15 minutes. The demapping complexity at the receiver side is lowered if compared with ML exhaustive search method. The condensation technique applied to the 2D-NUCs in the design process reduces the number of Euclidean distances computed at the demapping stage. The exhaustive search method for 2D-NUCs implies 2*M* Euclidean distances to be computed, where *M* is the number of the constellation symbols, i.e., 2048 and 8192 for 2D-1kNUC and 2D-4kNUC, respectively. The condensed 2D-NUCs proposed in this paper imply a minimum of 32 and maximum of 512 Euclidean distances.

Title: "Combining Advanced Constellations and SSD Techniques for Optimal BICM Capacity"

Authors: Barrueco J.; Regueiro, C.; Montalban, J.; Velez, M.; Angueira, P.; Kim, H-M.; Park, S-I.; Lee, J-Y.

Conference: IEEE International Symposium on Broadband Multimedia Systems and Broadcasting (BMSB)

Date: June 2015

Place: Belgium

Contributions: This paper evaluates the system performance of the latest modulation techniques developed, i.e., NUCs and RC technique. First, the system performance of NUCs and standard QAM schemes are compared for 4/15, 8/15 and 12/15 code rates to check out the feasibility of using NUCs. SNR versus BER results are obtained for BER threshold 10^{-6} at waterfall region of LDPC codes. The results show that NUCs outperform standard QAM schemes for all code rates and constellation orders. Besides, the higher the constellation order the higher the gain is and gains of up to 0.9 dB can be found for the highest constellation order evaluated (64 constellation points). Regarding RC technique, constellation orders from 4 to 64 constellation points and code rates from 5/15 to 13/15

are evaluated. RC technique is applied to NUCs in order to check out the feasibility of both techniques together and the results show that if RC is used together with NUCs, system performance gains of up to 2 dB are achieved for Rayleigh iid channel. An important conclusion is that RC technique only provides system gains for high code rates and low order constrellations. Finally, non-rotated standard QAM schemes are compared with rotated NUCs showing system performance gains of up to 0.5 dB for 12/15 code rate and 64 constellation points under Rayleigh iid channel.

2.3 International Consortiums for Regulation and Standardization

Title: "Rotation Gain Trend on NUC"

Organism: Advanced Television Systems Committee, ATSC

Date: October 2014

Contributions: This study was presented in the S32-2 ad-hoc subgroup during the ATSC 3.0 standardization process. The presentation contributes with the first BICM system performance results combining NUCs, RC and LDPC codes. The main conclusions are that RC technique provides up to 2 dB gain for NUCs and that RC technique is suitable for low order constellations with high code rates.

Title: "I/Q Interleaving Gain on NUC"

Organism: Advanced Television Systems Committee, ATSC

Date: October 2014

Contributions: This study was presented in the S32-2 ad-hoc subgroup during the ATSC 3.0 standardization process. The objective is to analyze the influence of the I/Q interleaving process if no rotation is applied. Some NUCs can be considered as QAM rotated and thus, only I/Q interleaver might be worthy. The results show that the interleaving process provides system performance gains of up to 0.6 dB for constellation orders from 64 points.

Title: "RC Performance in BICM and OFDM Chains and a Preliminary ModCod Reduction Analysis"

Organism: Advanced Television Systems Committee, ATSC

Date: October 2014

Contributions: This study was presented in the S32-2 ad-hoc subgroup during the ATSC 3.0 standardization process. System performance results of NUCs with RC technique and LDPC codes are shown for different code lengths (16K and 64K), channels (Rayleigh iid,

Rayleigh P1) and constellation orders (4, 16 and 64). Similar system performance is achieved independent of the FEC length block and channel (Rayleigh iid or P1) selected. Finally, a preliminary ModCod reduction is carried out considering ModCod combinations with similar thoughputs. The results conclude that ModCods with RC technique for high code rates and low order constellations need higher SNR level that those without RC technique with low code rates and high order constellations.

Title: "RC Gain on NUC over Rayleigh P1 and 0 dB Echo Channels"

Organism: Advanced Television Systems Committee, ATSC

Date: November 2014

Contributions: This study was presented in the S32-2 ad-hoc subgroup during the ATSC 3.0 standardization process. This contribution shows the system performance of NUCs with RC technique under Rayleigh P1 and 0 dB Echo at 90% GI channels. The conclusion is that NUCs with RC technique achieve higher system performance gains (up to 2 dB) under 0 dB Echo channels than Rayleigh P1 channels.

Title: "Verification and Validation (V&V) Platform for ATSC 3.0 Standardization"

Organism: Advanced Television Systems Committee, ATSC

Date: June 2015

Contributions: This platform is the first V&V platform developed and used during the ATSC 3.0 standardization process. Two different files can be compared and crosschecked in any of the functional blocks of the ATSC 3.0 physical layer.

Title: "ATSC 3.0 Recommended Practices"

Organism: Advanced Television Systems Committee, ATSC

Date: February 2017

Contributions: This work details the functional blocks and processes involved in the demapper of the ATSC 3.0 system. It is used as a guide to perform field and laboratory tests of the ATSC 3.0 system.

---

3. Future Work

Taking into consideration the work carried out and the results obtained in this thesis, there are several future research lines that can bring further improvements to the communication technologies such as:

- The design of massive order 2D-NUCs (from 1024 to higher constellation points) to provide ultra high spectral efficiency to future communication systems.

- Study coding techniques based on different schemes (LDPC, polar codes, turbo codes, neural codes...) for high SNR values in order to shorten the existing gap to the Shannon limit and design efficient CM and BICM system models.

- Create an advanced LDM profile consisting of non-uniform constellation schemes properly designed for such systems. The objective function to maximize is the LDM BICM system capacity and different upper and lower layer constellations are designed in order to obtain the best trade-off between data rate and robustness of both services.

- Develop advanced modulation techniques based on coding information bits in the injection level of the LDM systems. Design the detection block to demodulate the bit coded in the injection level.

- Extend the design of constellation schemes to provide low PAPR, sub-grouping ordering of different services inside the constellation scheme, adaptive configuration of the sub-grouping ordering and joint bit labelling and constellation points grouping for the delivery of different levels of service delivering.

- Study of novel orthonormal and bandwidth efficient polynomial functions to increase the spectral efficiency of the communication systems. Analyze the viability of using non-stationary signals in communication systems.

REFERENCES AND GLOSSARY

REFERENCES

[1] Digital Video Broadcasting (DVB); Framing Structure Channel Coding and Modulation for Digital Terrestrial Television, ETSI, 1997.

[2] A/53 – ATSC Digital Television Standard, ATSC, 2007.

[3] Transmission System for Digital Terrestrial Television Broadcasting, ARIB, 2014.

[4] Framing Structure, Channel Coding and Modulation for Digital Television Terrestrial Broadcasting System, Chinese National Standard, 2006.

[5] W. Y. Zou and Y. Wu, "COFDM: An Overview," *IEEE Trans. Broadcasting*, vol. 41, no. 1, pp. 1 – 8, 1995.

[6] Digital Video Broadcasting (DVB); Transmission System for Handheld Terminals (DVB-H), ETSI, 2004.

[7] Digital Video Broadcasting (DVB); Frame Structure Channel Coding and Modulation for a Second Generation Digital Terrestrial Television Broadcasting System (DVB-T2), ETSI, 2011.

[8] DVB WorldWide [Online]. Available: https://www.dvb.org/news/worldwide

[9] ATSC Standard – Physical Layer Protocol, ATSC, 2017.

[10] L. Fay, L. Michael, D. Gomez-Barquero, N. Ammar, and M. W. Caldwell, "An Overview of the ATSC 3.0 Physical Layer Specification," *IEEE Trans. Broadcasting*, vol. 62, no. 1, pp. 159 – 171, 2016.

[11] "Digital Dividend – Insights for Spectrum Decisions," ITU, Tech. Rep., 2012.

[12] "The Future of Terrestrial Broadcasting," European Broadcasting Union, Tech. Rep. 013, 2011.

[13] "Final Acts WRC-07," ITU, Geneva, Switzerland, Tech. Rep., 2007.

[14] "Final Acts WRC-15," ITU, Geneva, Switzerland, Tech. Rep., 2015.

[15] D. Gomez-Barquero and M. W. Caldwell, "Broadcast Television Spectrum Incentive Auctions in the U.S.: Trends, Challenges and Opportunities," *IEEE Communications Magazine*, vol. 53, no. 7, pp. 50 – 56, 2015.

[16] R. Farahbakhsh *et al*., "Understanding the Evolution of Multimedia Content in the Internet Through Bittorrent Glasses," in *IEEE Network*, vol.27, no.6, pp. 80 – 88, Dec. 2013.

[17] Commercial Requirements for DVB-T2, Digital Video Broadcasting, 2007.

[18] D. Gozalvez *et al*., "Time Diversity in Mobile DVB-T2 Systems," in *IEEE Trans. Broadcast*., vol.57, no.3, pp. 617 – 628, 2011.

[19] C. A. Nour and C. Douillard, "Rotated QAM constellations to improve BICM performance for DVB-T2," in *Proc. IEEE Int. Symp. Spread Spectrum Tech. Appl*., Bologna, Italy, Aug. 2008, pp. 354–359.

[20] ATSC Technology Group 3.0, "Call for Proposals for ATSC 3.0 Physical Layer", March 26, 2013.

[21] Going Global: ATSC 3.0 4K broadcasting launched in Korea, ATSC 3.0 Newsletter, July 2017.

[22] J. Montalban, "Solutions for New Terrestrial Broadcasting Systems Offering Simultaneously Stationary and Mobile Services," PhD thesis, Universidad del País Vasco / Euskal Herriko Unibertsitatea, 2014.

[23] L. Zhang *et al*., "Layered Division Multiplexing: Theory and Practice," in *IEEE Trans. Broadcast*., vol.62, no.1, pp. 216 – 232, 2016.

[24] L. Staldemeier *et al*., "Channel Bonding for ATSC 3.0," *IEEE Trans. Broadcasting*, vol. 62, no. 1, 2016.

[25] P. Klenner *et al*., "Physical Layer Time Interleaver for the ATSC 3.0 System," *IEEE Trans. Broadcasting*, vol. 62, no. 1, pp. 253 – 262, 2016.

[26] ATSC Recommended Practice: Guidelines for the Physical Layer Protocol, ATSC, 2018.

[27] S. Loghin *et al*., "Non-uniform constellations for ATSC 3.0," *IEEE Trans. Broadcast*., vol. 62, no. 1, pp. 197–203, Mar. 2016.

[28] M. Fuentes, "Non-Uniform Constellations for Next-Generation Digital Terrestrial Systems," PhD thesis, Universitat Politecnica de Valencia, 2017.

[29] C. E. Shannon, "A mathematical theory of communication," *Bell Labs System Journal*, vol. 27, p. 535, Jul./Oct. 1948.

[30] C. E. Shannon, "Communication in the presence of noise," *Proc. Institute of Radio Engineers*, vol. 37, no. 1, pp. 10–21, Jan. 1949. Reprint as classic paper in: Proc. IEEE, vol. 86, no. 2, Feb. 1998.

[31] H. Nyquist, "Certain Factors Affecting Telegraph Speed," *Bell System Tech. Jour*., vol. 3, p. 324, April 1924.

[32] H. Nyquist, "Certain Topis in Telegraph Transmission Theory," *A.I.E.E. Trans*., vol. 47, p. 617, April 1928.

[33] R. V. L. Hartley, "The Transmission of Information," *Bell System Tech. Jour.*, vol. 7, pp. 535 – 564, July 1928.

[34] D.J.C. Mackay and R.M. Neal, "Near Shannon limit performance of low density parity check codes," *IEEE Electronic Letters*, vol. 33, no.6, pp. 457 – 458, March 1997.

[35] C. Berrou, A. Glavieux, and P. Thitimajshima, "Near Shannon limit error-correcting coding and decoding: Turbo-codes," in *Proc. IEEE Int. Conf. Commun*., Geneva, Switzerland, May 1993, pp. 1064 – 1070.

[36] R. G. Gallager, "Low-density parity-check codes," Ph.D. dissertation, MIT, Cambridge, MA, 1962.

[37] Sae-Young *et al*., "On the Design of Low-Density Parity-Check Codes within 0.0045 dB of the Shannon Limit," in *IEEE Communications Letters*, vol.5, no.2, pp. 58 – 60, Feb. 2001.

[38] G. Ungerboeck, "Channel coding with multilevel/phase signals," *IEEE Trans. Inform. Theory*, vol. IT-28, pp. 55 – 67, 1982.

[39] G. Ungerboeck, "Trellis-coded modulation with redundant signal sets part I: introduction," *IEEE Communications Magazine*, vol. 25-2, pp. 5 – 11, 1987.

[40] H. Imai and S. Hirakawa, "A new multilevel coding method using error correcting codes," *IEEE Trans. Inform. Theory*, vol. IT–23, pp. 371–377, 1977.

[41] E. Zehavi, "8-PSK trellis codes for a Rayleigh channel," *IEEE Trans. Commun*., vol. 40, no. 5, pp. 873–884, May 1992.

[42] G. D. Forney, "The Viterbi Algorithm," *IEEE Proceedings of the IEEE*, vol. 61, no. 3, pp. 268 – 278, March 1973.

[43] R. Fischer, J. Huber, and U. Wachsmann, "Multilevel coding: Aspects from information theory," in *Proc. CTMC at IEEE Global Telecommun. Conf. (GLOBECOM'96*) (London, U.K., Nov. 1996), pp. 26–30.

[44] D-F. Yuan, P. Zhang and W.E. Stark, "A new MLC scheme with QAM constellations over AWGN and Rayleigh fading channels," *IEEE 55th Vehicular Technology Conference*, Birmingham, USA, May 2002.

[45] U. Wachsmann, R. F. H. Fischer, and J. B. Huber, "Multilevel codes: Theoretical concepts and practical design rules," *IEEE Trans. Inf. Theory*, vol. 45, no. 5, pp. 1361–1391, Jul. 1999.

[46] G. Caire, G. Taricco, and E. Biglieri, "Bit-interleaved coded modulation," *IEEE Trans. Inf. Theory*, vol. 44, no. 3, pp. 927–946, May 1998.

[47] E. Agrell and A. Alvarado, "Optimal Alphabets and Binary Labelings for BICM at Low SNR," *IEEE Trans. Inf. Theory*, vol. 57, no. 10, pp. 6650 – 6672, Oct. 2011.

[48] Chindapol and 1. A. Ritcey, "Design, analysis and performance evaluation for BICM-ID with square QAM constellations in Rayleigh fading channels," *IEEE Select. Areas Commun*, vol. 19 (5), pp. 944C957, May, 2001.

[49] S.X. Ng, T.H. Liew, L.L. Yang and L. Hanzo, "Comparative study of TCM, TTCM, BICM and BICM-ID schemes," in *Proc. of VTC2001 (Spring)*, pp. 2450–2454, Rhodes, Greece, May 2001.

[50] J.M. Cioffi, Signal Processing and Detection. Stanford University Web Page, Jul. 2017.

[51] W. Sung, S. Kang, P. Kim, D-I. Chang and D-J. Shin, "Performance analysis of APSK modulation for DVB-S2 transmission over nonlinear channels," in *International Journal of Satellite Communications and Networking*, vol. 27, no.6, Nov. 2009.

[52] M. K. Simon, "Bandwidth-Efficient Digital Modulation with Application to Deep-Space Communications," *Deep-Space Communications and Navigation Series*, Monograph 3, June 2001.

[53] J. Freudenberger and S. Shavgulidze, "Signal Constellations Based on Eisenstein Integers for Generalized Spatial Modulation," *IEEE Communications Letters*, vol. 21, no. 3, pp. 556 – 559, March 2017.

[54] G. Böcherer, "Labeling Non-Square QAM Constellations for One-Dimensional Bit-Metric Decoding," *IEEE Communications Letters*, vol. 18, no. 9, pp. 1515 – 1518, Sep. 2014.

[55] S-H. Han, J. M. Cioffi and J-H Lee, "On the Use of Hexagonal Constellation for Peak-to-Average Power Ratio Reduction of an OFDM Signal," *IEEE Transactions on Wireless Communications*, vol. 7, no. 3, pp. 781 – 786, March 2008.

[56] G. Foschini, R. D. Gitlin and S. B. Weinstein, "Optimization of Two-Dimensional Signal Constellation in the Presence of Gaussian Noise," *IEEE Trans. Communications*, vol. COM-22, no. 1, pp. 28 – 38, Jan. 1974.

[57] F-W. Sun and H. C. A. Van Tilborg, "Approaching Capacity by Equiprobable Signaling on the Gaussian Channel," *IEEE Trans. Infor. Theory*, vol. 39, no. 5, pp. 1714 – 1716, Sep. 1993.

[58] W. Betts, A. R. Calderbank and R. Laroia, "Performance of Nonuniform Constellations on the Gaussian Channel," *IEEE Trans. Infor. Theory*, vol. 40, no. 5, pp. 1633 – 1638, Sep. 1994.

[59] D. Sommer and G. P. Fettweis, "Signal Shaping by Non-Uniform QAM for AWGN Channels and Applications Using Turbo Coding," *RD ITG Conference Source and Channel Coding*, pp. 81 – 86, 2000.

[60] J. Kearsley, "Global and Local Optimization Algorithms for Optimal Signal Set Design," *Journal of Research of the National Institute of Standards and Technology*, vol. 106, no. 2, pp. 441 – 454, March 2001.

[61] Fragouli, R. D. Wesel, D. Sommer and G. P. Fettweis, "Turbo Codes with Non-Uniform Constellations," *IEEE International Conference on Communications*, Helsinki, Finland, June 2001.

[62] F. Zesong, K. Jingming and Y. Yu, "Shaping gain by non-uniform QAM constellation with binary turbo coded modulation," *IEEE Proceedings on Personal, Indoor and Mobile Radio Communications*, Beijing, China, Sept. 2003.

[63] M. F. Barsoum, C. Jones and M. Fitz, "Constellation Design via Capacity Maximization," *IEEE International Symposium on Information Theory*, Nice, France, June 2007.

[64] M. F. Barsoum, "On Constellation Design and Iterative Codes," Ph.D. dissertation, Univ. Of California, Los Angeles, 2008.

[65] N. S. Muhammad, "Coding and modulation for spectral efficient transmission," Ph.D. dissertation, Dept. Comput. Sci, Elect. Eng. Inf. Technol., Univ. Stuttgart, Stuttgart, Germany, 2010.

[66] F. Kayhan and G. Montorsi, "Constellation Design for Memoryless Phase Noise Channels," *IEEE Trans. Wireless Communications*, vol. 13, no. 5, pp. 2874 – 2883, May 2014.

[67] E. Agrell, "Voronoi Regions for Binary Linear Block Codes," *IEEE Trans. Information Theory*, vol. 42, no. 1, pp. 310 – 316, Jan 1996.

[68] G. D. Forney *et al.*, "Efficient Modulation for Band-Limited Channels," *IEEE Journal on Selected Areas in Communications*, vol. SAC-2, no. 5, pp. 632 – 647, Sep. 1984.

[69] R. Calderbank and L. H. Ozarow, "Nonequiprobable Signaling on the Gaussian Channel," *IEEE Trans. Infor. Theory*, vol. 36, no. 4, pp. 726 - 740, July 1990.

[70] F. R. Kschischang and S. Pasupathy, "Optimal Nonuniform Signaling for Gaussian Channels," *IEEE Trans. Infor. Theory*, vol. 39, no. 3, pp. 913 – 929, May 1993.

[71] Raphaeli and A. Gurevitz, "Constellation shaping for pragmatic turbo coded modulation," *IEEE Electronic Letters*, vol. 38, no. 14, pp. 717 – 719, July 2002.

[72] Raphaeli and A. Gurevitz, "Constellation Shaping for Pragmatic Turbo-Coded Modulation with High Spectral Efficiency," *IEEE Trans. Communications*, vol. 52, no. 3, pp. 341 – 345, March 2004.

[73] K. Khoo *et al.*, "Bit-interleaved Coded Modulation with Iterative Decoding Using Constellation Shaping," *European Signal Processing Conference*, Florence, Italy, Sept. 2006.

[74] S. Y. Le Goff *et al*., "Constellation Shaping for Bandwidth-Efficient Turbo-Coded Modulation with Iterative Receiver," *IEEE Trans. Wireless Communications*, vol. 6, no. 6, pp. 2223 – 2233, June 2007.

[75] Z. Mheich *et al*., "Constellation Shaping for Broadcast Channels in Practical Situations," *European Signal Processing Conference*, Barcelona, Spain, Sept. 2011.

[76] M. C. Valenti and X. Xiang, "Constellation Shaping for Bit-Interleaved LDPC Coded APSK," *IEEE Trans. Communications*, vol. 60, no. 10, pp. 2960 – 2970, Oct. 2012.

[77] M. Yankov *et al*., "Rate-adaptive Constellation Shaping for Near-capacity Achieving Turbo Coded BICM," *IEEE International Conference on Communications*, Sydney, Australia, June 2014.

[78] G. Böcherer, F. Steiner and P. Schulte, "Bandwidth Efficient and Rate-Matched Low-Density Parity-Check Coded Modulation," *IEEE Trans. Communications*, vol. 63, no. 12, pp. 4651 – 4665, Dec. 2015.

[79] S. G. Srinivasan and M. K. Varanasi, "Constellation Design for the Noncoherent MIMO Rayleigh-Fading Channel at General SNR," *IEEE Trans. Infor. Theory*, vol. 53, no. 4, pp. 1572 – 1584, April 2007.

[80] M. Maleki *et al*., "Space Modulation with CSI: Constellation Design and Performance Evaluation," *IEEE Trans. Vehicular Technology*, vol. 62, no. 4, pp. 1623 – 1634, May 2013.

[81] H-B. Cai *et al*., "Optimal Constellation Design for Indoor 2 x 2 MIMO Visible Light Communications," *IEEE Communications Letters*, vol. 20, no. 2, pp. 264 – 267, Feb. 2016.

[82] Mobasher and A. K. Khandani, "Integer-Based Constellation-Shaping Method for PAPR Reduction in OFDM Systems," *IEEE Trans. Communications*, vol. 54, no. 1, pp. 119 – 127, Jan. 2006.

[83] E. D. Sterian *et al*., "Reducing the peak and average power for OFDM systems using QAM by constellation shaping," *European Trans. On Telecommunications*, vol. 21, pp. 35 – 49, April 2009.

[84] L. Polak and T. Kratochvil, "Comparison of the Non-rotated and Rotated Constellations Used in DVB-T2 Standard," *International Conference Radioelektronika*, Brno, Czech Republic, April 2012.

[85] Gozálvez *et al*., "Rotated Constellations for Improved Time and Frequency Diversity in DVB-NGH," *IEEE Trans. Broadcasting*, vol. 59, no. 2, pp. 298 – 305, June 2013.

[86] Mouhouche, C. Barjau and H. Lee, "Design of Non Uniform Constellations for Layered Division Multiplexing," *IEEE International Symposium on Signal Processing and Information Technology*, Abu Dhabi, United Arab Emirates, Dec. 2015.

[87] M. Marey and O. A. Dobre, "Iterative Receiver Design for Uplink OFDMA Cooperative Systems," *IEEE Trans. Broadcasting*, vol. 62, no. 4, pp. 936 – 947, Dec. 2016.

[88] S. Chaabouni, N. Sellami and M. Siala, "Mapping Optimization for a MAP Turbo Detector Over a Frequency-Selective Channel," *IEEE Trans. Vehicular Technology*, vol. 63, no. 2, pp. 617 – 627, Feb. 2014.

[89] Viterbo and E. Biglieri, "A Universal Decoding Algorithm for Lattice Codes," *Quatorzieme Colloque Gretsi*, Sept. 1993.

[90] Viterbo and J. Boutros, "A Universal Lattice Code Decoder for Fading Channels," *IEEE Trans. Information Theory*, vol. 45, no. 5, pp. 1639 – 1642, July 1999.

[91] Agrell *et al*., "Closest Point Search in Lattices," *IEEE Trans. Information Theory*, vol. 48, no. 8, pp. 2201 – 2214, Aug. 2002.

[92] Yao and G. W. Wornell, "Lattice-reduction-aided detectors for MIMO communication systems," *IEEE Global Telecommunications Conference*, Taipei, Taiwan, Nov. 2002.

[93] M. O. Damen, H. El Gamal and G. Caire, "On Maximum-Likelihood Detection and the Search for the Closest Lattice Point," *IEEE Trans. Infor. Theory*, vol. 49, no. 10, pp. 2389 – 2402, Oct. 2003.

[94] Haroun *et al*., "Low-Complexity Soft Detection of QAM Demapper for a MIMO System," *IEEE Communications Letters*, vol. 20, no. 4, pp. 732 – 735, April 2016.

[95] Vikalo, "Sphere Decoding Algorithms for Digital Communications," Ph.D. dissertation, Dept., Elect. Eng., Stanford Univ., California, USA, 2002.

[96] Hassibi and H. Vikalo, "On the Sphere-Decoding Algorithm I. Expected Complexity," *IEEE Trans. Signal Processing*, vol. 53, no. 8, pp. 2806 – 2818, Aug. 2005.

[97] Boutros *et al*., "Soft-input soft-output lattice sphere decoder for linear channels," *IEEE Global Telecommunications Conference*, San Francisco, USA, Dec. 2003.

[98] M. Hochwald and S. ten Brink, "Achieving Near-Capacity on a Multiple-Antenna Channel," *IEEE Trans. Communicatons*, vol. 51, no. 3, pp. 389 – 399, March 2003.

[99] R. Wang and G. B. Giannakis, "Approaching MIMO Channel Capacity with Soft Detection Based on Hard Sphere Decoding," *IEEE Trans. Communications*, vol. 54, no. 4, pp. 587 – 590, April 2006.

[100] Z. Guo and P. Nilsson, "Algorithm and Implementation of the K-Best Sphere Decoding for MIMO Detection," *IEEE Journal on Selected Areas in Communications*, vol. 24, no. 3, pp. 491 – 503, March 2006.

[101] L. G. Barbero, T. Ratnarajah and C. Cowan, "A low-complexity soft-MIMO detector based on the fixed-complexity sphere decoder," *IEEE International Conference in Acoustics, Speech and Signal Processing*, Las Vegas, USA, 2008.

[102] L. Azzam and E. Ayanoglu, "Reduced Complexity Sphere Decoding via a Reordered Lattice Representation," *IEEE Trans. Communications*, vol. 57, no. 9, pp. 2564 – 2569, Sept. 2009.

[103] P. Wang and T. Le-Ngoc, "A List Sphere Decoding Algorithm with Improved Radius Setting Strategies," *Springer Wireless Personal Communications*, vol. 61, no. 1, pp. 189 – 200, May 2010.

[104] W. Park *et al*., "Low complexity soft-decision demapper for high order modulation of DVB-S2 system," *International SoC Design Conference*, Busan, South Korea, Nov. 2008.

[105] Lee, D. Yoon and K. Hyun, "Simple Signal Detection Algorithm for 4+12+16 APSK in Satellite and Space Communications," *Journal of Astronomy and Space Sciences*, vol. 27, no. 3, pp. 221 – 230, 2010.

[106] Zhang and S. Kim, "Efficient soft demapping for M-ary APSK," *International Conference on ICT Convergence*, Seoul, South Korea, Sept. 2011.

[107] Tosato and P. Bisaglia, "Simplified Soft-Output Demapper for Binary Interleaved COFDM with Application to HIPERLAN/2," *IEEE International Conference on Communications*, New York, USA, 2002.

[108] Akay and E. Ayanoglu, "Low Complexity Decoding of Bit-Interleaved Coded Modulation for M-ary QAM," *IEEE International Conference on Communications*, Paris, France, June 2004.

[109] R. S. Sherratt and R. Yang, "A Dual QPSK Soft-Demapper for Multiband OFDM Exploiting Time-Domain Spreading and Guard Interval Diversity," *IEEE Trans. Consumer Electronics*, vol. 53, no. 1, pp. 46 – 49, Feb. 2007.

[110] Q. Wang *et al*., "A Universal Low-Complexity Symbol-to-Bit Soft Demapper," *IEEE Trans. Vehicular Technology*, vol. 63, no. 1, pp. 119 – 130, Jan. 2014.

[111] T. Shitomi *et al*., "Evaluation of Simplified Demapping Algorithm for NUQAMs Using Urban MIMO Channel Response," *IEEE International Symposium on Broadband Multimedia Systems and Broadcasting*, Nara, Japan, June 2016.

[112] Barjau *et al*., "MIMO Sphere Decoding with Successive Interference Cancellation for Two-Dimensional Non-Uniform Constellations," *IEEE Communications Letters*, vol. 21, no. 5, pp. 1015 – 1018, May 2017.

[113] J. H. Stott, "CM and BICM limits for rectangular constellations. Where they come from, how to calculate them–and how to maximize them by optimizing the constellation," document JSC/BBC 022, Report produced under contract to BBC R&D, Aug. 2012.

[114] J. H. Stott, "Beyond NUQAM & ConQAM – overcoming their limitations, especially at lower SNRs," Report produced under contract to BBC R&D, document JSC/BBC 034. 2014.

[115] J. Zoellner and N. Loghin, "Optimization of high-order nonuniform QAM constellations," in *Proc. IEEE Int. Symp. Broadband Multimedia Syst. Broadcast*., London, U.K., Jun. 2013.

[116] R. H. Byrd, J. C. Gilbert, and J. Nocedal, "A trust region method based on interior point techniques for nonlinear programming," *Math. Program.*, vol. 89, no. 1, pp. 149–185, 2000.

[117] S. Loghin *et al*., "Non-uniform constellations for ATSC 3.0," *IEEE Trans. Broadcast*., vol. 62, no. 1, pp. 197–203, Mar. 2016.

[118] Fuentes, J. J. Giménez and D. Gómez-Barquero. "Optimization and Performance of Non-Uniform Rotated Constellations with Multi-RF Transmission Techniques," *IEEE Trans. Broadcasting*, vol. 62, no. 4, pp. 855 – 863, Dec. 2016.

[119] Steiner and G. Böcherer, "Comparison of Geometric and Probabilistic Shaping with Application to ATSC 3.0," arXiv preprint 1608.00474v2, 2016.

[120] M. Li *et al*., "Design of Rotated QAM Mapper/Demapper for the DVB-T2 Standard," *IEEE Workshop on Signal Processing Systems*, Tampere, Finland, Oct. 2009.

[121] Pérez-Calderón, V. Baena-Lecuyer, A. C. Oria, P. López, and J. G. Doblado, "Rotated constellation demapper for DVB-T2," *IEEE Electron. Lett*., vol. 47, no. 1, pp. 31–32, Jan. 2011.

[122] Pérez-Calderón, V. Baena-Lecuyer, A. C. Oria, P. López, and J. G. Doblado, "Simplified rotated constellation demapper for secon generation terrestrial digital video broadcasting," *IEEE Trans. Broadcast*., vol. 59, no. 1, pp. 160–167, Mar. 2013.

[123] S. Tomasin, and M. Butussi, "Low Complexity Demapping of Rotated and Cyclic Q Delayed Constellations for DVB-T2," *IEEE Wireless Communications Letters*, vol. 1, no. 2, pp. 81–84, Jan. 2012.

[124] K. Kim, N. Basutkar, K. Bae, P. Xue, and H. Yang, "One-Dimensional Soft-Demapping Algorithms for Rotated QAM and Software Implementation on DSP," *IEEE Trans. Signal Processing*, vol. 61, no. 15, pp. 3918–3930, May 2013.

[125] Y. Tao, H-J. Kim, S. Jeon, and J-S. Seo,"Low-complexity switched soft demapper for rotated non-uniform constellation DVB-NGH systems," in *Proc. IEEE Int. Symp. Broadband Multimedia Syst. Broadcast*. (BMSB), Jun. 2014.

[126] Y. Tao, H-J. Kim, S. Jeon, and J-S. Seo, "Low Complexity Switched Soft Demapper for Rotated QAM Constellations," *IEEE Trans. Broadcast*., vol. 62, no. 3, pp. 532–539, Jun. 2016.

[127] R. Jafri, A. Baghdadi, M. Waqas, and M. Najam-Ul-Islam, "High-Throughput and Area-Efficient Rotated and Cyclic Q Delayed Constellations Demapper for Future Wireless Standards," *IEEE Access.*, vol. 5, pp. 3077–3084, Jan. 2017.

[128] S. Kwon *et al*., "Simplified non-uniform constellation demapping scheme for the next broadcasting system," in *Proc. IEEE Int. Symp. Broadband Multimedia Syst. Broadcast*. (BMSB), Jun. 2015.

[129] M. Fuentes, D. Vargas, and D. Gómez-Barquero, "Low-Complexity Demapping Algorithm for Two-Dimensional Non-Uniform Constellations," *IEEE Trans. Broadcast*., vol. 62, no. 2, pp. 375–383, June 2016.

[130] K. P. Liolis and N. S. Alagha, "On 64-APSK Constellation Design Optimization," International Workshop on Signal Processing for Space Communications, Rhodes Island, Greece, Oct. 2008.

[131] K. P. Liolis, R. D. Gaudenzi, N. Alagha, A. Martínez, and A. Guillén I Fábregas (2010). Amplitude Phase Shift Keying Constellation Design and its Applications to Satellite Digital Video Broadcasting. Digital Video, Floriano de Rango (Ed.), ISBN: 978-953-7619-70-1, InTech, Available from: http://www.intechopen.com/books/digital-video/amplitude-phase-shift-keying-constellation-design-and-its-applications-to-satellite-digital-video-br

[132] X. Xiang, and M. C. Valenti, "Improving DVB-S2 Performance Through Constellation Shaping and Iterative Demapping," *Military Communications Conference*, Baltimore, USA, Nov. 2011.

[133] Kayhan, and G. Montorsi, "Constellation Design for Transmission over Nonlinear Satellite Channels," *Global Communications Conference*, Anaheim, USA, Dec. 2012.

[134] X. Xiang, and M. C. Valenti, "Closing the Gap to the Capacity of APSK: Constellation Shaping and Degree Distributions," arXiv preprint 1210.4831, Oct. 2012.

[135] Meloni, and M. Murroni, "On the genetic optimization of APSK constellations for satellite broadcasting," *Proc. IEEE Int. Symp. Broadband Multimedia Syst. Broadcast*. (BMSB), Beijing, China, Jun. 2014.

[136] M. Anedda, A. Meloni, and M. Murroni, "64-APSK Constellation and Mapping Optimization for Satellite Broadcasting Using Genetic Algorithms," *IEEE Trans. Broadcasting*, vol. 62, no. 1, pp. 1 – 9, March 2016.

[137] K. Cho *et al*., "An Approximated Soft Decoding Algorithm of 16-APSK Signal for DVB-S2," *International Conference on Consumer Electronics*, Las Vegas, USA, Jan. 2007.

[138] Q. Xie, Z. Wang, and Z. Yang, "Simplified Soft Demapper for APSK with Product Constellation Labeling," *IEEE Trans. Wireless Communications*, vol. 11, no. 7, pp. 2649 – 2657, Jul. 2012.

[139] R-J. Essiambre *et al*., "Capacity Limits of Optical Fiber Networks," *Journal of Lightwave Technology*, vol. 28, no. 4, pp. 662 – 701, Feb. 2010.

[140] P. Smith, and F. R. Kschischang, "A Pragmatic Coded Modulation Scheme for High-Spectral-Efficiency Fiber-Optic Communications," *Journal of Lightwave Technology*, vol. 30, no. 13, pp. 2047 – 2053, Jul. 2012.

[141] Djordjevic, T. Liu, and M. Cvijetic, "Optimum Signal Constellation Design for Ultra-High-Speed Optical Transport Networks," *International Conference on Transparent Optical Networks*, Coventry, UK, Jul. 2012.

[142] M. P. Yankov *et al*., "Constellation Shaping for Fiber-Optic Channels with QAM and High Spectral Efficiency," *IEEE Photonics Technology Letters*, vol. 26, no. 23, pp. 2407 – 2410, Dec. 2014.

[143] Buchali et al., "Experimental demonstration of capacity increase and rate adaption by probabilistically shaped 64-QAM," *European Conference on Optical Communication*, Valencia, Spain, 2015.

[144] T. Fehenberger et al., "Sensitivity Gains by Mismatched Probabilistic Shaping for Optical Communication Systems," *IEEE Photonics Technology Letters*, vol. 28, no. 7, pp. 786 – 789, Apr. 2016.

[145] T. Fehenberger et al., "On Probabilistic Shaping of Quadrature Amplitude Modulation for the Nonlinear Fiber Channel," *Journal of Lightwave Technology*, vol. 34, no. 21, pp. 5063 – 5073, Nov. 2016.

[146] J. Mao et al., "A Low Complexity 256QAM Soft Demapper for 5G Mobile System," *European Conference on Networks and Communications*, Athens, Greece, June 2016.

[147] J. Lee, J-Y. Jung, and J. M. Ahn, "Simplified Non-Square Amplitude Modulation Demapper for DOCSIS 3.1," *IEEE Trans. Broadcsating*, vol. 63, no. 1, pp. 156–161, Dec. 2016.

[148] *Ultra High Definition Television—Image Parameter Values for Program Production*, SMPTE Standard 2036-1, 2009.

[149] S.-I. Park *et al.*, "ADT-based UHDTV transmission for the existing ATSC terrestrial DTV broadcasting," *IEEE Trans. Broadcast.*, vol. 61, no. 1, pp. 105–110, Mar. 2015.

[150] T. Biatek *et al.*, "Optimal bitrate allocation in the scalable HEVC extension for the deployment of UHD services," *IEEE Trans. Broadcast*., vol. 62, no. 4, pp. 826–841, Dec. 2016.

[151] K. Northon. (Sep. 2015). *NASA, Harmonic Launch First Non- Commercial UHD Channel in North America. Washington.* [Online]. Available: https://www.nasa.gov/press-release/nasa-harmonic-launchfirst-non-commercial-uhd-channel-in-north-america

[152] D. Wood. (Mar. 2014). *The Nitty–Gritty of UHDTV Takes Shape DVB Scene*. [Online]. Available: https://www.dvb.org/resources/public/scene/DVB-SCENE43.pdf

[153] R. Chernock. (Jan. 2015). *ATSC 3.0: Where We Stand. Alexandria, VA, USA.* [Online]. Available: http://atsc.org/newsletter/atsc-3-0-where-we-stand/

[154] S.-H. Bae, J. Kim, M. Kim, S. Cho, and J.-S. Choi, "Assessments of subjective video quality on HEVC-encoded 4K-UHD video for beyond-HDTV broadcasting services," *IEEE Trans. Broadcast.*, vol. 59, no. 2, pp. 209–222, Jun. 2013.

[155] A. Ichigaya and Y. Nishida, "Required bit rates analysis for a new broadcasting service using HEVC/H.265," *IEEE Trans. Broadcast.*, vol. 62, no. 2, pp. 417–425, Jun. 2016.

[156] K.-J. Kim *et al.*, "Low-density parity-check codes for ATSC 3.0," *IEEE Trans. Broadcast*., vol. 62, no. 1, pp. 189–196, Mar. 2016.

[157] L. Stadelmeier, D. Schneider, J. Zollner, and J. J. Gimenez, "Channel bonding for ATSC3.0," *IEEE Trans. Broadcast*., vol. 62, no. 1, pp. 289–297, Mar. 2016.

[158] I. Eizmendi *et al.*, "DVB-T2: The second generation of terrestrial digital video broadcasting system," *IEEE Trans. Broadcast.*, vol. 60, no. 2, pp. 258–271, Jun. 2014.

[159] "Digital video broadcasting (DVB); Imlementation guidelines for a second generation digital cable transmission system (DVB-C2)," ETSI, Sophia Antipolis, France, Tech. Rep. ETSI TS 102 991 V1.2.1 (2011-06), Jun. 2011.

[160] D. Gomez-Barquero *et al.*, "MIMO for ATSC 3.0," *IEEE Trans.Broadcast*., vol. 62, no. 1, pp. 298–305, Mar. 2016.

[161] L. Zhang *et al.*, "Layered-division-multiplexing: Theory and practice," *IEEE Trans. Broadcast*., vol. 62, no. 1, pp. 216–232, Mar. 2016.

[162] K.-J. Kim *et al.*, "Low-density parity-check codes for ATSC 3.0," *IEEE Trans. Broadcast*., vol. 62, no. 1, pp. 189–196, Mar. 2016.

[163] S. I. Park, Y. Wu, H. M. Kim, N. Hur, and J. Kim, "Raptor-like rate compatible LDPC codes and their puncturing performance for the cloud transmission system," *IEEE Trans. Broadcast*., vol. 60, no. 2, pp. 239–245, Jun. 2014

[164] S. I. Park, H. M. Kim, Y. Wu, and J. Kim, "A newly designed quarter-rate QC-LDPC code for the cloud transmission system," *IEEE Trans. Broadcast*., vol. 59, no. 1, pp. 155–159, Mar. 2013.

[165] T. Jokela, M. Tupala, and J. Paavola, "Analysis of Physical Layer Signaling Transmission in DVB-T2 Systems," *IEEE Trans. Broadcast*., vol. 56, no. 3, pp. 410–417, June. 2010.

[166] J. Montalban *et al*., "Cloud Transmission: System Performance and Application Scenarios," *IEEE Trans. Broadcast*., vol. 60, no. 2, pp. 170–184, March. 2014.

[167] "Digital video broadcasting (DVB); Second generation framing structure, channel coding and modulation systems for broadcasting, interactive services, news gathering and other broadband satellite applications (DVB-S2)," ETSI, Sophia Antipolis, France, Tech. Rep. ETSI EN 302 307 V1.2.1 (2009-08), Aug. 2009.

[168] "Digital video broadcasting (DVB); Frame structure channel coding and modulation for a second generation digital transmission system for cable system (DVB-C2)," ETSI, Sophia Antipolis, France, Tech. Rep. ETSI EN 302 769 V1.1.1 (2010-04), Apr. 2010.

[169] C. A. Nour and C. Douillard, "Rotated QAM constellations to improve BICM performance for DVB-T2," in *Proc. IEEE Int. Symp. Spread Spectrum Tech. Appl*., Bologna, Italy, Aug. 2008, pp. 354–359.

[170] M. Breiling, J. Zollner, and J. Robert, "When do rotated constellations provide gains?," *IEEE International Symposium on Broadband Systems and Broadcasting*, Beijing, China, June 2014.

[171] T. Kratochvil, and L. Polak, " Measurement of the DVB-T2 with 256QAM rotated constellation and 32K extended mode in relation to variable pilot patterns," *IEEE International Symposium on Broadband Systems and Broadcasting*, London, UK, June 2013.

[172] L. Polak, and T. Kratochvil, "Comparison of the non-rotated and rotated constellations used in DVB-T2 standard," *International Conference Radioelektronika*, Brno, Czech Republic, April 2012.

[173] L. Michael and D. Gomez-Barquero, "Bit-Interleaved Coded Modulation (BICM) for ATSC 3.0," *IEEE Trans. Broadcast*., vol. 62, no. 1, Mar. 2016.

[174] T. Richardson and R. Urbanke, "Multi-edge type LDPC codes," Technical Report, LTHC-REPORT-2004-001, 2004

[175] D. Gozalvez, J.J. Gimenez, D. Gomez-Barquero, and N. Cardona, "Rotated Constellations for Improved Time and Frequency Diversity in DVB-NGH," *IEEE Trans. Broadcast*., vol. 59, no. 2, pp. 298–305, May. 2013.

[176] B. Mouhouche, D. Ansorregui, and A. Mourad, "High order non-uniform constellations for broadcasting UHDTV," in *Proc. IEEE Wireless Commun. Netw. Conf.*, Istanbul, Turkey, Apr. 2014, pp. 600–605.

[177] "Digital video broadcasting (DVB); Frame structure channel coding and modulation for a second generation digital terrestrial television broadcasting system (DVB-T2)," ETSI, Sophia Antipolis, France, Tech. Rep. ETSI EN 302 755 V1.1.1 (2009-09), Sep. 2009.

[178] D. Astely *et al*., "LTE: The evolution of mobile broadband," *IEEE Commun. Mag*., vol. 47, no. 4, pp. 44–51, Apr. 2009.

[179] *Part 11: Wireless LAN Medium Access Control (MAC) and Physical Layer (PHY) Specifications. Amendment 5: Enhancements for HigherThroughout*, IEEE Standard 802.11n-2009, Oct. 2009.

[180] J. Kennedy and R. Eberhart, "Particle swarm optimization," in *Proc. IEEE Int. Conf. Neural Netw.*, Piscataway, NJ, USA, 1995, pp. 1942–1948.

[181] D. W. Boeringer and D. H. Werner, "Particle swarm optimization versus genetic algorithms for phased array synthesis," *IEEE Trans. Antennas Propag.*, vol. 52, no. 3, pp. 771–779, Mar. 2004.

[182] K. K. Soo, Y. M. Siu, W. S. Chan, L. Yang, and R. S. Chen, "Particle-swarm-optimization-based multiuser detector for CDMA communications," *IEEE Trans. Veh. Technol.*, vol. 56, no. 5, pp. 3006–3013, Sep. 2007.

[183] R. Eberhart and Y. Shi, "Particle swarm optimization: Developments, applications and resources," *Proc. Congr. Evol. Comput.*, Seoul, South Korea, May 2001, pp. 81–86.

[184] K. E. Parsopoulos and M. N. Vrahatis, "Recent approaches to global optimization problems through particle swarm optimization," *Nat. Comput.*, vol. 1, no. 2, pp. 235–306, 2002.

[185] R. Shrestha, and R. Paily, "Hardware Implementation of Max-Log-MAP algorithm based on MacLaurin series for turbo decoder," *International Conference on Communications and Signal Processing*, Calicut, India, Feb. 2011.

[186] M. Sandell, F. Tosato, and A. Ismail, "Low-Complexity Max-log LLR Computation for Nonuniform PAM Constellations," *IEEE Communications Letters*, vol. 20, no. 5, pp. 838–841, May 2016.

[187] J. Barrueco *et al*., "Low complexity and high order two-dimensional non-uniform constellations for high capacity broadcasting systems," in *Proc. IEEE Int. Symp. Broadband Multimedia Syst. Broadcast. (BMSB)*, Jun. 2016.

[188] J. Barrueco *et al*., "Condensation Methodologies for Two-Dimensional Non-Uniform Constellations," in *Proc. IEEE Int. Symp. Broadband Multimedia Syst. Broadcast. (BMSB)*, Jun. 2017.

[189] 0. Edfors, M. Sandell, J.-J. van de Beek, S.K. Wilson and P. 0. Borjesson, Analysis of DFT-based channel estimators for OFDM. Research Report TULEA 1996:17, Div. of Signal Processing, Luleå University of Technology, Sept. 1996.

GLOSSARY

In this section there are alphabetically ordered the acronyms and abbreviations that appear through this document.

AMI	Average Mutual Information
ASIP	Application-Specific Instruction-Set Processor
ASK	Amplitude Shift Keying
ATSC	Advanced Television Systems Committee
ATSC 3.0	ATSC – Third Generation
AWGN	Additive White Gaussian Noise
BCH	Bose Chadhuri Hocquenghem
BER	Bit Error Rate
BICM	Bit-Interleaved Coded Modulation
BICM-ID	Iteratively Decoded BICM
BMD	Bit-Metric Decoding
BP	Belief Propagation
BPSK	Binary Phase Shift Keying
BTCM	Binary Turbo Coded Modulation
CAO	Condensation After Optimization
CB	Channel Bonding
CCSDS	Consultive Committee for Space Data Systems
CM	Coded-Modulation
CNR	Carrier-to-Noise Ratio
CR	Code Rate
CRC	Cyclic Redundancy Check

CSI	Channel State Information
CWO	Condensation With Optimization
DFT	Discrete Fourier Transform
DoF	Degrees of Freedom
DOCSIS	Data Over Cable Service Interface Specification
DSP	Digital Signal Processor
DTMB	Digital Terrestrial Multimedia Broadcast
DTT	Digital Terrestrial Television
DVB-C2	Digital Video Broadcasting – Cable Second Generation
DVB-H	DVB – Handheld
DVB-NGH	DVB – Next Generation Handheld
DVB-S2	DVB – Satellite Second Generation
DVB-T	DVB – Terrestrial
DVB-T2	DVB – Terrestrial Second Generation
ED	Euclidean Distance
ETSI	European Telecommunications Standards Institute
EXIT	Extrinsic Information Transfer Chart
FCC	Federal Communications Commission
FEC	Forward Error Correction
FFT	Fast Fourier Transform
FIFO	First In First Out
FSK	Frequency Shift Keying
GI	Guard Interval

GS	Geometrical Shaping
HDTV	High Definition TV
HDR	High Dynamic Range
HEVC	High Efficiency Video Coding
HFR	High Frame Rate
HM	Hierarchical Modulation
HPA	High Power Amplifier
HSD	Hard Sphere Decoder
I	In-phase
IAS	Interantenna Synchronization
iid	independent and identically distributed
IMT	International Mobile Telecommunications
IPM	Iterative Polar Modulation
ISDB-T	Integrated Services Digital Broadcasting - Terrestrial
ITU	International Telecommunications Union
JDD-ML	Joint Maximum-Likelihood Detection and Decoding
KPI	Key Performance Indicator
KSE	K-dimensional Schnorr-Euchner
LDM	Layered Division Multiplexing
LDPC	Low Density Parity Check
LLR	Log-Likelihood Ratios
LR	Lattice Reduction
LSB	Least Significant Bits

LSD	List Sphere Decoder
LST	Layered Space-Time
LTE	Long Term Evolution
LUT	Look-Up Table
MAP	Maximum A Posteriori
MIMO	Multple-Input Multiple-Output
ML	Maximum Likelihood
MLC	Multi-Level Coding
MLSL	Multi-Level Single Linkage
MMSE	Minimum Mean Square Error
MNO	Mobile Operator Network
ModCod	Modulation and Coding
MPEG	Moving Picture Experts Group
MSB	Most Significant Bit
MSC	Multi-Stage Coding
MSMod	Multi-antenna Spatial Modulation
MSSK	Modified Space Shift Keying
NOMA	Non-Orthogonal Multiple Access
NUC	Non-Uniform Constellation
OFDM	Orthogonal Frequency-Division Multiplexing
PAM	Pulse Amplitude Modulation
PAMI	Pragmatic Average Mutual Information
PAPR	Peak-to-Average Power Reduction

PAS	Probabilistic Amplitude Shaping
PCM	Parity Check Matrix
pdf	probability density function
PD-DEM	Per-Dimension Demapper
PDL	Parallel Decoding Level
PI	Power Imbalance
PLP	Physical Layer Pipes
PMF	Probability Mass Function
PP	Pilot Patern
PRBS	Pseudo-Random Binary Sequence
PS	Probabilistic Shaping
PSO	Particle Swarm Optimization
Q	Quadrature
QAM	Quadrature Amplitude Modulation
QPSK	Quadrature Phase Shift Keying
RC	Rotated Constellation
RF	Radio Frequency
RME	Rayleigh Memoryless with Erasures
RS	Reed-Solomon
RZ	Return to Zero
SCASR	Switched Condensed and Adaptive Sub-Region
SD	Sphere Decoder
SFN	Single Frequency Network

SFSD	Soft-output Fixed-complexity Sphere Decoder
SIC	Successive Interference Calculation
SISO	Single-Input Single-Output
SM	Spatial Multiplexing
SMD	Symbol-Metric Decoding
SNR	Signal-to-Noise Ratio
SQP	Sequencial Quadratic Programming
SSD	Signal Space Diversity
TCM	Trellis Coded Modulation
TDM	Time Division Multiplexing
TDS	Time Domain Spreading
TV	Television
UHDTV	Ultra-High Definition TV
UHF	Ultra-High Frequency
VHF	Very-High Frequency
VLC	Visible Light Communication
VLSI	Very-Large-Scale Integration
VSB	Vestigial Side Band
WCG	Wide Color Gamut
WRC	World Radiocommunication Conference
1D-NUC	One-Dimensional NUC
2D-NUC	Two-Dimensional NUC